



Technical University of Crete  
School of  
Electrical & Computer Engineering

Integrated Master's Thesis

**Determination of the  
Pharmaceutical Treatment-Dosage  
for Cancer Patients using  
Non-Linear Optimization Techniques**

author  
Mavromatakis Iason

Thesis Committee

Professor Stavrakakis Georgios (Supervisor)  
Professor Zervakis Michael  
Dr. Sergaki Eleftheria

Technical University of Crete, Chania  
February, 2020



Πολυτεχνείο Κρήτης  
Σχολή Ηλεκτρολόγων Μηχανικών  
& Μηχανικών Υπολογιστών

Διπλωματική Εργασία

**Προσδιορισμός της  
Χορήγησης Φαρμακευτικής Αγωγής-Δοσολογίας  
σε Καρκινοπαθείς με Χρήση Τεχνικών  
Μη-Γραμμικής Βελτιστοποίησης**

συγγραφέας  
Μαυροματάκης Ιάσων

Εξεταστική επιτροπή  
Καθηγητής Σταυρακάκης Γεώργιος (Επιβλέπων)  
Καθηγητής Ζερβάκης Μιχαήλ  
Δρ. Σεργάκη Ελευθερία

Πολυτεχνείο Κρήτης, Χανιά  
Φεβρουάριος, 2020

# Abstract

---

Cancer, a disease first documented thousands of years ago, remains one of the most important issues of medicine, troubling numerous scientists and researchers, as well as individual patients. In this study, a non-linear mathematical model of tumor growth with immune response, under the effects of chemotherapeutic treatment, is presented. After analyzing the dynamics of the cells and the possible equilibria of the drug-free system, their interactions with the drug are examined. Later on, two cost-efficient optimal control approaches are reviewed, based on direct collocation and state-dependent Riccati equation methods, and then they are extended further so that they can be practically applied to patients. Ultimately, the results from each method are presented, providing an overall better regimen, when compared to previous studies, by successfully eradicating the tumor and keeping the side-effects of chemotherapy to a minimum.

**Keywords:** Cancer, Tumor growth, Cancer model, Chemotherapy, Drug Dosage, Toxicity, Mathematical modelling, Immune system, Ordinary differential equations, Direct Collocation, SDRE control, Optimal control.

# Πρόλογος

---

Ο καρκίνος αποτελεί μια ασθένεια που πρωτοεμφανίστηκε πριν από χιλιάδες χρόνια και εξακολουθεί να παραμένει ένα από τα σημαντικότερα ζητήματα της ιατρικής. Στην παρούσα μελέτη παρουσιάζεται και αναλύεται ένα μη γραμμικό μαθηματικό μοντέλο που προσομοιώνει την εξέλιξη ενός αρχικά μεγάλου όγκου, υπό την επήρεια ενός αποδυναμωμένου ανοσοποιητικού συστήματος και χημειοθεραπευτικής αγωγής. Το πρόβλημα εύρεσης της βέλτιστης δοσολογίας για αυτήν την περίπτωση αποτελεί μία πρόκληση. Για τον λόγο αυτό, αναπτύσσονται δύο μέθοδοι θεραπείας, εφαρμόζονται και συγκρίνονται, βάσει των αποτελεσμάτων τους.

Αρχικά, παρουσιάζεται το μη γραμμικό μαθηματικό μοντέλο, βάσει του οποίου προσομοιώνονται οι αντιδράσεις μεταξύ των καρκινικών κυττάρων, των υγιών κυττάρων και των κυττάρων του ανοσοποιητικού συστήματος του ασθενή. Έπειτα, γίνεται μια ανάλυση σχετικά με τα σημεία ισορροπίας του συστήματος και την ευστάθεια τους, χωρίς την επίδραση της χημειοθεραπείας. Όμως, προκειμένου να μετατοπιστεί το σύστημα σε ένα ευσταθές «υγιές» σημείο ισορροπίας, πρέπει να χορηγηθεί κάποια ποσότητα φαρμάκου. Επομένως, εισάγεται η επίδραση του φαρμάκου στο μαθηματικό μοντέλο και εξετάζονται δύο προσεγγίσεις για τη χημειοθεραπευτική αγωγή του ασθενή.

Στην πρώτη προσέγγιση εφαρμόζεται η μέθοδος ελέγχου άμεσης ταξινόμησης Hermite-Simpson, ώστε να βρεθεί ένα βέλτιστο πρόγραμμα χορήγησης φαρμάκου, αποφέροντας πολύ ικανοποιητικά αποτελέσματα (η μέθοδος παρουσιάζεται αναλυτικά στο Παράρτημα 1). Ωστόσο, η απαίτηση της για χορήγηση φαρμάκου κάθε μέρα, καθ' όλη τη διάρκεια της θεραπείας, δεν την καθιστά υλοποιήσιμη. Συνεπώς, μετατρέπεται σε μέθοδο ελέγχου Bang-Bang, διατηρώντας την ίδια συνολική ποσότητα φαρμάκου, αλλά επιλέγοντας συγκεκριμένες ημέρες για τη χορήγησή του. Τα αποτελέσματα που λαμβάνονται είναι εξίσου ικανοποιητικά, καθώς ο όγκος εξαλείφεται, αποφεύγονται επικίνδυνα επίπεδα τοξικότητας και μειώνεται παράλληλα η διάρκεια της διαδικασίας.

Στη δεύτερη προσέγγιση, εφαρμόζεται η μέθοδος ελέγχου State-Dependent Riccati Equation (SDRE), η οποία απαιτεί μικρότερο όγκο υπολογισμών, άρα και λιγότερο χρόνο για την προσομοίωση (η μέθοδος παρουσιάζεται αναλυτικά στο Παράρτημα 2). Δυστυχώς, η προσέγγιση βάσει της SDRE εισάγει το ζήτημα της υψηλής τοξικότητας (συγκέντρωση φαρμάκου στη περιοχή του όγκου), το οποίο αντιμετωπίζεται, είτε ορίζοντας ένα άνω φράγμα στην ποσότητα του χορηγούμενου φαρμάκου, είτε δημιουργώντας ένα περιοδικό πρόγραμμα ενεργών και ανενεργών ημερών χορήγησης. Και τα δύο σενάρια προσφέρουν αποτελεσματικές θεραπευτικές αγωγές, με το περιοδικό πρόγραμμα να ξεχωρίζει, καθώς επιτυγχάνει να ελαττώσει τη συνολική ποσότητα φαρμάκου που απαιτείται, περιορίζοντας ταυτόχρονα τις αρνητικές παρενέργειες της χημειοθεραπείας.

Εν κατακλείδι, συγκρίνονται τα αποτελέσματα των προσομοιώσεων από τις παραπάνω προσεγγίσεις χημειοθεραπευτικής αγωγής. Και οι δύο περιπτώσεις είναι αποτελεσματικές κατά των καρκινικών κυττάρων, εξαλείφοντας τον όγκο που είχε δημιουργηθεί, ενώ ταυτόχρονα ελαχιστοποιούν την συνολική ποσότητα χορηγούμενου φαρμάκου και διατηρούν τα επίπεδα τοξικότητας, στο σώμα του ασθενή, σε χαμηλές τιμές. Με αυτόν τον τρόπο, περιορίζονται οι παρενέργειες της χημειοθεραπείας και ο πληθυσμός των υγιών κυττάρων ανακάμπτει πιο γρήγορα.

# Acknowledgments

---

A period of five and a half years has reached its end. In this journey, I have had the opportunity to meet a lot of people, make friends, and to get to know myself better. Even though I was not completely sure of what to expect at the beginning, I had the good fortune to discover many interests and paths to become creative. It was the welcoming environment and caring community of the department of Electrical and Computer Engineering at the Technical University of Crete that made this possible; thus I feel truly blessed that I had the opportunity of being an undergraduate student there, surrounded by many individuals who influenced me and provided crucial stimuli and knowledge. I am deeply grateful to all of them.

The educational process needs a student and a teacher in order to be defined. In my opinion, the most successful way for a teacher to motivate his/her students is to help them see, from a different perspective, the magic that lies underneath the courses or the research he/she carries out. For me, this person was Prof. Stavrakakis Georgios, who not only convinced me, but also guided me with enthusiasm, patience and care, in the fields of research, mathematics, and engineering, alongside with the support and counsel of the thesis committee members, Prof. Zervakis Michalis and Dr. Sergaki Eleftheria. Moreover, the crucial aid of my fellow student Liliopoulos Sotirios and the former Prof. Pouliezos Anastasios had a great impact on the theoretical and implementational correctness of this research. Without the contribution of all the above individuals, this thesis would not have been the same. I am greatly indebted to them and I will always be thankful for the inspiration they have given me.

Every journey has its happy and sad moments. I had the pleasure to share many of them with my family and friends, who celebrated with me the good moments and supported me through the bad ones. I am truly grateful to them for being there for me. Finally, I would like to thank any fellow students who helped and supported me, throughout all these years, reminding me that teamwork is a very powerful tool and should be used as often as possible.

# Table of contents

---

Acknowledgments.....	iv
Table of contents.....	v
Abbreviations.....	viii
List of figures.....	ix
Chapter 1 : Introduction.....	1
Topic of interest.....	1
Definition of the cancer chemotherapy optimization problem.....	2
Related work.....	3
The present thesis' contribution.....	6
Chapter 2 : Presentation and analysis of the cancer growth non-linear dynamic mathematical model first proposed by L. G. de Pillis and A. Radunskaya.....	7
Tumor dormancy.....	7
Key elements of the cancer growth mathematical model.....	9
Differential equations of the non-linear cancer growth mathematical model.....	11
Drug-free mathematical model analysis.....	13
Tumor-free equilibria.....	15
Normal cells' dead equilibria.....	16
Coexisting normal and tumor cells equilibria.....	16
Numerical values of the parameters of the tumor growth mathematical model eq. (2) .....	21
Chapter 3 : Optimal cancer chemotherapy treatment based on the Direct Collocation method.....	25
The Direct Collocation (DirCol) method.....	25
The Hermite-Simpson Collocation method.....	27
Formulation of the problem.....	28

The Bang-Bang conversion of the Direct Collocation method .....	30
Simulation results of the application of the determined treatment by using the Hermite-Simpson Collocation method and its modified Bang-Bang approach .....	31
Case 1 : Highly weakened immune system, $I_0 = 0.10$ .....	32
Case 2 : Less weakened immune system, $I_0 = 0.15$ .....	36
Chapter 4 : Optimal cancer chemotherapy treatment based on the State-Dependent Riccati Equation (SDRE) optimal non-linear control method .....	42
Pseudo-linear state space equations formulation.....	43
Reconstruction of the mathematical model of eq. (2) in pseudo-linear form.....	47
Periodic application of the determined optimal chemotherapy treatment .....	51
Simulation results of the application of the determined treatment by using the pseudo-linear SDRE optimal control method of eq. (7a) ... (7e) .....	52
Case 1 : The drug input's weight $R(x)$ has a constant value .....	54
Case 2 : The tumor increases the drug input's weight $R(\underline{x}(t))$ .....	55
Case 3 : The tumor decreases the drug input's weight $R(\underline{x}(t))$ .....	56
Case 4 : The drug input is bounded and the drug input's weight $R(\underline{x})$ has a constant value.....	57
Case 5 : Reevaluation of the chemotherapeutic schedule by applying a periodic drug input dosage .....	59
Case 6 : Reevaluation of the chemotherapeutic schedule by applying a periodic bounded drug input dosage.....	62
Chapter 5 : Conclusion.....	68
Interpretation of the Results .....	69
Future Work.....	74
References .....	75
Bibliography.....	80
Appendix 1 : Hermite-Simpson Direct Collocation method.....	83
Discretize the time domain .....	83

Compute state derivatives at the collocation point .....	83
Express the cost function in terms of optimization parameters.....	85
Define Additional Constraints .....	86
Appendix 2 : State-Dependent Riccati Equation (SDRE) method .....	87
Problem formulation .....	87
Extended linearization .....	88
Controller structure.....	89
Existence of stabilizing feedback controls.....	90
Local asymptotic stability.....	91

# Abbreviations

---

ARE	:	Algebraic Riccati Equation
BSA	:	Body Surface Area
DIRCOL	:	Direct Collocation
EKF	:	Extended Kalman Filter
HJB	:	Hamilton Jacobi Bellman
LPV	:	Linear Parameter Varying
LQR	:	Linear Quadratic Regulator
LTI	:	Linear Time Invariant
LTV	:	Linear Time Varying
NLP	:	Non-linear Programming
ODE	:	Ordinary Differential Equation
SDC	:	State-Dependent Coefficient
SDRE	:	State-Dependent Riccati Equation
TP	:	Tensor Product
TPBVP	:	Two Point Boundary Value Problem
$x(t), x$	:	$n$ -dimensional state vector symbols
$\underline{x}(t), \underline{x}$	:	$n$ -dimensional state vector symbols
$u(t), u$	:	$m$ -dimensional control vector symbols

## List of figures

---

<b>Figure 1</b> – Plane surfaces corresponding to the cells’ populations recalculated and reevaluated in the present work.....	14
<b>Figure 2</b> – Stability of coexisting equilibria in relation to $s$ and $\rho$ reevaluated in the present work. ....	17
<b>Figure 3</b> – Normal, tumor and immune cell populations’ evolution and stability recalculated in the present work. ....	19
<b>Figure 4</b> – Tumor cells’ population and stability evolution and stability recalculated in the present work.....	20
<b>Figure 5</b> – Drug-free mathematical model response for varying initial immune cells’ populations $I_0$ , recalculated and reevaluated in the present work.....	24
<b>Figure 6</b> – Hermite-Simpson collocation method. ....	28
<b>Figure 7</b> – Cell populations and drug input for DirCol treatment (case 1). ....	32
<b>Figure 8</b> – Maximum/minimum state values for DirCol treatment (case 1). ....	33
<b>Figure 9</b> – Cell populations and drug input for bang-bang conversion (case 1). ....	34
<b>Figure 10</b> – Maximum/minimum state values for bang-bang conversion (case 1).....	35
<b>Figure 11</b> – Cell populations and drug input for DirCol treatment (case 2). ....	36
<b>Figure 12</b> – Maximum/minimum state values for DirCol treatment (case 2). ....	37
<b>Figure 13</b> – Cell populations and drug input for bang-bang conversion (case 2). ....	38
<b>Figure 14</b> – Maximum/minimum state values for bang-bang conversion (case 2).....	39
<b>Figure 15</b> – Mathematical model’s response and drug input for constant $R(x) = 4.7$ . ....	54
<b>Figure 16</b> – Mathematical model’s response and drug input for $R(x(t))$ as an increasing function of the tumor evolution, i.e. $x_2(t)$ , that is as a function of the state vector $x(t)$ . ...	55
<b>Figure 17</b> – Mathematical model’s response and drug input for $R(x(t))$ as a decreasing function of the tumor evolution, i.e. $x_2(t)$ , that is as a function of the state vector $x(t)$ . ...	56
<b>Figure 18</b> – Mathematical model’s response and drug input for bounded drug dosage. ....	57

<b>Figure 19</b> – Comparison of global minima in normal cells when applying a variety of periodic treatments (case 5).....	59
<b>Figure 20</b> – Comparison of total drug amount administered when applying a variety of periodic treatments (case 5).....	60
<b>Figure 21</b> – Mathematical model’s response and drug input when a periodic treatment of [3/1] days is applied, the drug input is unbounded and the input weight $R(x(t))$ is a decreasing function of the tumor evolution, i.e. $x_2(t)$ .....	61
<b>Figure 22</b> – Comparison of global minima in normal cells when applying a variety of periodic treatments (case 6).....	62
<b>Figure 23</b> – Comparison of total drug amount administered when applying a variety of periodic treatments (case 6).....	63
<b>Figure 24</b> – Mathematical model’s response and drug input when a periodic treatment of [4/3] days is applied, the drug input is bounded and the input weight $R(x(t))$ has a constant value.....	64
<b>Figure 25</b> – Comparison of the normal cells’ minimum population (best cases).....	69
<b>Figure 26</b> – Comparison of the total amount of administered drug (best cases). ....	70
<b>Figure 27</b> – Comparison of the maximum drug concentration (best cases). ....	71
<b>Figure 28</b> – Comparison of the treatment’s duration (best cases). ....	72
<b>Figure 29</b> – Comparison of the tumor cells’ maximum population (best cases).....	73

*To my beloved family...*



# Chapter 1 : Introduction

---

## Topic of interest

Our bodies' tissues are made of billions of individual cells. These cells divide throughout our whole lifespan, by splitting into two identical new cells. Thus, where there was one cell, there are now two, later will be four, eight and so on. Once we are fully grown, the multiplication rate of those cells is reduced and mainly occurs if there is any sort of damage, so that it can be repaired. However, because of various reasons, certain cells keep on dividing irregularly, until a mass is formed. This mass of cells eventually becomes a lump, which is called a tumor. Cancer research focuses on how and when these abnormal cells start developing, as well as their ability to infiltrate and destroy the normal body tissue.

This disease has troubled the scientific society for many years and definitely lies among the most important issues of modern medicine. It is the second-leading cause of death in the world, especially in developing countries, due to the increased appearance of established risk factors such as smoking, alcohol, physical inactivity, obesity, unhealthy lifestyle and varying reproductive patterns related with urbanization and monetary development. However, survival rates are improving for many types of cancer, thanks to improved screening and treatment techniques.

Many methods have been developed, in order to deal with cancer, such as surgery, radiotherapy, chemotherapy, hormone therapy, and immunotherapy. Amidst the above, chemotherapy has been established as an essential approach and is applied frequently to patients. Its primary goal is to inhibit the division of the cancerous cells or destroy them. Halting the cells' division process (mitosis) is the reason why chemotherapy is such an effective treatment method. Some drugs damage cells at the point of splitting, while others damage the cells while they are making copies of all their genes before they split. In general, chemotherapy is much less likely to damage cells that are not proliferating, such as most normal cells, making it more precise.

Cancer cells are easily distinct, since their growth and division rates are higher and without order or control, compared to those of normal cells. Hence, chemotherapy can focus on them more efficiently. Nevertheless, some types of normal cells, such as cells in hair follicles, nails, the mouth, the digestive tract and bone marrow do not grow and divide in an accurate, structured manner. Chemotherapy can, also, damage these other types of frequently dividing cells unintentionally, causing what is known as side effects. Commonly, a combination of different chemotherapy drugs is used, in order to damage cells at different stages, throughout the process of mitosis. Therefore, the chances of killing more cancerous cells are higher.

Along with the process described above, some efforts have been made in the scientific and engineering fields to portray the dynamics of cancer. One of the most promising approaches is mathematical modeling, which includes identification of the cells responsible for the cancer propagation, interactions between these bodies and description of the dynamics of these interactions. This powerful tool has helped us identify and formulate such problems (e.g. calculation of biologically relevant parameters), perform stability analysis, and understand clinically observed phenomena such as tumor dormancy, tumor size oscillations and regressions, nonspatial mathematical models of tumor and immune system interactions and the relation between tumor growth and chemotherapy. Last but not least, mathematical modeling offers a low-cost and time-efficient solution to what would otherwise require months of experiments in labs alongside with a significant financial investment.

## Definition of the cancer chemotherapy optimization problem

Up to this day, the issue of drug dosage in cancer chemotherapy eludes consistent quantitative responses, even though it is extremely crucial for a successful treatment. Modern oncology increasingly takes the point of view of a tumor as an aggregation of cancer cells subgroups, with a variety of therapeutic sensitivities embedded into its microenvironment. This microenvironment is formed by the tumor vasculature, the tumor-immune system interactions, and several other structures (e.g., fibroblasts and the extracellular matrix), all of

which are located into healthy tissue. When all these excessive factors are ignored, the concept of ideal chemotherapy protocols can be applied and provide us with clear and simple answers. For example, if a homogenous tumor population of chemotherapeutically sensitive cells is assumed and other aspects of the tumor microenvironment are ignored, then undoubtedly an optimal treatment schedule would come up with correct and realistic results.

The purpose of the drug is to control the populations of three major biological cell types (normal, immune and tumor cells) under given cancer mathematical model parameters, by finding the optimal regimen for its administration. Optimality can be translated into either a quick eradication of the tumor, by destroying healthy cells as well for a short period of time, or a moderate regimen, lasting longer but keeping any side effects to the bare minimum. In order to achieve this goal, an optimal controller is proposed for a non-linear mathematical model, which describes the interactions between the drug, normal, immune and tumor cells. The drug dosage is constantly adapted to the current state of the mathematical model, in order to control the tumor growth and preserve immune and normal cells within the desired levels.

Having said all the above, the scientific community has resulted in a series of regimens (e.g. bang-bang control, quadratic control, state-dependent Riccati equation (SDRE) based optimal control, maximum tolerated doses (MTD), etc.), most of which are commonly used in control theory. Yet, when they are applied in practice, other characteristics of the tumor microenvironment are also taken into consideration, making the bigger picture fuzzy, and the question of proper drug dosage remains unanswered.

## Related work

To analyze the dynamics between tumor and immune systems under chemotherapy, numerous mathematical models have been proposed and extensively studied by many researchers. Initial studies focused on exponential, Gompertz, Bertalanffy and logistic mathematical models, with analysis of the data based on non-linear regression methods [88]. It is crucial to highlight how much useful work has been done on simplified yet fundamental

mathematical models, shedding light on the interactions between tumor cells and immune cells alone [36][60][78], between tumor cells and normal cells alone [20][21][32] and between tumor cells and chemotherapy drugs alone [1][39][40][50][54][55][68][77].

While these mathematical models were extremely useful in offering an interpretation of the tumor growth and treatment from different perspectives, they were not able to imprint certain qualitative factors, concerning the clinicians who applied them in practice. Therefore, they became a stepping stone to the more recent research, leading to the production of a mathematical model that incorporates the interactions among tumor cells, normal cells, immune cells and chemotherapy drugs [13][14][17][18][82].

Advancing even further, scientists took under consideration the regimen of the drug administration and later confirmed that, if it had been optimal, the patients' survival rates in cancer treatment were higher. A mathematical model of the above form has allowed researchers to test and compare various optimal control strategies, some of which are linear control, quadratic control, (by taking advantage of Pontryagin's Maximum/Minimum Principle) and state-constraints [14]. Once the existence of the optimal control is proved, it is applied in both the quadratic and the linear case. Although, when the problem is approached linearly, we are confronted with the problem of singular control.

Various techniques in the literature [8][9][37][39][77] attempted to solve optimal control problems for non-linear systems; specifically, cancer mathematical models, which are highly non-linear and high dimensional. Unfortunately, since they were carefully addressed to have an optimal solution, the methods produced cannot be generalized, because of the considerable computational efforts to obtain them. An additional optimal control method for cancer treatment is then suggested, in which the non-linear cancer dynamics are presented as Linear Time Varying (LTV) approximations [26]. Thus, the well-known Linear Quadratic Regulator (LQR) techniques could take place. This approach, despite the valid results which produces by recursively solving an infinite series of LQR problems for LTV systems, is bound to the pre-computation of the optimal control parameters.

This issue can be dealt with a more recent technique, which is called State-Dependent Riccati Equation (SDRE) optimal control and has been applied effectively to plenty non-linear systems, not only in theory, but also in practice [3][6][10][41][42][70]. Given its computational simplicity and satisfactory performance in simulations and practice, SDRE optimal control can be considered an appealing approach for the control of certain non-linear systems, as long as they can be represented as a series of Linear Time Invariant (LTI) systems.

A lot of research has also been carried out in the development of stochastic mathematical models [64][75][80]. A stochastic approach can be useful, specifically when studying the interactions among populations with low densities. On the contrary, other parties have developed continuous-time deterministic mathematical models of tumor growth and treatment [17]. This approach seems to be more efficient, since classical optimal control theory can be applied, which, as one would expect, suggests an improved chemotherapy administration schedule. Thus, the optimal control problem of tumors, in cancer treatment under chemotherapy and/or immunotherapy has been highlighted as a research topic in cancer treatment strategies [8][14][17][18][77][40][41][56][61][66]. Specifically, De Pillis and Radunskaya (2003) [18] focused on the phase-space analysis of an Ordinary Differential Equations (ODE) mathematical model of tumor growth, including interactions with the immune response and chemotherapy, and proved that if the drug administration follows an optimal control method, the state trajectory can be moved into a basin of attraction of a healthy equilibrium point.

Other studies have taken advantage of the Extended Kalman Filter (EKF) in order to estimate the drug level, in cases where it is considered unmeasurable. Linear Parameter Varying (LPV) mathematical models are used both at controller design (difference-based control oriented LPV mathematical model) and EKF development. By using the Tensor Product (TP) model transformation accompanied by the Linear Matrix Inequality (LMI) optimization technique, a Parallel Distributed Compensator (PDC) kind controller is designed [33][43][63][69][70][73][84].

## The present thesis' contribution

In this study, the dynamics of a non-linear mathematical tumor model based on the previous work of L. G. de Pillis and A. Radunskaya in [17][18] are reviewed, with emphasis on the equilibria points. Afterwards, two optimal control methods of previous research, based on the Direct Collocation method [18] and on the State-Dependent Riccati Equation method [41], are examined for this certain mathematical model and, later on, are modified, so that better results can be obtained. More specifically, the effectiveness of the methods is enhanced and at the same time their cost-efficiency is increased. In other words, the cost function presented in [18] is extended, so that the total amount of drug can be reduced even further, and a periodic optimal chemotherapy treatment is determined and applied by modifying the method initially proposed in [41], which limits the side-effects of chemotherapy and at the same time decreases the total amount of administered drug, while maintaining the efficacy of the treatment against the tumor.

## **Chapter 2 : Presentation and analysis of the cancer growth non-linear dynamic mathematical model first proposed by L. G. de Pillis and A. Radunskaya [17][18]**

---

The design of a biological system's mathematical model is driven by the need to synthesize the system's basic actions and to address specific questions about it. Specifically, the aim is to use the mathematical model in order to develop an improved chemotherapy regimen, which delivers a better result, by reducing the final size of the tumor without causing significant losses in the population of normal cells. Moreover, the mathematical model should explain clinically observed phenomena brought to light by the oncologists working on this area, such as “Jeff’s phenomenon” and tumor dormancy.

In this chapter, an Ordinary Differential Equation (ODE) based tumor growth mathematical model is presented. ODE-based cancer dynamics mathematical modeling is an active research area, and many different mathematical models have been proposed. Among many of these, the mathematical model proposed by de Pillis and Radunskaya (2003) [18] stands out, since its composition combines some of the most useful aspects of previously existing mathematical models and at the same time considers the growth of tumor cells and their interaction with normal cells and immune cells, alongside with the effects of chemotherapy.

### **Tumor dormancy**

Under hostile conditions, microorganisms adopt different mechanisms for survival. They are undergoing drastic changes in cell physiology to form the surrounding microenvironment in order to best meet their needs [27]. In response to a stressor such as chemotherapy, stressed tumor cells that survive apoptosis become dormant. After the therapy

has been discontinued, the dormant cells may repopulate, resulting in tumor recurrence and development of chemotherapy-resistant cancer cells [87][89].

Dormant cells may be identified as circulating tumor cells (CTCs) in the bloodstream or disseminated cells (DTCs) within secondary sites, such as bone marrow. When metastatic cells find a new place to reside, they can take different destinies: either they die, remain silent (restrictive soil), or develop with an even more violent and lethal behavior than before (permissive soil). The implication of tumor cell dormancy is very well established in the development of tumor outgrowth and metastatic relapse, leading to cancer treatment failure.

Previous mathematical models [31][36] have shown that immune and tumor cells compete in what is known as a "predator-prey" relationship, in which the immune cells play the role of the predator and the tumor cells play the role of the prey. This competition can lead to repetitive procedure of growth and reduction of the cell population. Firstly, the existence of tumor cells biochemically stimulates the production of immune cells. At the same time, the presence of immune cells counters the multiplication of the tumor cells' population. When a considerable number of tumor cells has perished, the immune cell population inevitably decreases, since they are no longer needed. However, this decrease will enable the regrowth of the tumor cells. This cycle could either keep on going indefinitely, or eventually converge to an equilibrium point, depending on the system parameters.

As a result, the mathematical model's equations have embedded the interaction of the immune and tumor cells, since it greatly affects the dynamics of the tumor growth. Should the immune system be removed, the cyclical routine cannot arise. Instead, there would be either one globally stable equilibrium point (stable competition) or two stable equilibria and a saddle point (competitive exclusion) [7]. For the mathematical model of this study, the existence of possible periodic orbits is analyzed in [18] in detail. When applying the parameters presented below and initial values from the positive octant, all orbits of the system have exactly one of the equilibria as their limit set. More specifically, all orbits are bounded and the system does not have any nontrivial periodic orbits.

## Key elements of the cancer growth mathematical model

The mathematical model presented below is a mixture of previously developed mathematical models, with its key features being:

- Immune response: The presence of tumor cells causes an increase in the immune cells' population, whose purpose is to combat the tumor first through a kinetic process. A phenomenon often observed, even though cancerous cells are immunogenic, is that the immune system response fails to effectively combat the rapid growth of cancerous cells on its own, leading to the formation of a tumor. Thus, the tumor has not completely escaped active immunosurveillance; it is simply strong enough to encounter it.
- Competition terms: There is antagonism between normal and tumor cells, competing for available resources required for their survival and multiplication, and between immune and tumor cells competing in a predator-prey fashion.
- Optimal control theory for chemotherapy: a method of optimal treatment regimen is presented, in order to keep the tumor population at the bare minimum by the end of the treatment period, while keeping the normal cells above a percentage considered safe; these solutions are then put to practice, simulation a practical administration protocol.
- Chemotherapy effects: every type of cell is affected by the drug used in the process. Tumor cells are targeted the most, but immune and normal cells die as well, with a lower rate, as a negative side effect.

The framework of the mathematical model is near the tumor site, assuming a homogeneous tumor, whose reactions with the immune system follows the same concept as in [36].

A comparison has been carried out for the growth law terms, considering mathematical models based on exponential, Gompertz or logistic growth. Should the exponential growth law be applied, the rate of multiplication of the tumor cells, at any given moment, is expected to be proportional to the size of the tumor population at that time; without restricting the exponential curve as time progresses. Likewise, Gompertz law dictates an increase rate similar

to that of the exponential growth in the early stages, but reaches an upper limit as tumor size increases, since its curve is sigmoid. Lastly, the logistic growth law again does not differ from the exponential growth law, with the addition of including a built-in upper bound for the size of the population, beyond which it cannot expand.

Since the mathematical model which is presented has a qualitative character and is meant to handle a wide variety of tumor types, it is vague which growth law reflects reality better. It turns out, however, that none of them has any significant difference from the others, until a certain point in tumor size is reached. Due to the initially small tumor mass, relative to the carrying capacity of the system, alternating between the growth laws mentioned above has no significant effect to the end result, thus the qualitative behavior of the mathematical model is retained.

## Differential equations of the non-linear cancer growth mathematical model

Moving on to the mathematical analysis of the model, the major cell types presented are three. Given a specific time  $t$ , immune, tumor and normal (host) cells are denoted by  $I(t)$ ,  $T(t)$  and  $N(t)$  respectively. The increase of immune cells in the tumor area is achieved by an external source (immune system), therefore a constant influx rate  $s$  is expected. Moreover, should the tumor be eliminated, immune cells will no longer be required, thus they will start decreasing at a per capita rate  $d_1$ , converging to a long-term population size of  $s/d_1$  cells. In other words, a scenario where the tumor area is overwhelmed by immune cells is not feasible. The existence of a tumor triggers the defensive mechanism of the body (immune response), thus the growth rate of immune cells is presented by the non-linear term

$$\frac{\rho I(t)T(t)}{\alpha + T(t)}$$

where  $\rho$  and  $\alpha$  are positive constants, representing the intensity and threshold rate of the immune system respectively.

Additionally, when immune and tumor cells come in contact, the outcome is the elimination of either the first or the second, resulting in the two competition terms of the populations

$$\frac{dI}{dt} = -c_1 I(t)T(t) \quad \text{and} \quad \frac{dT}{dt} = -c_2 I(t)T(t).$$

As far as the proliferation of the tumor and normal cells is concerned, it follows a logistic growth law with growth rate  $r_i$  and maximum carrying capacity  $b_i^{-1}$ , where the index  $i = \{1,2\}$  refers to tumor or normal cells accordingly. Combining all the above, the following equations occur

$$\begin{aligned}
\dot{N} &= r_2N(1 - b_2N) - c_4TN, \\
\dot{T} &= r_1T(1 - b_1T) - c_2IT - c_3TN, \\
\dot{I} &= s + \frac{\rho IT}{\alpha + T} - c_1IT - d_1I,
\end{aligned} \tag{1}$$

which express the dynamics of the mathematical model, without the injection of any drug.

In order to combat the tumor, however, a dose of drug  $v(t)$  in  $mg/m^2$  will have to be administered to the patient, at time  $t$ . Its concentration at the tumor site is denoted by  $M(t)$  in  $mg/L$ . It is rational to consider that all types of cells are affected by the drug, but in a different extent, with the response curve being in the exponential form of

$$a_i(1 - e^{-kM}).$$

Given the unknown pharmacokinetics and pharmacodynamics, it is considered that  $k = 1$ . The coefficients regarding how each cell type is affected by the drug are denoted by  $a_1, a_2, a_3$  for immune, tumor and normal cells respectively. Also, the drug is metabolized by the organism as time progresses, displaying a per capita decay rate  $d_2$ , starting from the moment it enters the patient's body. By merging all the above terms, the final form of the mathematical model becomes

$$\begin{aligned}
\dot{N} &= r_2N(1 - b_2N) - c_4TN - a_3(1 - e^{-M})N, \\
\dot{T} &= r_1T(1 - b_1T) - c_2IT - c_3TN - a_2(1 - e^{-M})T, \\
\dot{I} &= s + \frac{\rho IT}{\alpha + T} - c_1IT - d_1I - a_1(1 - e^{-M})I, \\
\dot{M} &= v(t) - d_2M.
\end{aligned} \tag{2}$$

## Drug-free mathematical model analysis

In order to achieve the best result, the dynamics of the mathematical model have to be studied without any perturbation. The state of the mathematical model is considered healthy when it has reached either a tumor-free equilibrium point or a coexisting state, where the size of the tumor is small enough to no longer be considered a threat.

The null-surfaces occurring from the equations in eq. ( 2 ) are presented below.

- Normal cells:

$$\dot{N} = 0 \Rightarrow \begin{cases} N = 0, & (I - T \text{ coordinate plane}) \\ N = \frac{1}{b_2} - \frac{c_4}{r_2 b_2} T, & (P_N \text{ plane}) \end{cases}$$

Thus, a function describing  $P_N$  proportionally to the tumor population, could be defined as

$$g(T) \equiv \frac{1}{b_2} - \frac{c_4}{r_2 b_2} T$$

- Tumor cells:

$$\dot{T} = 0 \Rightarrow \begin{cases} T = 0, & (I - N \text{ coordinate plane}) \\ T = \frac{1}{b_1} - \frac{c_2}{r_1 b_1} I - \frac{c_3}{r_1 b_1} N, & (P_T \text{ plane}) \end{cases}$$

- Immune cells:

$$\dot{I} = 0 \Rightarrow I = \frac{s(\alpha + T)}{(c_1 T + d_1)(\alpha + T) - \rho T}, \quad (P_I \text{ plane})$$

as long as  $(c_1 T + d_1)(\alpha + T) \neq \rho T$ . The  $P_I$  plane has the form of a cylinder, parallel to the N-axis and it can be expressed proportionally to the tumor population by defining

$$f(T) \equiv \frac{s(\alpha + T)}{c_1 T(\alpha + T) + d_1(\alpha + T) - \rho T}.$$

The planes are depicted in Figure 1, given a specific set of parameter values.

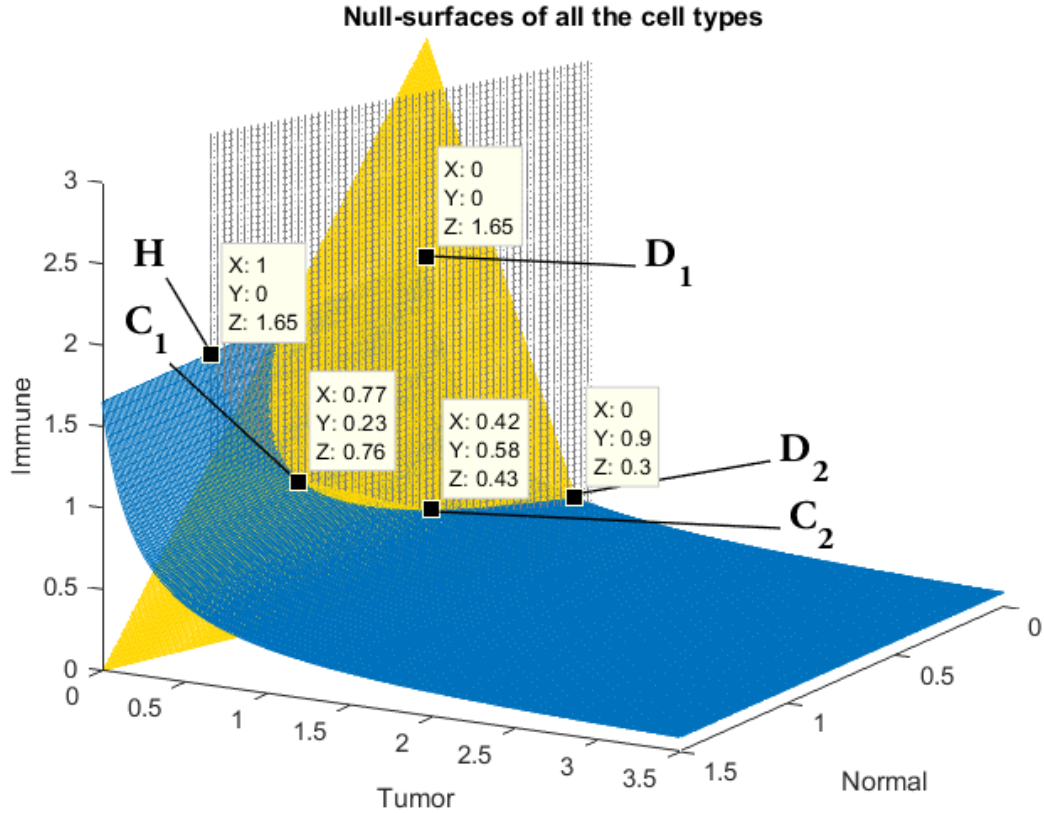


**Figure 1** – Plane surfaces corresponding to the cells’ populations recalculated and reevaluated in the present work.

The planes  $P_N, P_T, P_I$  as described above. The marked points correspond to equilibrium points. The healthy tumor-free point is marked as “H”, the two dead points are marked as “D1”, “D2” (indicating the absence of normal cells) and the two points where all three types of cells coexist are marked as “C1”, “C2”.

The types of the equilibrium points are divided into three categories:

- Tumor-free: A healthy organism, without any tumor cells. The equilibrium point has the form

$$\left( \frac{1}{b_2}, 0, \frac{s}{d_1} \right)$$

- Dead: An organism overwhelmed by cancer, leaving no room to normal cells, hence, the population of the latter is equal to zero. There are two types of these equilibria
  1. Tumor cells have died as well, producing the form  $(0, 0, s/d_1)$ .

2. Tumor cells have survived, producing the form  $(0, \alpha, f(\alpha))$ , where  $\alpha \geq 0$  and is a solution of

$$\alpha + \left(\frac{c_2}{r_1 b_1}\right) f(\alpha) - \frac{1}{b_1} = 0. \quad (3)$$

- Coexisting: Both normal and tumor cells' populations are positive and the equilibrium point is in the form

$$(g(b), b, f(b)),$$

where  $b \geq 0$  and  $b$  is a solution of

$$b + \left(\frac{c_2}{r_1 b_1}\right) f(b) + \left(\frac{c_3}{r_1 b_1}\right) g(b) - \frac{1}{b_1} = 0. \quad (4)$$

The optimal result for the mathematical model is to reach any equilibrium point which is tumor-free or coexisting with a trivial amount of tumor cells ( $b$  tends to zero and  $g(b)$  tends to one), since such a point would ultimately drive the mathematical model to a healthy state.

## Tumor-free equilibria

In order to reach a tumor-free equilibrium point (which is the mathematical model's ultimate goal), it has to be locally stable. To ensure that, the linearization of the equations around this point produces the mathematical model

$$\begin{bmatrix} \dot{N} \\ \dot{T} \\ \dot{I} \end{bmatrix} = \begin{bmatrix} r_2 - 2r_2 b_2 & -c_4 & 0 \\ 0 & r_1 - \frac{c_2 S}{d_1} - c_3 & 0 \\ 0 & \frac{\rho S}{d_1 \alpha} - \frac{c_1 S}{d_1} & -d_1 \end{bmatrix} \begin{bmatrix} N \\ T \\ I \end{bmatrix}$$

with eigenvalues

$$\lambda_1 = r_2 - 2r_2 b_2, \quad \lambda_2 = r_1 - \frac{c_2 S}{d_1} - c_3, \quad \lambda_3 = -d_1.$$

The condition for the tumor-free equilibrium to be stable is  $\lambda_1, \lambda_2$  and  $\lambda_3$  to have negative real parts, as control theory dictates. The death rate  $d_1$  is a positive constant, as presented in previous work [36], thus  $\lambda_3 < 0$ . Also, the normal cells' population is normalized, therefore  $b_2 = 1$ , making  $\lambda_1 < 0$ . Last but not least, for  $\lambda_2 < 0$  it is required that

$$r_1 < \frac{c_2 s}{d_1} + c_3.$$

The latter inequality sets a bound to the “resistance coefficient”  $(c_2 s)/d_1$ , which represents the efficiency of the immune system against the per capita growth rate of the tumor cells  $r_1$ . If the above condition is not met, the current mathematical model is pointless, since no amount of chemotherapy drug will be able to successfully combat the tumor. Such a mathematical model is presented in [78].

## Normal cells' dead equilibria

Following the same steps as above, it is easily proved that all Type 1 dead equilibria  $(0, 0, s/d_1)$  are always unstable. On the contrary, the stability of Type 2 dead equilibria  $(0, \alpha, f(\alpha))$  depends on the selection of the parameters, making them either stable or unstable. In any case, normal cells' dead equilibria are not a desired state and their analysis is not crucial.

## Coexisting normal and tumor cells equilibria

This sort of equilibria points occurs where all three planes  $P_N, P_T, P_I$  intersect, excluding coordinate planes. There are two points where these conditions are met and are presented in Figure 1. Further analysis of these equilibria needs to be done, since they are considered an intermediate state of the mathematical model towards the healthy state  $(1, 0, s/d_1)$ , should the treatment be successful.

The stability of the coexisting equilibria points, as previously mentioned, depends on the values of the parameters. Below is portrayed the relation between the stability of these points and the range of parameters  $s \in [0, 0.35]$  and  $\rho \in [0, 2]$ .

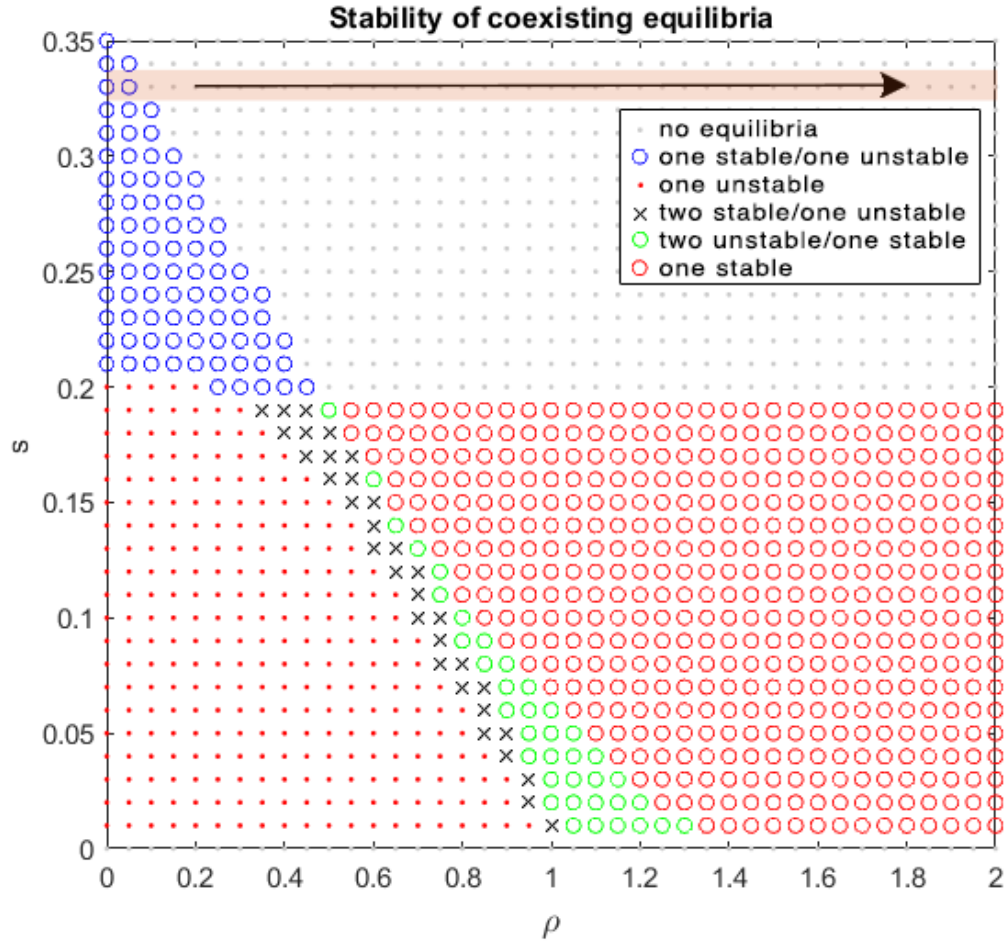


**Figure 2** – Stability of coexisting equilibria in relation to  $s$  and  $\rho$  reevaluated in the present work.

Each set of  $(\rho, s)$  values produces a different number and/or stability of coexisting equilibria points. The highlighted area refers to the analysis of figure 3, where  $s$  has a constant value of 0.33.

The surface  $\rho - s$  can be divided into regions, in order to make the distinction of the points clearer.

- Region 1 (grey dots) has no equilibria.
- Region 2 (blue circles) has one stable and one unstable equilibrium.

- Region 3 (red dots) has one unstable equilibrium.
- Region 4 (black x) has two stable and one unstable equilibrium.
- Region 5 (green circles) has two unstable and one stable equilibrium.
- Region 6 (red circles) has one stable equilibrium.

To further explain the nature of the equilibria, one of the variables is restricted to a constant value ( $s = 0.33$ ) and the other ( $\rho$ ) remains an element of the same set as previously. When  $\rho = 0.09$  all three populations transit from Region 2 to Region 1. Also, the value of  $b$  (i.e.  $T$ ) and therefore  $g(b)$  and  $f(b)$  defines the stability of the equilibrium. By examining the value of the derivative  $\dot{b}$  within an offset  $\dot{b}_{offset} = 0.01$ , it becomes clear that as long as the tumor population remains above a threshold,  $b_{thres} = 0.4103$ , the equilibrium point is stable, otherwise it is unstable.

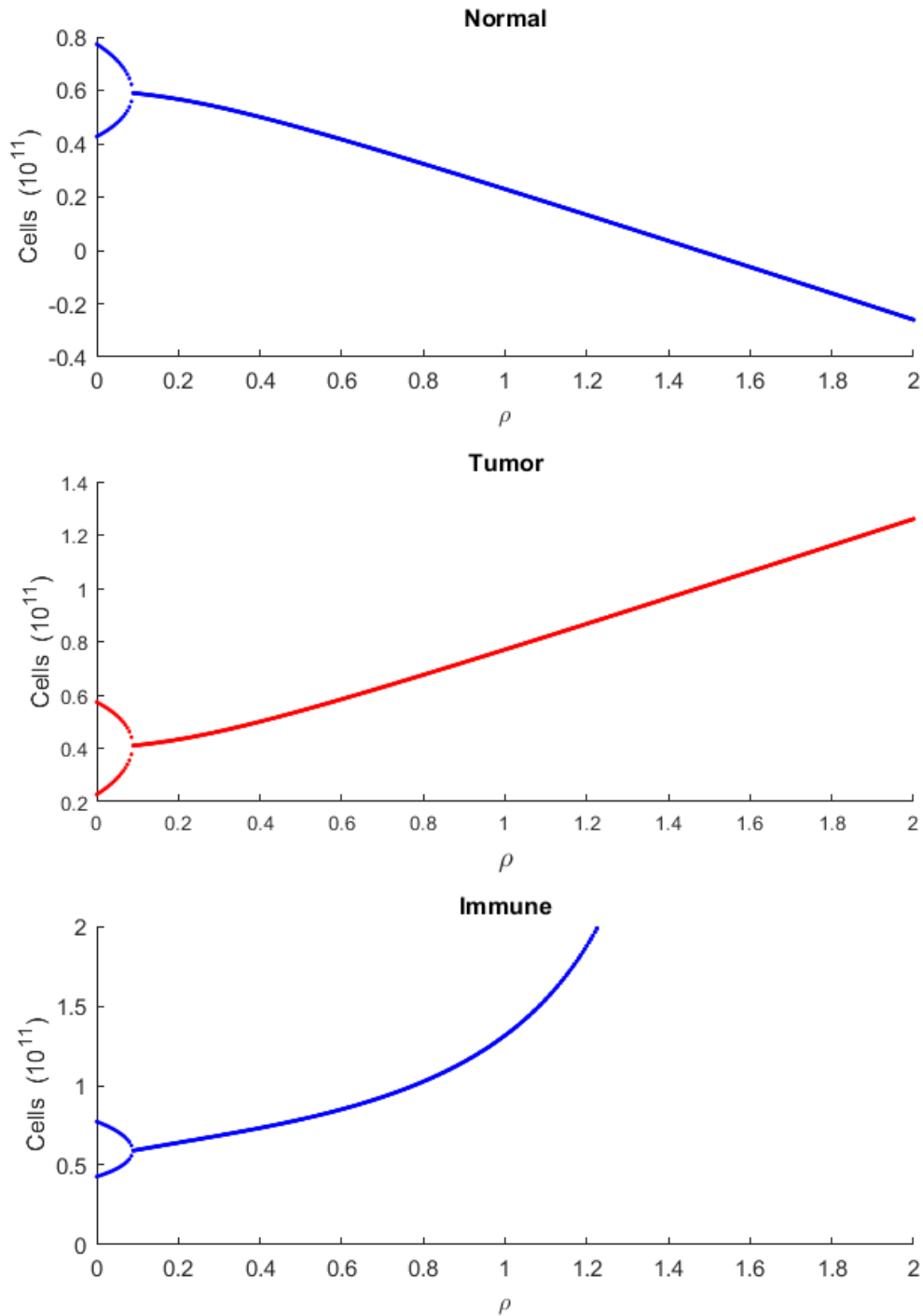


**Figure 3** – Normal, tumor and immune cell populations' evolution and stability recalculated in the present work.

As  $\rho$  starts increasing from zero, there are two possible states for each population, both of which are coexisting equilibria, followed by only one, which does not represent an equilibrium point. Immune cells' population is hidden for  $\rho > 1.25$  due to very high values. This progression is also highlighted with orange color in figure 2.

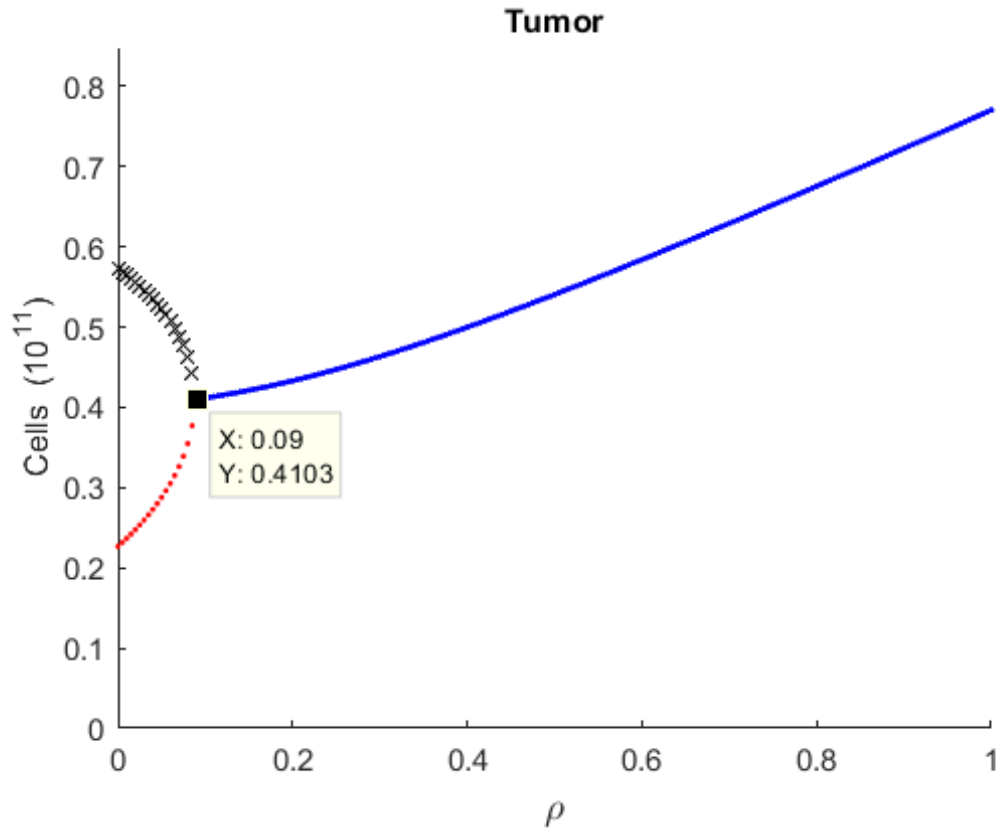


**Figure 4** – Tumor cells’ population and stability evolution and stability recalculated in the present work.

The threshold  $b_{thres} = 0.4103$  is shown, separating the stable from the unstable equilibria, as long as  $\rho < 0.09$ . When  $\rho$  exceeds that value, the mathematical model no longer has any equilibria.

It is evident that the mathematical model is very sensitive to the selection of  $\rho$ , the tumor response rate, and  $s$ , the steady source rate of immune cells to the tumor site, because a slight change in their values leads to different equilibria. In the final mathematical model, the values  $\rho = 0.01$  and  $s = 0.33$  were chosen, which place the mathematical model within Region 2.

## Numerical values of the parameters of the tumor growth mathematical model eq. (2)

The complete list of the parameters used are presented in the following table

$a_1 = 0.2$	$a_2 = 0.3$	$a_3 = 0.1$	$\alpha = 0.3$
$b_1 = 1.0$	$b_2 = 1.0$	$s = 0.33$	$\rho = 0.01$
$c_1 = 1.0$	$c_2 = 0.5$	$c_3 = 1.0$	$c_4 = 1.0$
$d_1 = 0.2$	$d_2 = 1.0$	$r_1 = 1.5$	$r_2 = 1.0$

The cells' units of all three populations ( $N, T, I$ ) have been rescaled, so that one unit is at the order of the carrying capacity of the normal cells at the cancerous area. There can be some variations, depending on the type of tumor, but a realistic number to consider is  $10^{11}$  cells per unit in the y axis [17]. As a result, all cell populations are normalized at the value of  $10^{11}$ . By assuming that healthy body tissue consists of  $10^8$  to  $10^9$  cells per  $cm^3$ , the normal cells' population at carrying capacity form an area with a diameter between 5.8 and 12.4  $cm$ . The purpose of each parameter in the mathematical model is analyzed further below.

- $a_i$  ( $L/mg$ ) : Fraction cell kill rate, representing how much each cell type is affected by chemotherapy. Cancerous cells are the main target, followed by immune and then normal cells, as a side effect. Thus  $a_2 > a_1 > a_3$ .
- $b_i$  ( $cells^{-1}$ ) : Carrying capacities for the proliferation of normal and tumor cells.
- $c_i$  ( $cells^{-1} * day^{-1}$ ) : Competition terms between cell types. Positive values indicate that normal and immune cells are destroyed once they encounter tumor cells and vice versa.
- $d_i$  ( $day^{-1}$ ) : Per capita death rates of normal cells and injected drug,  $d_1$  and  $d_2$  respectively.
- $r_i$  ( $day^{-1}$ ) : Per unit growth rates of tumor and normal cells. Time is normalized so that normal cells increase at a constant rate  $r_2 = 1$ . Cancerous cells are known to have a more aggressive behavior than healthy ones, which gives  $r_1 > r_2$ . There are types of cancer, however, where  $r_1$  can be smaller than  $r_2$ , [34][53].

- $s$  (*cells/day*) : Immune source rate, providing constantly the cancerous area with immune cells, in order to combat the tumor cells.
- $\alpha$  (*cells*) : Immune threshold rate, determining how fast the response of the immune system is. If the value of tumor cells' population  $T$  is equal to  $\alpha$ , the immune response rate is located at the half of its maximum value ( $\rho = 1.25$ ).
- $\rho$  ( $day^{-1}$ ) : Immune response rate, a term of high importance for the behavior of the mathematical model, ranging within a set of values  $(0, 2.5)$  [17]. Different values of the term reflect different states of the mathematical model. Figure 3 and Figure 4 show how all populations are affected by the choice of  $\rho$ . A low value of immune response rate, as in the current study ( $\rho = 0.01$ ), is interpreted as a weakened immune system, making the treatment process even more challenging.
- $v(t)$  ( $mg/m^2$ ) : Drug input at time  $t$ , proportional to the surface of the patient's body in  $m^2$ , calculated by the body surface area (BSA) formula. [25][32][50].
- $N(t)$  (*cells*) : Population of the normal cells, normalized at  $10^{11}$ .
- $T(t)$  (*cells*) : Population of the tumor cells, normalized at  $10^{11}$ .
- $I(t)$  (*cells*) : Population of the immune cells, normalized at  $10^{11}$ .
- $M(t)$  ( $mg/L$ ) : Drug concentration, proportional to the liters of plasma at the area of the tumor. The maximum value of this term ( $M_{max}$ ) determines the toxicity effects of the drug to the patient; therefore, it is crucial to keep the drug input to a minimum, yet effective, level. [25][32].

By applying these values to the normal, tumor and immune cells ( $N, T, I$ ) equations, the equilibria which occur are

- Two unstable dead equilibria, located at  $(0, 0, 1.65)$  and  $(0, 0.899244, 0.302268)$ .
- Two coexisting equilibria
  - one stable at  $(0.435204, 0.564796, 0.435204)$  and
  - one unstable at  $(0.763197, 0.236803, 0.763197)$ .
- One stable tumor-free equilibrium at  $(1, 0, 1.65)$ .

A tumor can be detected by clinical equipment as long as its radius is above  $1.2 \text{ mm}$  [52], which translates to approximately  $1.05 * 10^5$  cells. The experiments carried out in this study consider a large initial tumor population of  $T(0) = 0.25 * 10^{11}$  cells, a number within the detection limits of modern technology. It is important to note that the presence of such a tumor does not indicate that immuno-surveillance has failed to recognize it, but that the actions of the immune system alone are not enough to eliminate it. Also, the initial normal cells' population is  $N(0) = 1 * 10^{11}$ , considering the tumor has not started spreading yet and immune cells start at two possible values  $I(0) = 0.10 * 10^{11}$  and  $I(0) = 0.15 * 10^{11}$ , both of which indicate a weakened immune system. A numerical simulation of the mathematical model under the above conditions is executed in Figure 5.

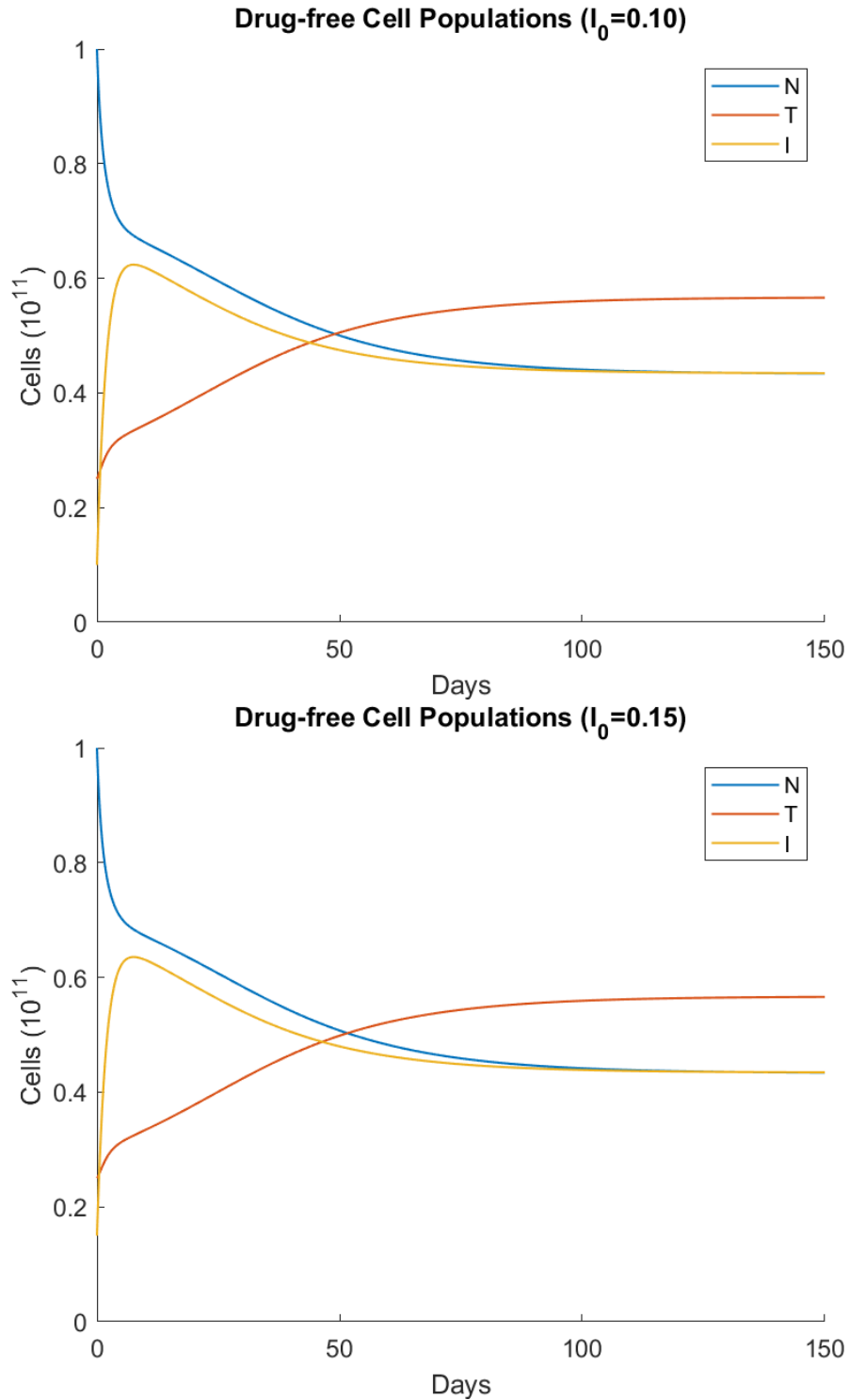


**Figure 5** – Drug-free mathematical model response for varying initial immune cells’ populations  $I_0$ , recalculated and reevaluated in the present work.

On the first figure, the initial immune cells’ population is  $I(0) = 0.10$  and on the second,  $I(0) = 0.15$ . Both cases are ineffective, resulting in a state where the tumor spreads and surpasses the population of normal and immune cells.

## Chapter 3 : Optimal cancer chemotherapy treatment based on the Direct Collocation method

---

The problem of finding an optimal solution of therapy to the presented mathematical model arises. In order to provide such a solution, the **Direct Collocation** (DirCol) method will be used. This method belongs to the family of transcription methods, alongside with shooting methods, and is a very effective non-linear programming (NLP) optimization technique [28][29][49][59]. It aims to simplify the complex calculations of the system equations' integrals by estimating the state and control values of the mathematical model, using a piecewise linear function of time for the control and piecewise continuous polynomials, of a certain degree, for the states. The values of the states and control at each point in the time domain (knot point) are the decision variables. The concept is to correlate these polynomials with a second set of points in the time domain (collocation points) and to enforce them to satisfy the dynamics of the mathematical model at the collocation points. Consequently, the differentiations and any other calculations involved are replaced by algebraic equations, which require less computational power, thus the time of execution is significantly reduced. Moreover, collocation methods are suitable for problems with state constraints, as is the one presented in this study. The behavior of each collocation method relies on the way the state and control variables are discretized and how the dynamic constraints are satisfied [47]. In this chapter a treatment regimen based on the DirCol method is proposed.

### The Direct Collocation (DirCol) method

**Direct Collocation** methods are categorized according to the choice of polynomials which represent the state dynamics, the method of numerical integration (quadrature) of the cost function and the state propagation scheme, producing the correlated non-linear programming method. The above three main components are further analyzed below:

1. Piece-wise polynomial for state and control: The selection of the polynomial is of high importance. For states, as in the current analysis, piecewise cubic polynomials produce good results. However, depending on the specific problem domain, some methods may be preferred over another. For example, in the trajectory optimization of a robot's gait, Bezier polynomials are used, while in the determination of wave functions of electrons, Legendre polynomials are more common.
2. Integrating method of the cost function: Cost function, in most cases, is defined as an integral term that depends on the entire trajectory. Quadrature, the process of constructing a square with an area equal to that of a figure bounded by a curve, is then used to calculate the integral at each timestep. Therefore, the integration process is converted to a summation, using fewer intermediate values. The manner in which quadrature is performed produces different results [44].
3. Propagation method: In order to represent the mathematical model, the states in each timestep must be propagated to the next one, which is achieved by writing the equations of the mathematical model dynamics in either integral or derivative form. In the first case, the state trajectory must match the integral of the dynamics with respect to time ( $x(t) = \int f(x(t), u(t)) dt$ ). In the second, the derivative of the current state with respect to time must be equal to the dynamics function ( $\dot{x}(t) = f(x(t), u(t))$ ). The derivative is estimated at the segment's midpoint, using the state and dynamics values at knot points. The midpoint is chosen for differentiation, because for a cubic polynomial with fixed end points (value and derivative), the derivative is farthest away from either of the end points' derivatives. It is important to note that, for a cubic polynomial, once the derivatives and state values are defined at a segment, the cubic is completely defined in the corresponding segment, thus the values at midpoint can be changed only if the state values and their derivatives also change.

The above steps are repeated, until a feasible solution is found. In each iteration, the direct collocation method attempts to minimize the error between the mathematical model's dynamics and state variables' derivatives at the collocation points, which occur from polynomial differentiation. That error tends to zero with only a few iterations. Additionally, there is a divergence between the optimal control and the control obtained from direct collocation, which is greatly reduced when the time domain is divided in additional segments. Therefore, the solution becomes more accurate. Below, a specific direct collocation method, called Hermite-Simpson collocation method, is presented and is, afterwards, applied for optimal control.

## The Hermite-Simpson Collocation method

A basic form of collocation is the **Hermite-Simpson Collocation** method [23], illustrated in Figure 6. For each segment of time  $[t_k, t_{k+1}]$  the two knot points (denoted as blue dots) represent the state and control NLP variables, which correspond to  $[x_k, u_k, x_{k+1}, u_{k+1}]$ . The dynamics of the mathematical model are used to provide time derivative values at the two knot points, so the four datasets  $[x_k, x_{k+1}, f(x_k, u_k), f(x_{k+1}, u_{k+1})]$  can be used to generate a third-order Hermite interpolation polynomial (cubic spline), which satisfies the equations of the mathematical model only at the knot points  $t_k, t_{k+1}$ , but not at any other given time within  $(t_k, t_{k+1})$ . Let  $[x_c, u_c]$  be the state and control at  $t_c$ , the middle point of  $[t_k, t_{k+1}]$ ; the collocation point (red diamond). By enforcing  $\Delta = \dot{x}_c - f(x_c, u_c) = 0$  it is possible to have a polynomial that not only satisfies the dynamics at the two knot points but also does that at the collocation point. If a large number of segments is used, the approximation of the state approaches the real dynamics throughout the whole time domain (see **Appendix 1** for further details). Moreover, this method is based on the hypothesis that the dynamics and control are quadratic, which is true for the states of the current mathematical model.

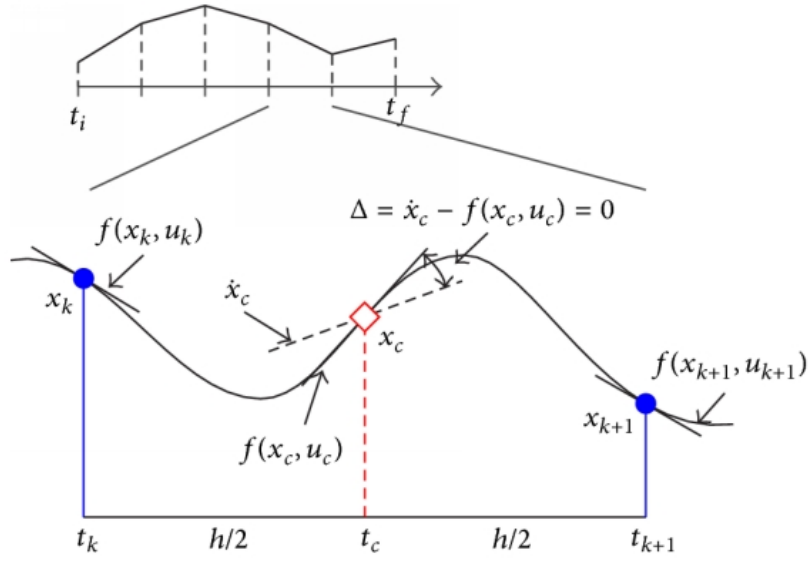


**Figure 6** – Hermite-Simpson collocation method.

A time segment of the algorithm, where  $t_k, t_{k+1}$  are the knot points and  $t_c$  is the collocation point. If  $\Delta$  is enforced, the dynamics  $f(x, u)$  apply to the collocation point as well, not only to the knot points. Figure taken from [57].

## Formulation of the problem

After having thoroughly examined the mathematical model and the algorithm which will be used, it is time to add the effects of chemotherapy, in order to formulate an optimal administration protocol for the treatment. The goal is to determine the quantity of drug that should enter the mathematical model and the exact day it should be done, so that the tumor will be eradicated by the end of the chemotherapy. For brevity, the four states of the mathematical model and the drug input will be denoted as

$$\{x_1, x_2, x_3, x_4\} = \{N, T, I, M\},$$

$$u = v.$$

The optimal control problem of treatment for the mathematical model of this analysis can be expressed as an objective function  $J$  which must be minimized by the final time  $t_f$ , subject to the states

$$\dot{x} = f(x, u) = \begin{bmatrix} \dot{x}_1 \\ \dot{x}_2 \\ \dot{x}_3 \\ \dot{x}_4 \end{bmatrix} = \begin{bmatrix} r_2 x_1 (1 - b_2 x_1) - c_4 x_2 x_1 - a_3 (1 - e^{-x_4}) x_1 \\ r_1 x_2 (1 - b_1 x_2) - c_2 x_3 x_2 - c_3 x_2 x_1 - a_2 (1 - e^{-x_4}) x_2 \\ s + \frac{\rho x_3 x_2}{\alpha + x_2} - c_1 x_3 x_2 - d_1 x_3 - a_1 (1 - e^{-x_4}) x_3 \\ u - d_2 x_4 \end{bmatrix},$$

with initial conditions  $x(0) = x_0$ , the control input (drug)  $u$  and the following constraints

$$u_{min} \leq u \leq u_{max}, \quad x_{min} \leq x \leq x_{max},$$

where  $u_{min} = 0$  and  $x_{max} = \infty$ , because the amount of drug input cannot be negative and the saturation point of the states is embedded in the growth terms of the above eq. (2).

As long as the lower bound  $x_{min}$  is concerned, the constraint of keeping the normal cells' population at a healthy level is depicted, so that rehabilitation of the organism can be achieved after the tumor has been confronted. A robust organism is one which maintains the population of normal cells at levels above 75% of its carrying capacity, throughout the entire process [17][18]. All cell populations have been normalized in such a manner ( $10^{11}$ ), so that the carrying capacity of normal cells is 1 ( $b_2 = 1$ ) for the presented mathematical model, therefore, the above constraint is expressed as the following lower bound

$$x_1(t) \geq x_{1min}(t) = 0.75, \quad t \in [0, t_f].$$

The rest of the cell populations (tumor, immune) and drug concentration are considered non-negative quantities, thus

$$x_{min} = \begin{bmatrix} 0.75 \\ 0 \\ 0 \\ 0 \end{bmatrix}.$$

An additional constraint is set for the previous issue, but this time from the perspective of the input. High toxicity levels in the tumor area are prevented, by setting an upper bound to the amount of drug administered each day, which is translated to

$$u \leq u_{max} = 1, \quad t \in [0, t_f].$$

Primal studies have presented objective functions, which focus only on the tumor size at final time  $x_2(t_f)$  and later evolved, by including the total tumor population  $\int_0^{t_f} x_2(t) dt$ ,

the maximum value it could reach  $\max x_2(t)$  and weights  $w_1, w_2, w_3$ , for each of those terms accordingly, indicating the degree of their impact. In this study, the objective function is further evolved, including the total amount of drug given  $v_{total} = \sum_{t=0}^{t_f} v(t)$ , with a corresponding weight  $w_4$ , making the approach more cost-efficient. Final time  $t_f$  is set to 150 days, approximating the four to six months chemotherapy usually lasts. The resulting objective function weighted by  $w_1 = 1500$ ,  $w_2 = 150$ ,  $w_3 = 1000$ ,  $w_4 = 40$  is

$$J(u) = w_1 * x_2(t_f) + w_2 * \int_0^{t_f} x_2(t)dt + w_3 * \max_{t \in (0, t_f)} x_2(t) + w_4 * v_{total}.$$

## The Bang-Bang conversion of the Direct Collocation method

By executing simulations with the above approach, the final results are very satisfying, since the main goal, which is the tumor eradication, is achieved and at the same time, the healthy tissue is not critically damaged, allowing the normal cells to rebuild their population and return to the desired healthy level. However, a practical matter arises. Optimal control dictates that drug should be administered in a daily basis, even though a number of days the amount of drug is trivial, making it very difficult for patients to be present every day at the place of administration e.g. hospital, continuously, for a period of five months ( $t_f = 150$ ). Thus, a slight modification to the regimen is required, keeping the current results as guidelines.

The solution is to force the regimen to have a bang-bang style, by finding a threshold for the drug input  $u_{th}$  and maximize or set to zero all values above or below that, respectively. In other words

$$u_{bb}(t) = \begin{cases} u_{max}, & u(t) \geq u_{th} \\ 0, & u(t) < u_{th} \end{cases},$$

where  $u_{max} = 1$ ,  $u(t)$  is the drug dosage as DirCol dictates and  $u_{bb}(t)$  is the converted drug dosage, on day  $t$ . The threshold value has derived from a number of experimental simulations and aims to force the bang-bang approach use the same amount of drug as in DirCol, so that the effectiveness of these methods can be compared clearly.

## Simulation results of the application of the determined treatment by using the Hermite-Simpson Collocation method and its modified Bang-Bang approach

In the following section, the simulations for the above control method are presented. As originally mentioned, there are two cases, each one starting from different populations of immune cells  $x_3(0) = 0.10$  (case 1) and  $x_3(0) = 0.15$  (case 2). The initial values for the populations of the tumor and normal cells are  $x_2(0) = 0.25$  and  $x_1(0) = 1$  in both cases, while the desired final values are  $\{x_1(t_f), x_2(t_f), x_3(t_f)\} = \{1, 0, 1.65\}$ , which correspond to the tumor-free equilibrium, as discussed in Chapter 2. The drug concentration starts at a zero value  $x_4(0) = 0$ , considering that this is the first treatment of the patient or a considerable amount of time has passed since his last one, and the desired final value is again zero  $x_4(t_f) = 0$ , indicating that the tumor has been eradicated at some point before the period of  $t_f = 150$  days ends. The aim is to generate a schedule which will be effective against the tumor, gentle with normal cells and economic for production.

For clarity, the previous notation  $\{N, T, I, M\}$  is used for the states and  $\{v\}$  for the control input in the following diagrams. The tool which implements the direct collocation method is “**OptimTraj**” by M.P. Kelly [30], the segments for the Hermite-Simpson method are 149 and the iterations’ limit is set to 50, the combination of which yields very efficient results, as seen below. All cell populations are normalized at the value of  $10^{11}$  *cells* which corresponds to the normalized cells’ population value 1 (one). The drug concentration and drug input dosage are measured in *mg* per *liter* of blood plasma in the tumor area and *mg* per  $m^2$  of the patient’s body surface, respectively.

### Case 1 : Highly weakened immune system, $I_0 = 0.10$

Starting with case 1, the DirCol simulation results for the states (cell populations  $N, T, I$ ) and the control (drug input  $v$ ) are the following

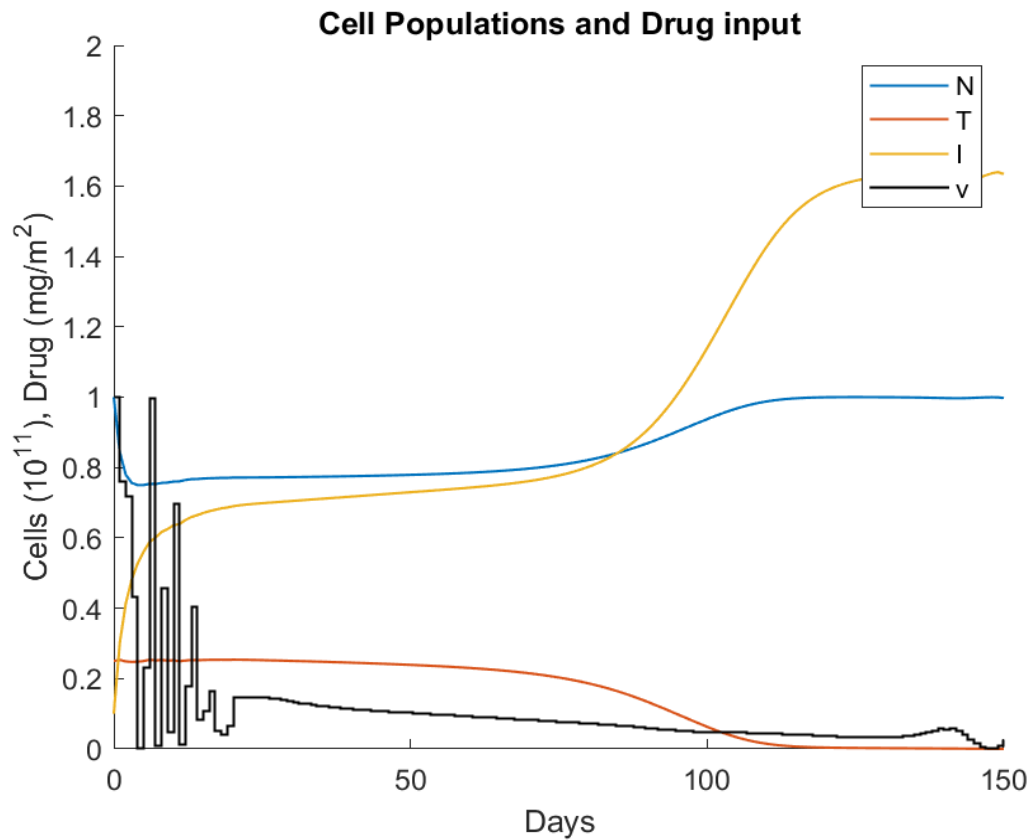


**Figure 7** – Cell populations and drug input for DirCol treatment (case 1).

The treatment is effective with a total drug administration of  $15.8379 mg/m^2$ . The eradication of the tumor is achieved on and the  $t_{zero} = 118$ th day.

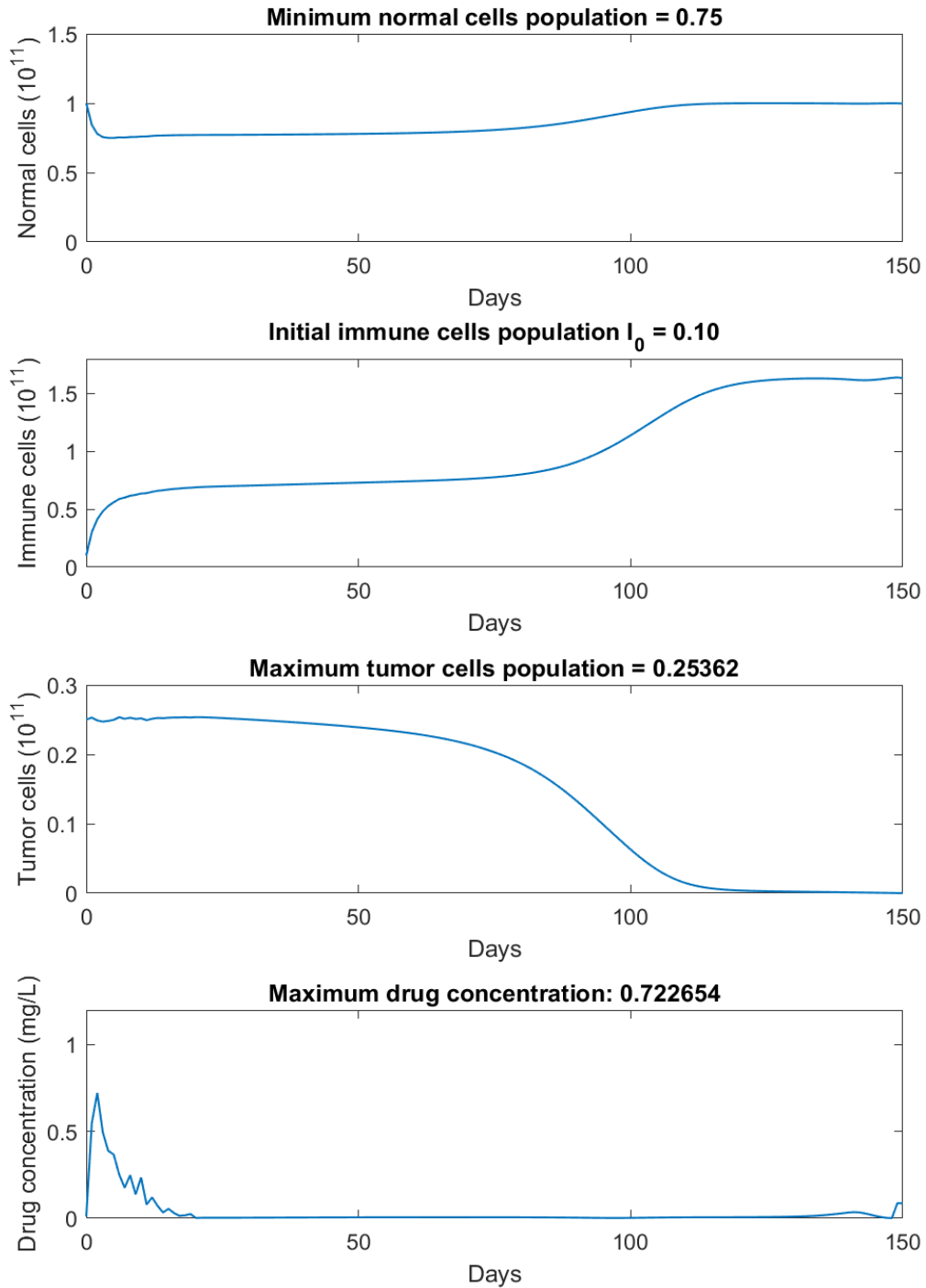


**Figure 8** – Maximum/minimum state values for DirCol treatment (case 1).

The constraint of  $N_{min} \geq 0.75$  is satisfied, while at the same time tumor cells do not increase noticeably, compared to their initial value  $T(0) = 0.25$ . Drug concentration, after an initial increase, remains at trivial levels.

By converting the above data to a bang-bang regimen, following the ruleset presented in the previous section, with a threshold  $v_{th} = 0.1455 \text{ mg/m}^2$ , the results for the states (cell populations  $N, T, I$ ) and the control (drug input  $v$ ) are the following

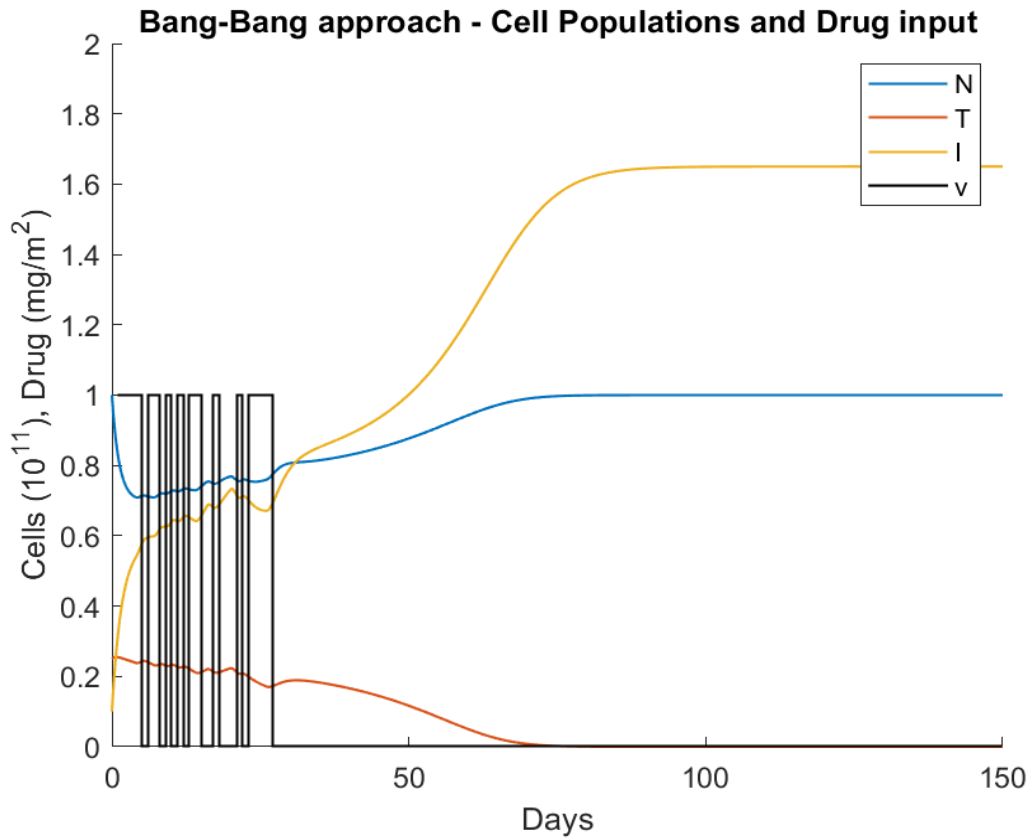


**Figure 9** – Cell populations and drug input for bang-bang conversion (case 1). The treatment is effective with a total drug administration of  $16 \text{ mg/m}^2$ . The eradication of the tumor is achieved on and the  $t_{zero} = 72$ th day.

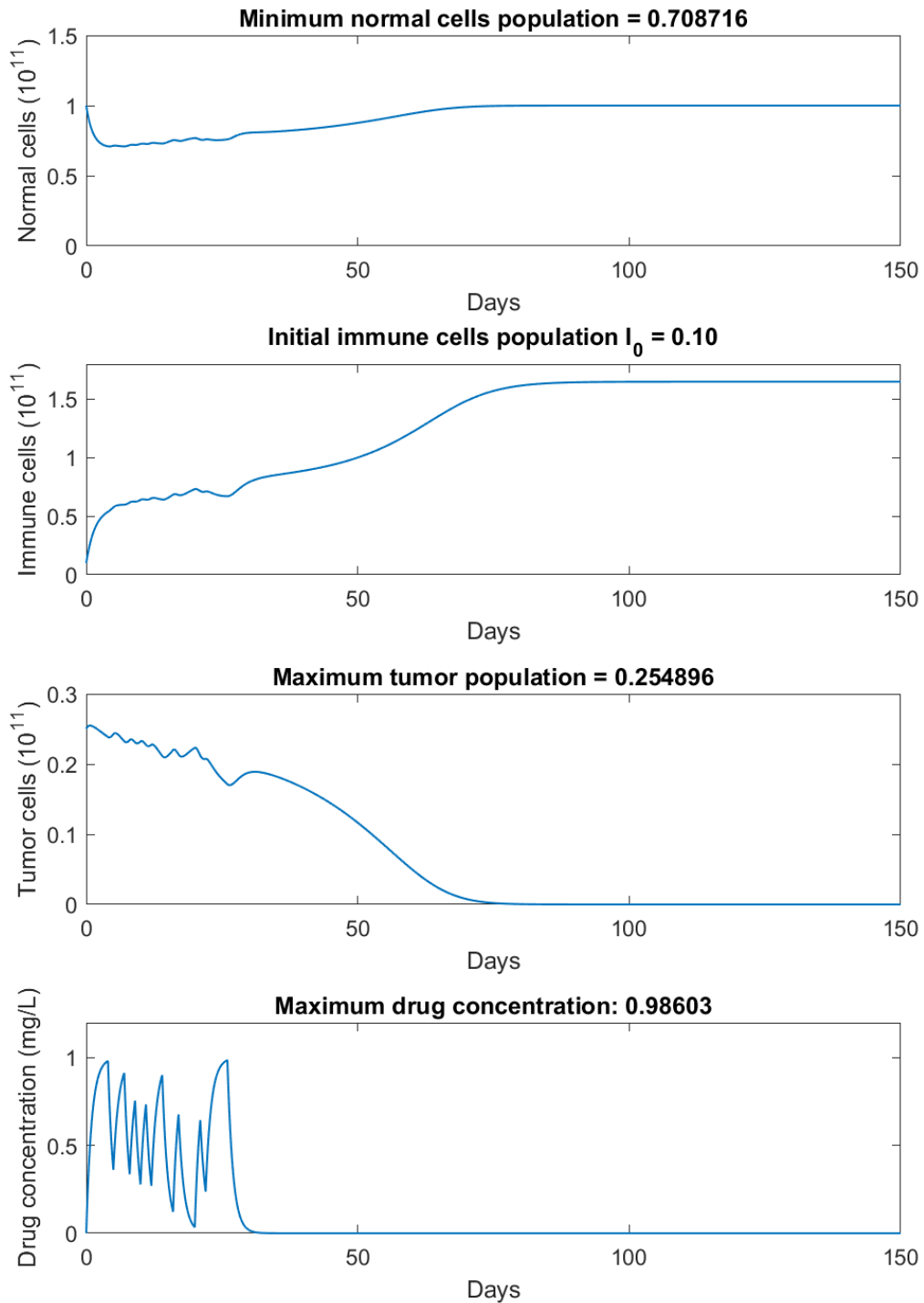


**Figure 10** – Maximum/minimum state values for bang-bang conversion (case 1).

The constraint of  $N_{min} \geq 0.75$  is not satisfied, however it is close to that value and the tumor is countered effectively. Drug concentration has a few peaks at the beginning and then drops to zero.

## Case 2 : Less weakened immune system, $I_0 = 0.15$

Continuing with case 2, the DirCol simulation results for the states (cell populations  $N, T, I$ ) and the control (drug input  $v$ ) are the following

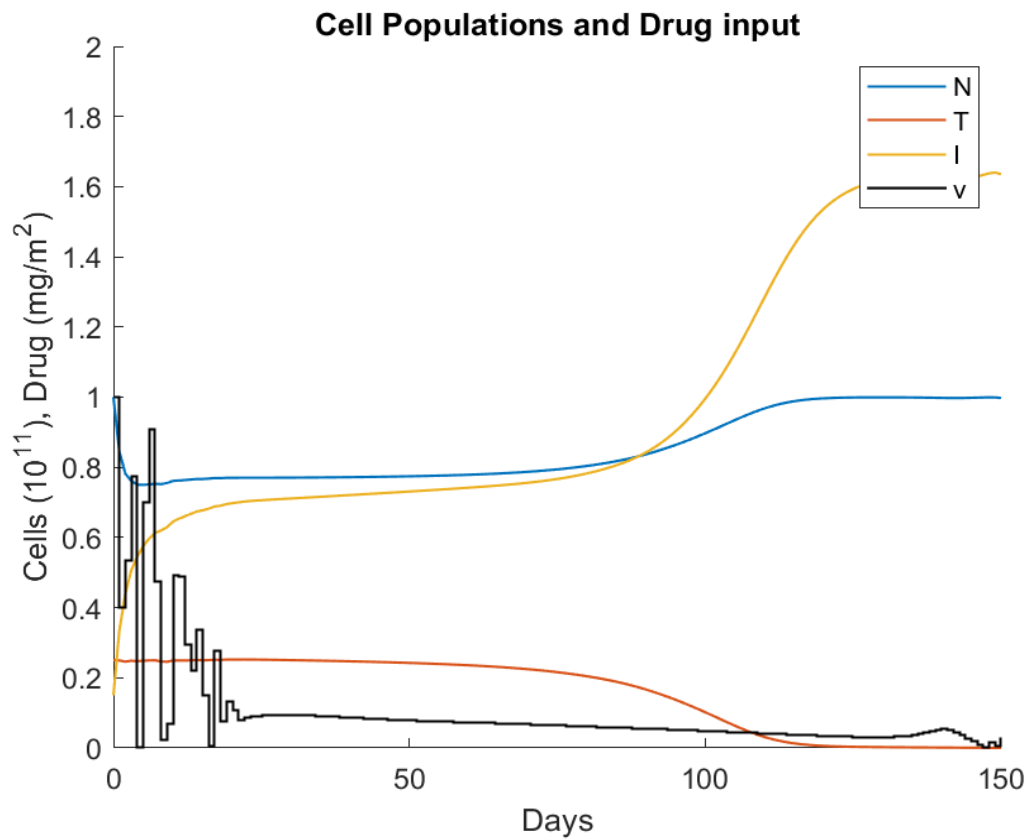


**Figure 11** – Cell populations and drug input for DirCol treatment (case 2).

The treatment is effective with a total drug administration of  $14.9764 \text{ mg}/m^2$ . The eradication of the tumor is achieved on and the  $t_{zero} = 122$ th day.

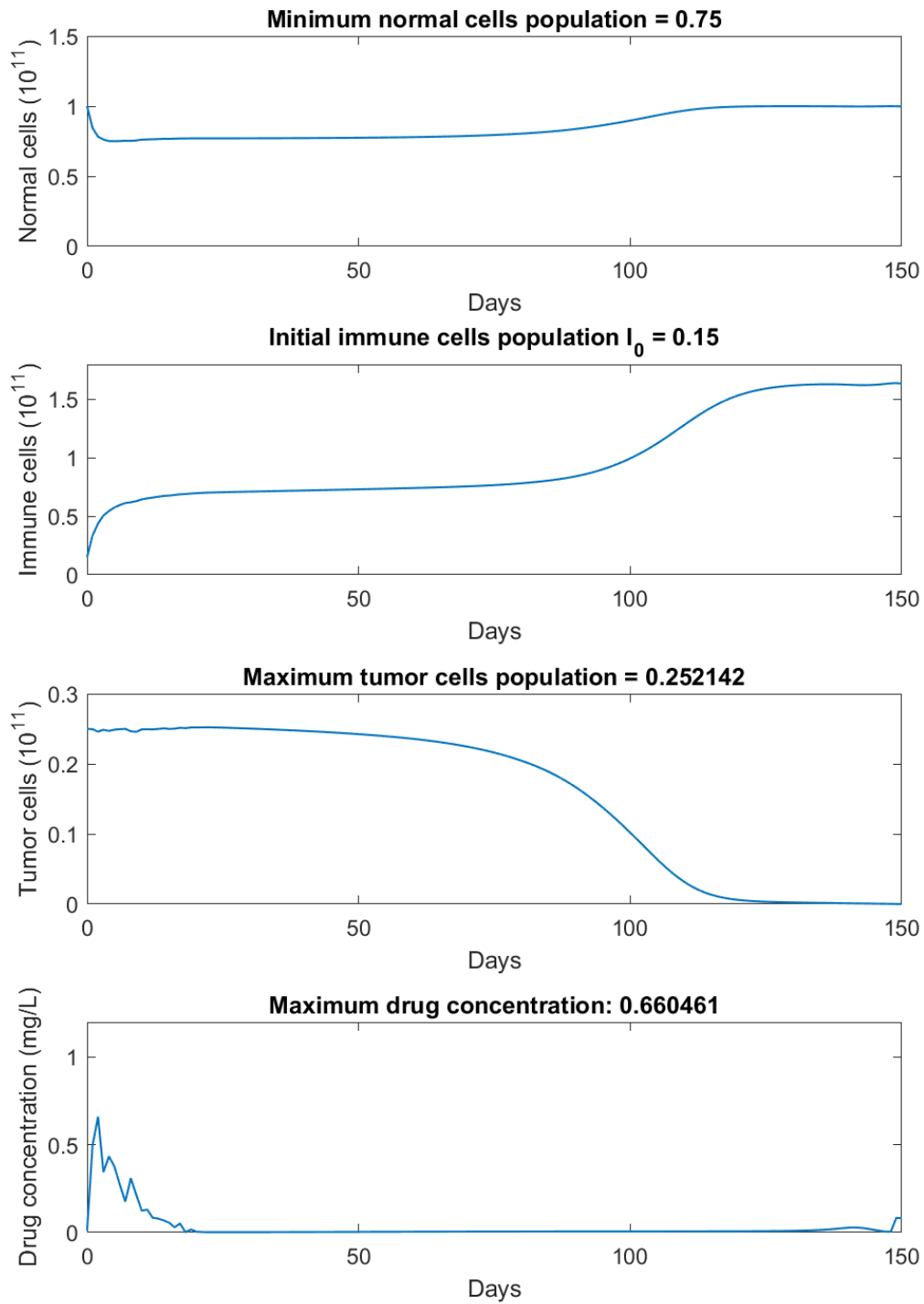


**Figure 12** – Maximum/minimum state values for DirCol treatment (case 2).

The constraint of  $N_{min} \geq 0.75$  is satisfied, while at the same time tumor cells do not increase noticeably, compared to their initial value  $T(0) = 0.25$ . Drug concentration, after an initial increase, remains at trivial levels.

Again, the above data are converted to a bang-bang regimen, which has a threshold  $v_{th} = 0.12 \text{ mg/m}^2$ . The results for the states (cell populations  $N, T, I$ ) and the control (drug input  $v$ ) are the following

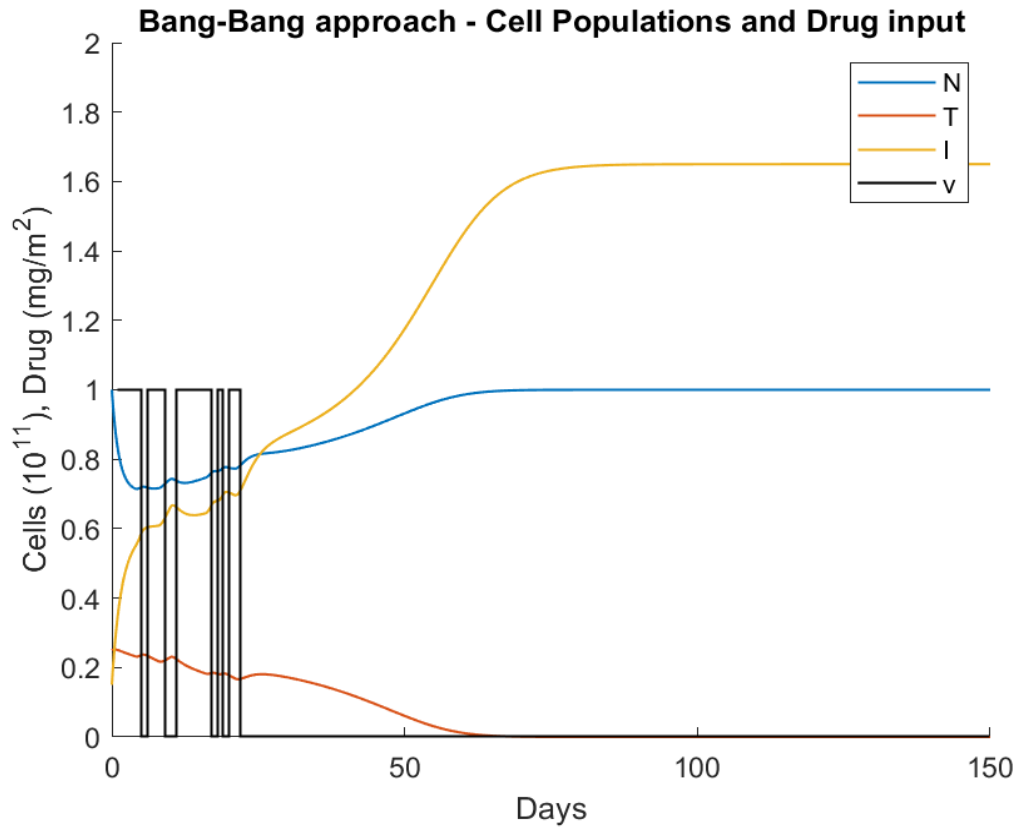


**Figure 13** – Cell populations and drug input for bang-bang conversion (case 2). The treatment is effective with a total drug administration of  $15 \text{ mg/m}^2$ . The eradication of the tumor is achieved on and the  $t_{zero} = 63$ th day.

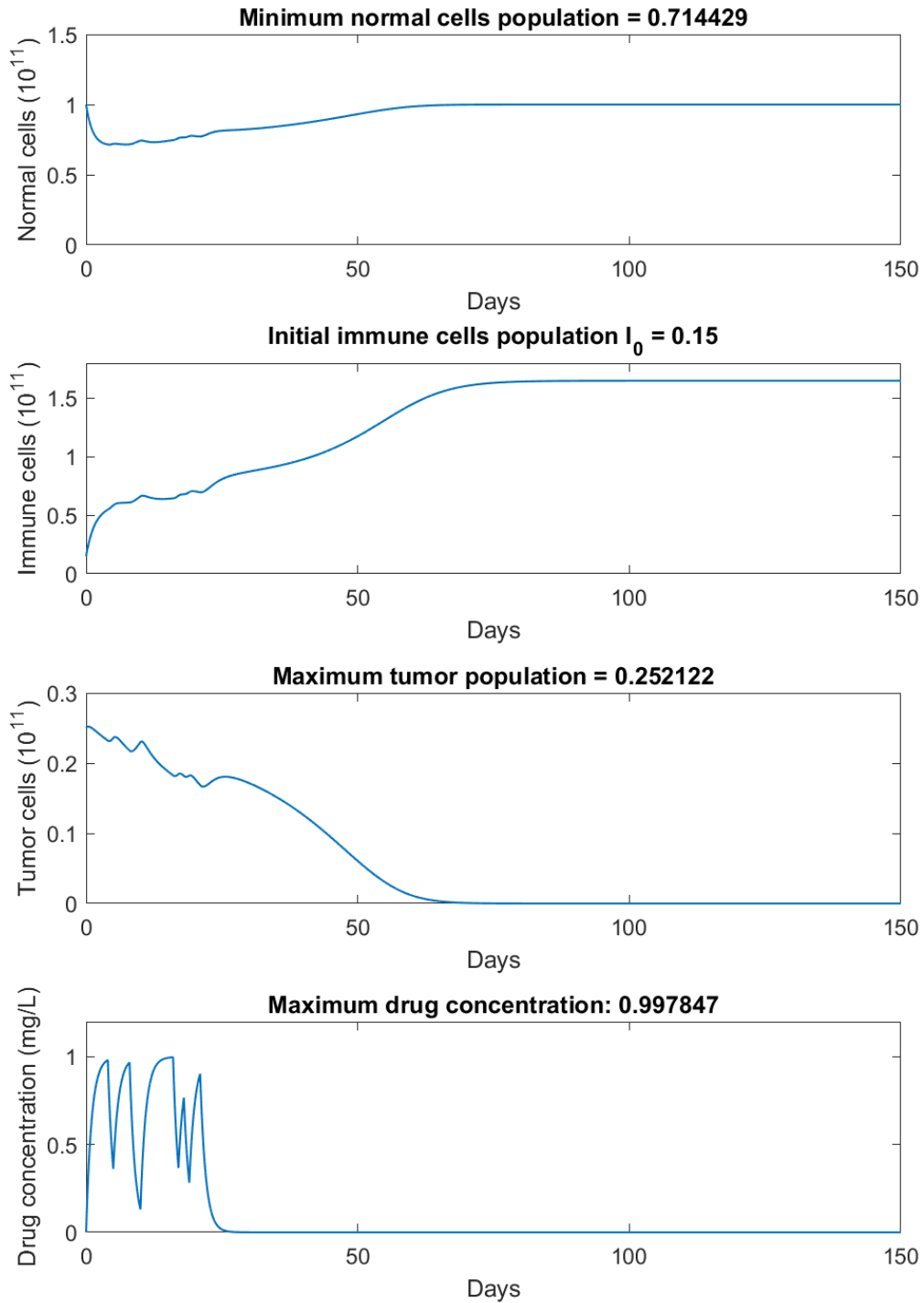


**Figure 14** – Maximum/minimum state values for bang-bang conversion (case 2).

The constraint of  $N_{min} \geq 0.75$  is not satisfied, however it is close to that value and the tumor is countered effectively. Drug concentration has a few peaks at the beginning and then drops to zero.

A **synopsis** of the simulations' final data is presented in the table below. The variables of particular interest are:

- $I_0$  ( $cells * 10^{11}$ ): initial immune cells' population.
- $N_{min}$  ( $cells * 10^{11}$ ): minimum normal cells' population.
- $T_{max}$  ( $cells * 10^{11}$ ): maximum tumor cells' population.
- $M_{max}$  ( $mg/L$ ): maximum drug concentration.
- $v_{total}$  ( $mg/m^2$ ): total amount of administered drug.
- $v_{th}$  ( $mg/m$ )<sup>2</sup>: threshold for DirCol to Bang-Bang conversion.
- $t_{zero}$  ( $day$ ): day of tumor eradication ( $T(t_{zero}) < 0.005$ , practically 0).

**Table 1:** DirCol treatment results.

	Case 1		Case 2	
	DirCol	Bang-Bang	DirCol	Bang-Bang
$I_0$	0.10		0.15	
$N_{min}$	0.75	0.708716	0.75	0.714429
$T_{max}$	0.25362	0.254896	0.252142	0.252122
$M_{max}$	0.722654	0.98603	0.660461	0.997847
$v_{total}$	15.8379	16	14.9764	15
$v_{th}$	0.1455		0.12	
$t_{zero}$	118	72	122	63

To begin with, the main difference which is noted concerns the case selection. When  $I_0$  is low, in the first case, the amount of drug suggested ( $15.8379 \text{ mg/m}^2$ ) is slightly higher than the amount suggested in the second case ( $14.9764 \text{ mg/m}^2$ ). That can be explained, since the immune system is more fatigued and cannot combat the tumor to the same extent, thus it demands an additional aid, i.e. drug, in order to achieve the desired results.

Moving on, the DirCol and Bang-Bang approaches diverge in most results. As far as the lower bound of normal cells  $N_{min}$  is concerned, DirCol manages to satisfy it in both cases, but Bang-Bang does not. That does not translate to ineffectiveness of the latter, since Bang-Bang suggests that all of the drug must be given at the early days, a fact confirmed by the increase in maximum drug concentration  $M_{max}$ . On the other hand, DirCol proposes a smoother regimen, with a significant amount of drug being administered during the initial days, followed by smaller amounts throughout the entire treatment period. Therefore, the side effects of the drug can be seen clearly now, due to which  $N_{min}$  has a lower value when the drug concentration in the tumor area is higher. Ultimately, the differences between these two methods have an obvious impact on the swiftness of the treatment, making DirCol 1.6-2 times slower than Bang-Bang, when the day of tumor eradication  $t_{zero}$  is compared.

Last but not least, all of the above cases present a peak value in the tumor cells' population which is very close to the initial  $T(0) = 0.25$ . This value indicates the efficacy of the treatment regimens, because there is no further increase of an already notably sized tumor. However, Bang-Bang is preferred, due to practicality issues, as previously discussed.

## Chapter 4 : Optimal cancer chemotherapy treatment based on the State-Dependent Riccati Equation (SDRE) optimal non-linear control method

---

The optimal control problem of dynamical mathematical models has been studied in depth for a given cost function to be minimized and is well-established for Linear Time Invariant (LTI) mathematical models, subjected to linear quadratic functions. In most cases, the solution of Algebraic Riccati Equations (ARE) yields enough information to compute the optimal feedback gain(s). Hence, the stabilization problem of LTI mathematical models, which is known as Linear Quadratic Regulator (LQR), is solved in optimal way.

On the other hand, the above approach cannot be generally applied to non-linear mathematical models, because Hamilton Jacobi Bellman (HJB) equations do not yield straightforward solutions. Analytical solutions for the optimal control may be obtained for only a few restricted cases, since the control equations for optimality are also non-linear and their solutions should satisfy the state conditions. Moreover, numerical solutions for the optimal control cannot be obtained with precision, due to the unknown number of possible candidates for the optimal solution. This issue has forced researchers to form approximate solutions to the HJB equation, which are suboptimal to the optimal control problem of non-linear dynamical mathematical models.

One of these approaches is the State-Dependent Riccati Equation (SDRE) technique. This method presents a systematic way of designing non-linear feedback controllers that approximates the solution of the infinite time horizon optimal control problem and is described in detail in **Appendix 2**, as well as [6][10][42][65]. Firstly, the non-linear mathematical model is converted to a pseudo-linear mathematical formulation of a non-linear dynamics mathematical model, also referred to as extended linear form, in which it is treated as a sequence of LTI mathematical models. Afterwards, the suboptimal solution is computed via solving the ARE for the LTI mathematical models obtained in each time step.

Over the past decade, SDRE has become very well-known within the control community, providing a very effective algorithm for implementing non-linear feedback controllers, including non-linearities in the mathematical model's states, and offering great design flexibility through its state-dependent weighting matrices. Moreover, SDRE gives the time responses of the non-linear mathematical model in real time, making it feasible to be implemented on-line by using microprocessors with adequate computational power in the controller structure. As a result, it has been applied successfully to non-linear mathematical models both in theory and in experimental practice [3][41][65][76]. Among the various applications of SDRE optimal control, control of drug administration in cancer dynamics is also included [3][41]. In this chapter, that application will be extended further, by adding a periodic character of active and inactive days to the control input, introducing a periodic SDRE drug administration.

## Pseudo-linear state space equations formulation

In this section, the mathematical model's equations presented in eq. ( 2 ) will be converted to a pseudo-linear mathematical model, which will later allow the SDRE technique to find an optimal solution for the drug input (for more detail see **Appendix 2**). Therefore, the non-linear mathematical model can be represented as

$$\dot{\underline{x}}(t) = f(\underline{x}(t)) + G(\underline{x}(t))u(t), \quad \underline{x}(0) = \underline{x}_0, \quad (5)$$

where  $\underline{x} \in \mathbb{R}^n$  is the state vector and  $u \in \mathbb{R}^m$  is the input vector. The above mathematical model can be written in the pseudo-linear form

$$\dot{\underline{x}} = A(\underline{x})\underline{x} + B(\underline{x})u, \quad (6)$$

where  $f(\underline{x}) = A(\underline{x})\underline{x}$ ,  $A(\underline{x}) \in \mathbb{R}^{n \times n}$  and  $G(\underline{x}) = B(\underline{x})$ ,  $B(\underline{x}) \in \mathbb{R}^{n \times m}$ . The  $A(\underline{x})$  and  $B(\underline{x})$  are called state-dependent coefficient (SDC) matrices and their role is to transform the mathematical model in eq. ( 5 ) into a linearized form. There are many alternative parameterizations to choose from when constructing the SDC matrices, but the one which

will be chosen must ensure pointwise controllability, in order to apply the SDRE control law [42]. That can be achieved if the state-dependent controllability matrix

$$M(\underline{x}) = [B(\underline{x}) \quad A(\underline{x})B(\underline{x}) \quad \cdots \quad A^{n-2}(\underline{x})B(\underline{x}) \quad A^{n-1}(\underline{x})B(\underline{x})]$$

has full rank for the time segment where the control is applied to the mathematical model.

Moving on to the control strategy, SDRE attempts to determine the sub-optimal controller of the mathematical model in eq. ( 6 ), in order to minimize to cost function

$$J = \frac{1}{2} \int_0^{\infty} (\underline{x}^T Q(\underline{x}) \underline{x} + u^T R(\underline{x}) u) dt,$$

where  $Q(\underline{x}) \in \mathbb{R}^{n \times n}$  and  $R(\underline{x}) \in \mathbb{R}^{m \times m}$  are state-dependent matrices and determine the weight of each state and the control, thus  $Q(\underline{x}) \geq 0$  and  $R(\underline{x}) \geq 0$  for  $\forall \underline{x}$  [48]. Some optimal control problems require constraints on the mathematical model states and/or control input to be satisfied, as the current is concerned with drug toxicity and the normal cells' minimum population. Satisfying such requirements heavily depends on the proper selection of the matrices  $Q(\underline{x})$  and  $R(\underline{x})$  for the optimal control problem. Another approach is introducing hard bounds on the control input by penalizing the Hamiltonian [5]. The Hamiltonian for the optimal control problem is given by

$$H(\underline{x}, u, \lambda) = \frac{1}{2} (\underline{x}^T Q(\underline{x}) \underline{x} + u^T R(\underline{x}) u) + \lambda^T (A(\underline{x}) \underline{x} + B(\underline{x}) u) - \bar{w}^T (u - u_{min}) - \hat{w}^T (u_{max} - u),$$

where  $\bar{w}$  and  $\hat{w}$  represent the penalty, as non-negative  $m$ -dimensional multiplier vectors.

Their role is to constrain the control input so that it satisfies the conditions

$$\bar{w}^T (u - u_{min}) = \hat{w}^T (u_{max} - u) = 0.$$

The Hamiltonian dictates that the necessary conditions for optimality are

$$\begin{aligned}\dot{\underline{x}} &= \frac{\partial H}{\partial \lambda} = A(\underline{x})\underline{x} + B(\underline{x})u, \\ \dot{\lambda} &= -\frac{\partial H}{\partial \lambda} = -Q(\underline{x}) - \left[ \frac{dA(\underline{x})\underline{x}}{d\underline{x}} \right]^T \lambda - \left[ \frac{dB(\underline{x})u}{d\underline{x}} \right]^T \lambda, \\ 0 &= \frac{\partial H}{\partial u} = R(\underline{x})u + B^T(\underline{x})\lambda - \bar{w} + \hat{w}.\end{aligned}\tag{7}$$

The last equation of eq. (7) produces the optimal control input, which is

$$u(\underline{x}) = -R^{-1}(\underline{x})(B^T(\underline{x})\lambda - \bar{w} + \hat{w}).\tag{7a}$$

It is important to always keep in mind that the current research embodies a simulation, not a real-life experiment. It is practically impossible, from both the economic and time aspect to measure the response of the patient's body to the tumor progression following a chemotherapy, on a daily or even more frequent basis; it is done more scarcely. Hence, the value of the control input of the feedback loop is calculated using the same realistic non-linear mathematical model developed and presented previously in Chapter 2. Afterwards, an optimized chemotherapeutic cancer treatment schedule is generated off-line, which could be applied in the real clinical practice. Its effectiveness could be evaluated by applying the protocol of the clinical examinations, and if there would be any deviations from those expected (the tumor remains the same or increases in size), then a re-run of the chemotherapy optimization should take place, by setting as initial states of the mathematical model and of the chemotherapy optimization procedure those of the current states-measurements of the normal, tumor, immune cell populations and the drug concentration, as obtained by the most recent patient's tumor evolution examinations. Such an approach would lead to an adaptive control.

When the control of LQR is applied, the adjoint state matrix obtains the form of  $\lambda = P(\underline{x})\underline{x}$ , where  $P(\underline{x}) \in \mathbb{R}^{n \times n}$  is a state-dependent symmetric matrix. Therefore, if the control is unbounded, by substituting  $\lambda$ , it becomes

$$u(\underline{x}) = -R^{-1}(\underline{x})B^T(\underline{x})P(\underline{x})\underline{x} \triangleq -K(\underline{x})\underline{x}.\tag{7b}$$

In the case of a bounded control input, the sub-optimal input for the mathematical model is

$$u_{bound}(\underline{x}) = \min(\max(u, u_{min}), u_{max}), \quad (7c)$$

with  $u_{min}$  and  $u_{max}$  being the lower and upper bounds, accordingly. The term  $-R^{-1}(\underline{x})B^T(\underline{x})P(\underline{x})$  is also referred to as feedback gain matrix, with  $P(\underline{x})$  being a symmetric positive definite matrix and a solution of the algebraic Riccati equation

$$A^T(\underline{x})P(\underline{x}) + P(\underline{x})A(\underline{x}) - P(\underline{x})B(\underline{x})R^{-1}(\underline{x})B^T(\underline{x})P(\underline{x}) + Q(\underline{x}) = 0, \quad (7d)$$

where it is prerequisite that  $A(\underline{x}), B(\underline{x})$  are pointwise controllable  $\forall \underline{x}$ . As a result, the dynamics of the pseudo-linearized closed-loop mathematical model become

$$\dot{\underline{x}} = \left( A(\underline{x}) - B(\underline{x})K(\underline{x}) \right) \underline{x} = A_{CL}(\underline{x})\underline{x}. \quad (7e)$$

The local asymptotic stability of this final form of the mathematical model is proved in **Appendix 2**, as well as in [6][10][42].

## Reconstruction of the mathematical model of eq. (2) in pseudo-linear form

The mathematical model of the previous chapters, presented in eq. (2), is examined once again. The dynamics of growth, death and interactions between cell populations remain the same, apart from the regression rate  $1 - e^{-M}$ , caused by the drug, which is now a linear function of the drug concentration  $M$ . The equivalent of a regression rate as in eq. (2) can be achieved by setting an upper bound to the drug input  $v_{max} = 1$ . This modification provides the possibility to apply SDRE to a practically similar cancer growth mathematical model, which also enables the examination of the possible effects of higher drug dosages.

$$\begin{aligned}
 \dot{N} &= r_2 N(1 - b_2 N) - c_4 TN - a_3 MN, \\
 \dot{T} &= r_1 T(1 - b_1 T) - c_2 IT - c_3 TN - a_2 MT, \\
 \dot{I} &= s + \frac{\rho IT}{\alpha + T} - c_1 IT - d_1 I - a_1 MI, \\
 \dot{M} &= v(t) - d_2 M.
 \end{aligned} \tag{8}$$

In the previous chapter, a cost function was defined in terms of drug input and tumor cells' population, which was later minimized by using special computer software [30], through an iterative method, following the non-linear dynamics. The final result was the proposed optimal control input. Moreover, the existence of such an optimal control had to be proved beforehand.

On the other hand, the SDRE control method does not require any additional burden, neither in computing the optimal drug regimen, nor in proving the existence of an optimal control, since the original LQR algorithm is used for the optimal control's computation. In order to implement the SDRE based optimal control, the mathematical model of eq. (8) must be rewritten in the form of eq. (6).

Thus, the tumor-free equilibrium point  $(1/b_2, 0, s/d_1, 0)$  is shifted to the origin, in terms of the following states

$$x_1 = N - \frac{1}{b_2}, \quad x_2 = T, \quad x_3 = I - \frac{s}{d_1}, \quad x_4 = M,$$

where  $\underline{x}^T = [x_1, x_2, x_3, x_4]^T$  represents the shifted state vector for the normal, tumor, immune cells and drug concentration  $\underline{x}$  vector elements, respectively. As a result, the mathematical model's equations are rewritten as

$$\begin{aligned} \dot{x}_1 &= -r_2 x_1 (1 + b_2 x_1) - \frac{c_4}{b_2} x_2 - \frac{a_3}{b_2} x_4 - c_4 x_2 x_1 - a_3 x_4 x_1, \\ \dot{x}_2 &= r_1 x_2 (1 - b_1 x_2) - \left( \frac{c_2 s}{d_1} + \frac{c_3}{b_2} \right) x_2 - c_2 x_3 x_2 - c_3 x_2 x_1 - a_2 x_4 x_2, \\ \dot{x}_3 &= -\frac{c_2 s}{d_1} x_2 - d_1 x_3 - \frac{a_1 s}{d_1} x_4 + \frac{\rho s}{d_1} \frac{x_2}{(a + x_2)} + \frac{\rho x_3 x_2}{\alpha + x_2} - c_1 x_3 x_2 - a_1 x_4 x_3, \\ \dot{x}_4 &= u(t) - d_2 x_4, \end{aligned} \tag{9}$$

where  $u(t)$  is the control input (drug dosage).

The non-linear mathematical model of the above equations is now in the form of eq. (5), thus it can be written in the form of  $\dot{\underline{x}} = A(\underline{x})\underline{x} + B(\underline{x})u$ , eq. (6). In order to achieve this, the SDC matrices  $A(\underline{x}), B(\underline{x})$  must be defined, one of the main difficulties of the SDRE technique, because the SDC representation is not unique and the selection procedure for the factorization of  $f(\underline{x}) = A(\underline{x})\underline{x}$  cannot be expressed with clear steps. However, this obstacle can be used in our favor, producing a variety of different sub-optimal solutions, as long as the selected SDC matrices are pointwise controllable. It is important to remember that the pointwise controllability of the selected pair  $(A(\underline{x}), B(\underline{x}))$  does not have any implication on the controllability of the non-linear mathematical model [10][42]. Therefore, the resulting SDC matrices, as suggested in [41], are

$$A(\underline{x}) \triangleq \begin{bmatrix} -r_2(1 + b_2x_1) & -c_4\left(x_1 + \frac{1}{b_2}\right) & 0 & -a_3\left(x_1 + \frac{1}{b_2}\right) \\ -c_3x_2 & r_1(1 - b_1x_2) - \left(\frac{c_2s}{d_1} + \frac{c_3}{b_2}\right) & -c_2x_2 & -a_2x_2 \\ 0 & \frac{\rho\left(x_3 + \frac{s}{d_1}\right)}{(a + x_2)} - c_1\left(x_3 + \frac{s}{d_1}\right) - x_4 & -d_1 & -a_1\left(x_3 + \frac{s}{d_1}\right) + x_2 \\ 0 & 0 & 0 & -d_2 \end{bmatrix},$$

$$B(\underline{x})^T \triangleq [0, 0, 0, 1]^T.$$

By combining all the above, the final non-linear state space equations take the form

$$\dot{\underline{x}} = \begin{bmatrix} -r_2(1 + b_2x_1) & -c_4\left(x_1 + \frac{1}{b_2}\right) & 0 & -a_3\left(x_1 + \frac{1}{b_2}\right) \\ -c_3x_2 & r_1(1 - b_1x_2) - \left(\frac{c_2s}{d_1} + \frac{c_3}{b_2}\right) & -c_2x_2 & -a_2x_2 \\ 0 & \frac{\rho\left(x_3 + \frac{s}{d_1}\right)}{(a + x_2)} - c_1\left(x_3 + \frac{s}{d_1}\right) - x_4 & -d_1 & -a_1\left(x_3 + \frac{s}{d_1}\right) + x_2 \\ 0 & 0 & 0 & -d_2 \end{bmatrix} \begin{bmatrix} x_1 \\ x_2 \\ x_3 \\ x_4 \end{bmatrix} + \begin{bmatrix} 0 \\ 0 \\ 0 \\ 1 \end{bmatrix} u.$$

As a result, the relation  $f(\underline{x}) = A(\underline{x})\underline{x}$  is verified and the optimal control attempts to minimize the quadratic cost function  $J = \int_0^\infty (\underline{x}^T Q(\underline{x})\underline{x} + R(\underline{x})u^2) dt$ ,

where  $Q(\underline{x})$  and  $R(\underline{x})$  are the state-dependent weighting matrices for the states and the input, accordingly [48]. Their role is very important, since they determine the level of impact each term has on the regulation process; a great advantage the SDRE technique provides.

More specifically, the states which have to be minimized are the tumor cells' population and the drug concentration, so that the mathematical model ends up to the tumor-free equilibrium point. Thus, the form of  $Q(\underline{x})$  will be

$$Q(\underline{x}) = Q = \begin{bmatrix} 0 & 0 & 0 & 0 \\ 0 & w_2 & 0 & 0 \\ 0 & 0 & 0 & 0 \\ 0 & 0 & 0 & w_4 \end{bmatrix},$$

where  $w_2, w_4$  are non-negative constants, with values  $w_2 = 150, w_4 = 0.1$  [41]. The elements of the main diagonal of the weighting matrix  $Q$ ,  $\{Q_{11}, Q_{22}, Q_{33}, Q_{44}\} = \{0, w_2, 0, w_4\}$ , correspond to the weights of each state  $(x_1, x_2, x_3, x_4)$ . In other words, by

setting a zero value to the weights  $Q_{11}, Q_{33}$ , which refer to the populations of normal ( $x_1$ ) and immune ( $x_3$ ) cells, the proliferation of these cells is not inhibited at all by the controller; a desirable result, since they aim to shift the mathematical model to a healthy state. On the other hand, the positive values of the weights  $Q_{22}, Q_{44}$ , which refer to the population of tumor cells and the drug concentration, indicate that the controller must focus on minimizing the values of  $x_2$  and  $x_4$ . Moreover, the notable difference between the values of these weights ( $w_2 = 150$  compared to  $w_4 = 0.1$ ), does not represent any relation between them, since they refer to different units (*cells* compared to *mg/m<sup>2</sup>*).

For the weight matrix  $R(\underline{x})$  three scenarios will be examined. A constant value and two functions of the tumor cells' population, affected incrementally or decrementally. The scenarios can be expressed as

$$R(\underline{x}) = \begin{cases} r_c, & \text{or} \\ r_c + \beta_1 * x_2(t), & \text{or} \\ r_c - \beta_2 * x_2(t), \end{cases}$$

where  $r_c, \beta_1, \beta_2$  are positive constants, with values  $r_c = 4.7, \beta_1 = 2, \beta_2 = 15$  [41]. The value of  $R(\underline{x})$  determines the cost of the input (drug). A low value of  $R(\underline{x})$  will allow a greater amount of drug to be administered, compared to a higher one. When  $R(\underline{x})$  remains constant, the drug intake rate is related only to the factor  $r_c$ . On the contrary, when  $R(\underline{x})$  is a function of the tumor population ( $x_2$ ), the drug input can vary according to the state of the tumor. In the case where the tumor expands ( $x_2$  increases), the cost of the control input is affected and, as a result, the amount of suggested drug is decremented when  $R(\underline{x}) = r_c + \beta_1 * x_2(t)$ , or it is incremented when  $R(\underline{x}) = r_c - \beta_2 * x_2(t)$ .

The estimation of both  $Q(\underline{x})$  and  $R(\underline{x})$  is a very delicate process (see [48]). An initial calculation of their values has been done in [41], yet in this approach they are reevaluated through trial and error, so that the tumor can be eradicated with a lesser amount of drug, which also results in lower toxicity levels in the patient's body.

By inserting the above terms into the cost function, the following form is obtained

$$J = \int_0^{\infty} (w_2(x_2(t))^2 + w_4(x_4(t))^2 + R(\underline{x})(u(t))^2) dt,$$

where  $x_2(t)$  are the tumor cells,  $x_4(t)$  is the drug concentration and  $u(t)$  is the drug input, at a specific time (day)  $t$ .

## Periodic application of the determined optimal chemotherapy treatment

The above approach can be extended even further, by adding a restriction of active and inactive days. SDRE technique as much as effective it can be, it might need to be slowed down slightly, in cases of excessive drug dosage, so that high toxicity scenarios can be avoided. Therefore, a periodic controller is proposed, with a period of  $t_p$  days,  $t_p \geq 2$ . If the control is active during the first  $t_{on}$  days, where  $1 \leq t_{on} < t_p$ , it is then turned off for the remaining  $t_{off} = t_p - t_{on}$  days. An active controller is one which applies the control input suggested by SDRE, based on the state and control responses of the previous timestep, while an inactive controller sets the control input to zero, ignoring what SDRE dictates as optimal control.

As one might speculate, during the time window of inactive days  $t_{off}$ , the state's values change according to the mathematical model's dynamics. When a new period is about to start, the control input based on SDRE is applied once again, throughout the whole set of active days  $t_{on}$ . As simulations have shown, the mathematical model's state and control in this approach differ from those of a mathematical model with continuous SDRE control input, a phenomenon which was anticipated, since the absence of drug input during the inactive days allowed the normal, tumor and immune cells to recover, up to a certain point. Such a recovery, can produce improved results by reducing the toxicity levels, thus preventing the normal cells' population from degenerating below a safe level. However, it can also be damaging, if the inactive days are unreasonably more than the active, offering a lot of time for the tumor to

regrow. In such cases, either a great amount of drug is required to restore the mathematical model to a treatable state, which also critically reduces the normal cells' population, or the tumor has reached an uncontrollable level, implying a great risk for the patient's health. Subsequently, examining numerous combinations of active and inactive days is of high importance, so that the periodic effects can be determined for the mathematical model of the current analysis.

Simulation results of the application of the determined treatment by using the pseudo-linear SDRE optimal control method of eq. (7a) ... (7e)

In this section, the simulations for the above control method are presented. This time, only the initial value of  $x_3(0) = 0.15$  will be taken under consideration, keeping the rest of the starting cells' populations the same as in Chapter 3. Therefore the initial values of the mathematical model are  $\{x_1(0), x_2(0), x_3(0), x_4(0)\} = \{1, 0.25, 0.15, 0\}$ , referring to normal, tumor, immune cells and drug concentration in the tumor area, respectively. The desired final values are once again the tumor-free equilibrium, as discussed in Chapter 2, which translates to  $\{x_1(t_f), x_2(t_f), x_3(t_f)\} = \{1, 0, 1.65\}$ . The drug concentration starts and ends at a zero value  $x_4(0) = x_4(t_f) = 0$ , indicating a pure organism at first, as far as drug existence goes, which will no longer require medicine by the end of the treatment, since the tumor will have been eradicated. Lastly, the final time  $t_f$  does not require any constraints for the SDRE approach.

A number of cases will be reviewed. At first, the impact of different values in the weight matrix of the control  $R(\underline{x})$  will be examined. In case 1,  $R(\underline{x})$  will be set to a constant value of  $r_c = 4.7$ , which will also represent the base value for the following cases. In case 2,  $R(\underline{x})$  will be affected incrementally by a linear function of the tumor cells' population, thus  $R(\underline{x}) = r_c + \beta_1 x_2(t)$ ,  $\beta_1 = 2$ . Case 3 will follow the same idea of case 2, but with a negative

coefficient for the tumor cells' population, that is  $R(\underline{x}) = r_c - \beta_2 x_2(t)$ ,  $\beta_2 = 15$ . Afterwards, case 4 will be similar to case 1, but with the introduction of an upper bound  $v_{max} = 1$  to the control input, in an attempt to minimize the toxicity levels in the tumor area, while maintaining the effectiveness of the treatment. As the results will later tell, the differences between the above cases are mainly located between case 1 and case 4. Thus, in a second phase, a periodic-SDRE approach will be applied to both of them, in order to examine how the mathematical model corresponds to various periods of active and inactive days.

The main goal is, once again, to limit the drug side effects to the normal cells, by keeping the global minimum of their population  $N_{min}$  at a relatively safe level. Moreover, the total amount of drug administered  $v_{total}$  needs to be monitored. An unreasonably high amount of drug is used as an indicator, showing that the tumor was able to regrow during the inactive days. The above terms are directly related to the maximum concentration of the drug  $u_{max}$  and the day of tumor eradication  $t_{zero}$ , all of which are recorded, alongside with the maximum population reached by the tumor cells  $T_{max}$ .

For clarity, the notation  $\{N, T, I, M\}$  will be used for the states and  $\{v\}$  for the drug input in the following diagrams. All cell populations are normalized at the value of  $10^{11}$  cells, drug concentration and drug input are measured in *mg* per *liter* of plasma in the tumor area and *mg* per  $m^2$  of the patient's body surface, respectively.

Case 1 : The drug input's weight  $R(\underline{x})$  has a constant value

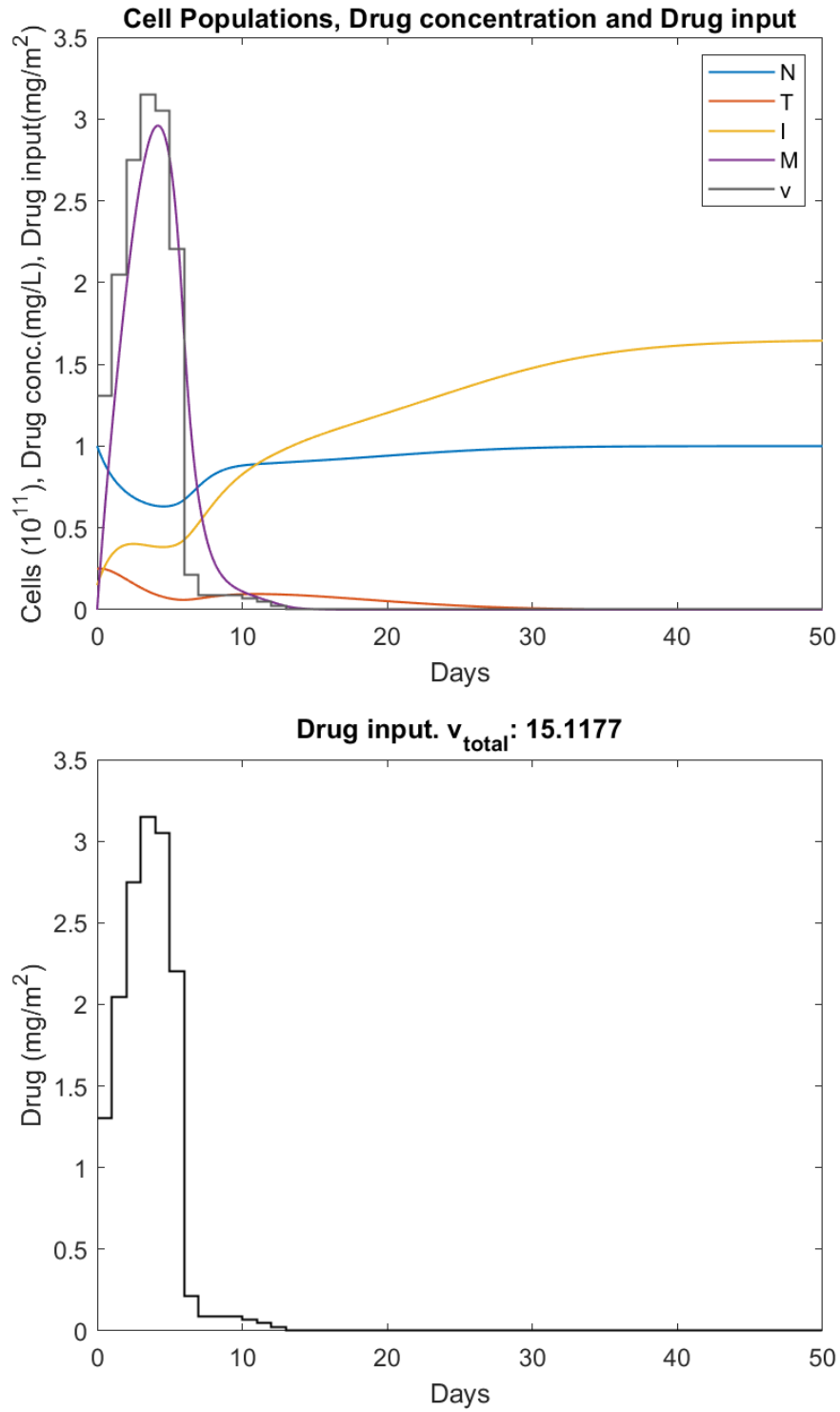


**Figure 15** – Mathematical model's response and drug input for constant  $R(\underline{x}) = 4.7$ . The tumor is eradicated with a total amount of drug  $v_{total} = 15.1177 \text{ mg/m}^2$ .

Case 2 : The tumor increases the drug input's weight  $R(\underline{x}(t))$

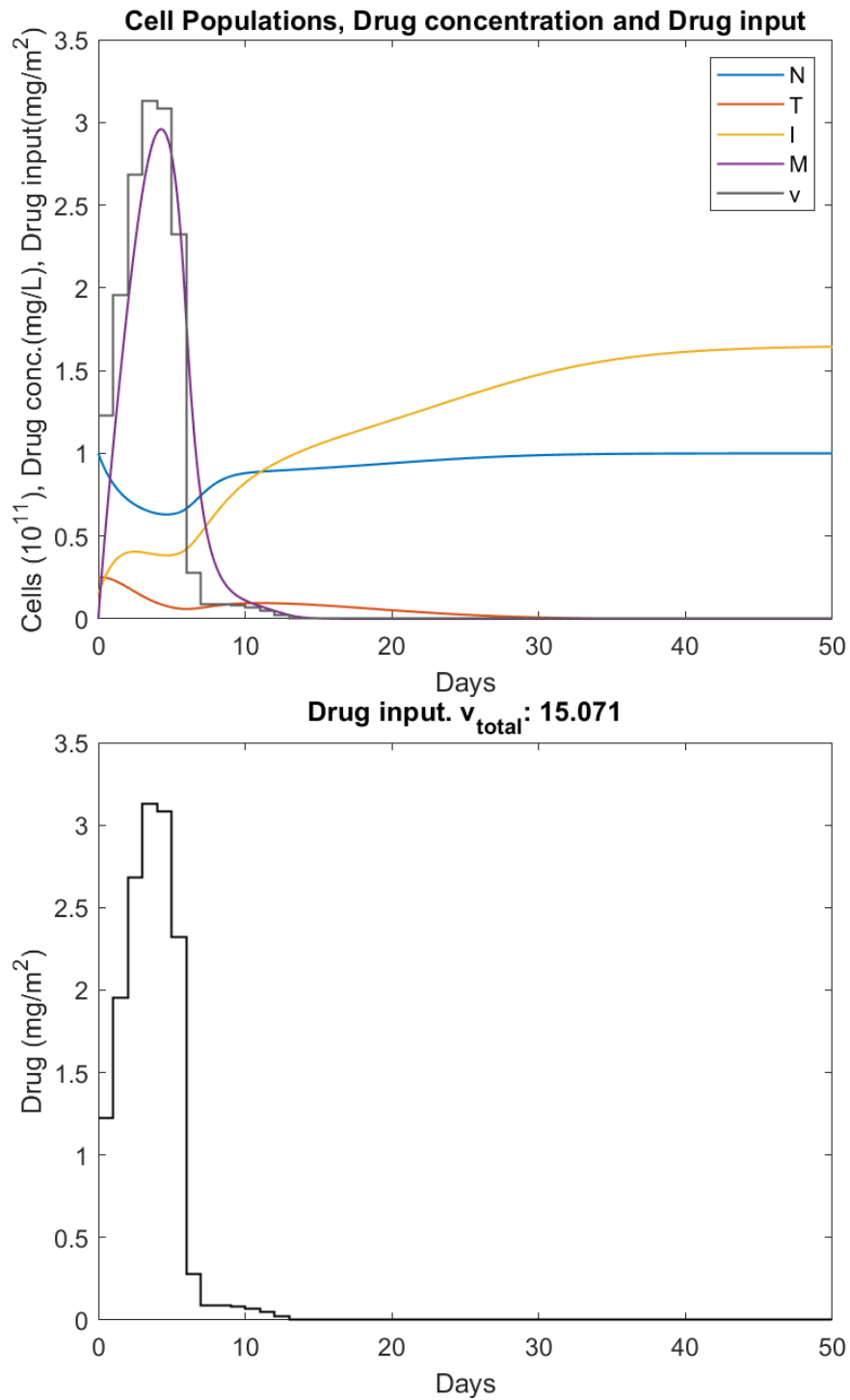


**Figure 16** – Mathematical model's response and drug input for  $R(\underline{x}(t))$  as an increasing function of the tumor evolution, i.e. of  $x_2(t)$ , that is as a function of the state vector  $\underline{x}(t)$ . An increased input weight, when the tumor exists, results in a slightly delayed drug dosage.

Case 3 : The tumor decreases the drug input's weight  $R(\underline{x}(t))$

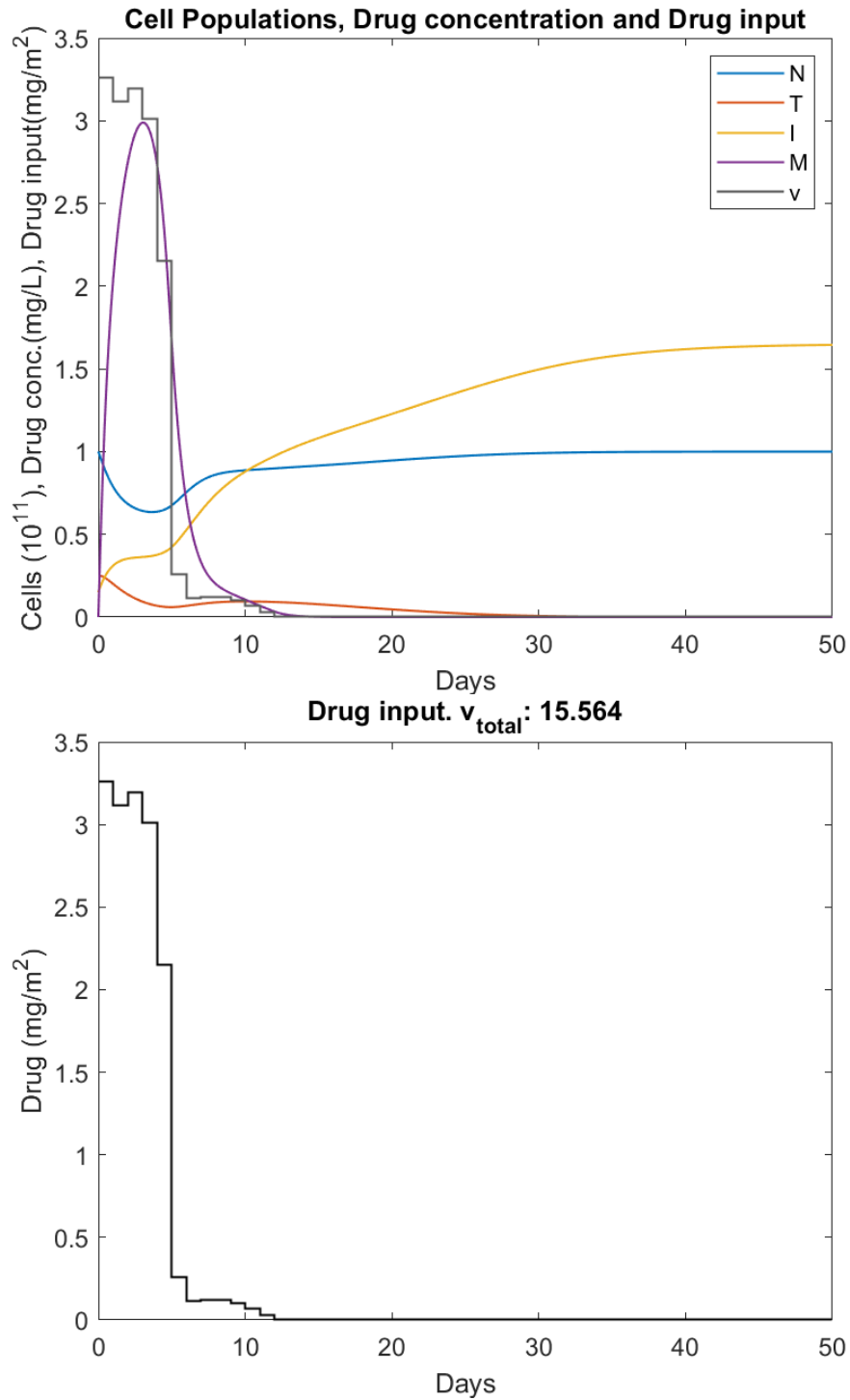


**Figure 17** – Mathematical model's response and drug input for  $R(\underline{x}(t))$  as a decreasing function of the tumor evolution, i.e. of  $x_2(t)$ , that is as a function of the state vector  $\underline{x}(t)$ . A decreased input weight, when the tumor exists, results in a slightly hastened drug dosage.

Case 4 : The drug input is bounded and the drug input's weight  $R(x)$  has a constant value

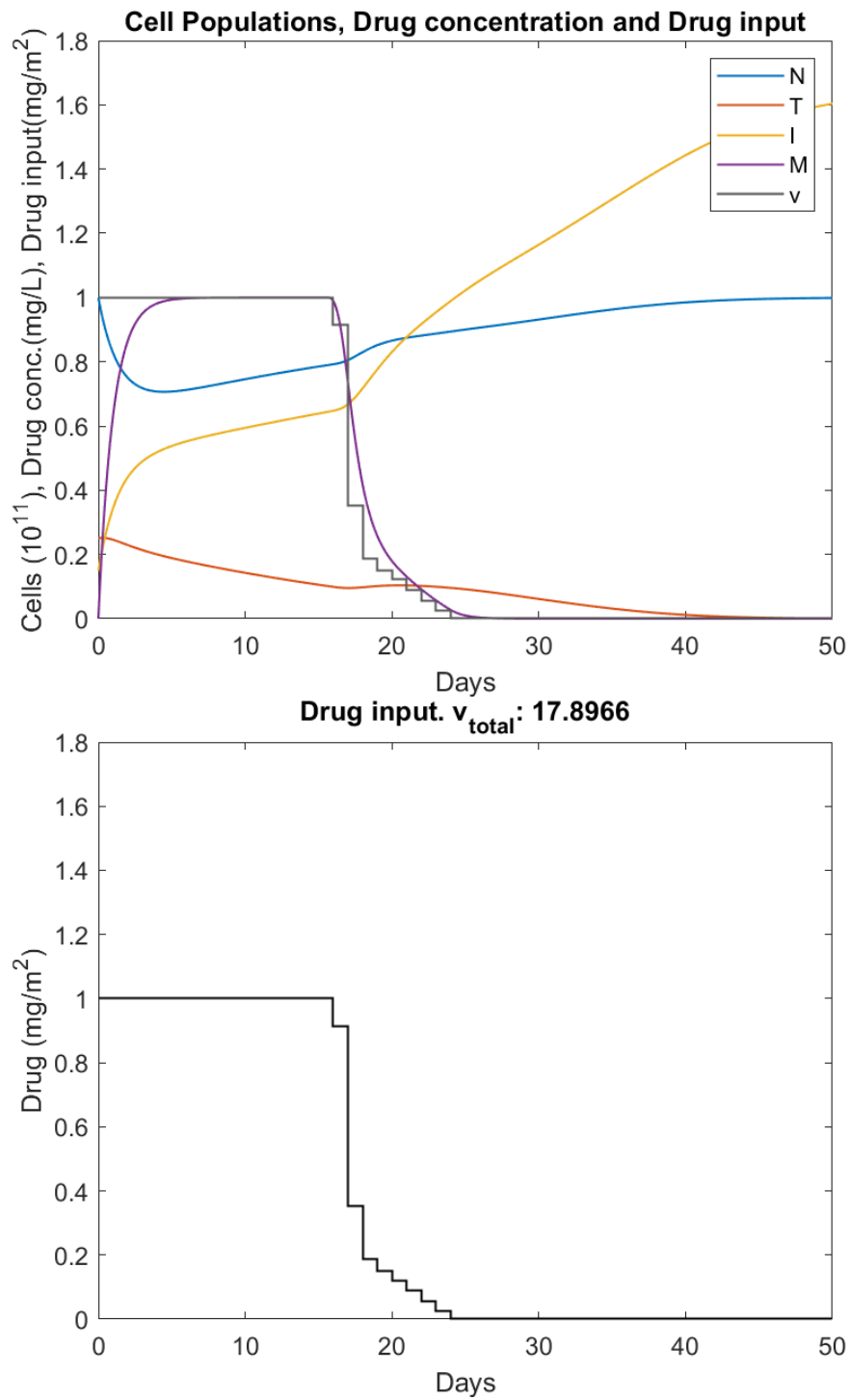


**Figure 18** – Mathematical model's response and drug input for bounded drug dosage. By setting an upper bound to the drug input, the toxicity levels are reduced dramatically.

Based on the previous simulations, case 3 and case 4 seem to be the most interesting, since they damage the normal cells the least and combat the tumor successfully. Therefore, the periodic-SDRE will be applied to them. The number of active and inactive days will be represented as  $t_{on}$  and  $t_{off}$ , creating a total period of  $t_p = t_{on} + t_{off}$  days. The examined values of the period are  $t_p = \{2, 3, 4, 5, 7, 10, 14\}$  days and the active days lie within the range of values  $1 \leq t_{on} < t_p$ . It has been observed that 7 continuous active days of drug administration are almost the equivalent of a continuous-SDRE approach (see Figures 17-18), thus the constrain  $t_{on} \leq 7$  is also applied. The most important term, according to which the effectiveness of the periodic approach will be determined, is the minimum population of the normal cells during the treatment. Additionally, the total amount of drug administered will be compared, so that the advantages of this approach can be shown better.

## Case 5 : Reevaluation of the chemotherapeutic schedule by applying a periodic drug input dosage

In case 5, the periodic treatment is being applied and the input weight matrix used is  $R(\underline{x}) = r_c - \beta_2 x_2(t) = 4.7 - 15 * x_2(t)$  (same as case 3). Below, the minimum values of normal cells  $N_{min}$  are compared for each combination of  $[t_p/t_{on}]$  days, followed by the total amount of drug administered  $v_{total}$ .

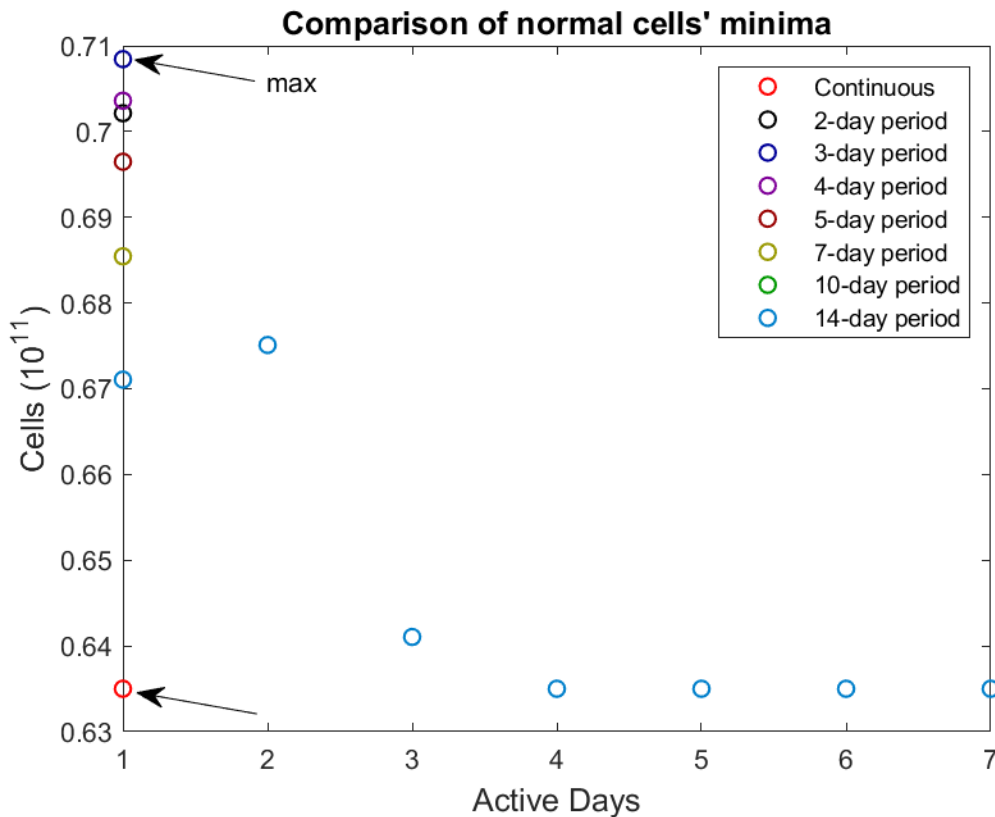


**Figure 19** – Comparison of global minima in normal cells when applying a variety of periodic treatments (case 5).

As the scatter plot shows, different combinations of active and inactive days produce different results, compared to the continuous treatment (red circle). Of particular interest is the case of  $[t_p/t_{on}] = [3/1]$ , where the drug is administered every first day of a three-day period, allowing the normal cells' population to remain close to 0.71, the maximum value of all the combinations. This value is significantly higher than the one which results from a continuous regimen (0.635). Thus, the drug's side effects are diminished. For active days  $t_{on} \geq 2$ , the minima seem to be overlapping and as the number of active days increases, the populations' minima converge to the continuous treatment's value.

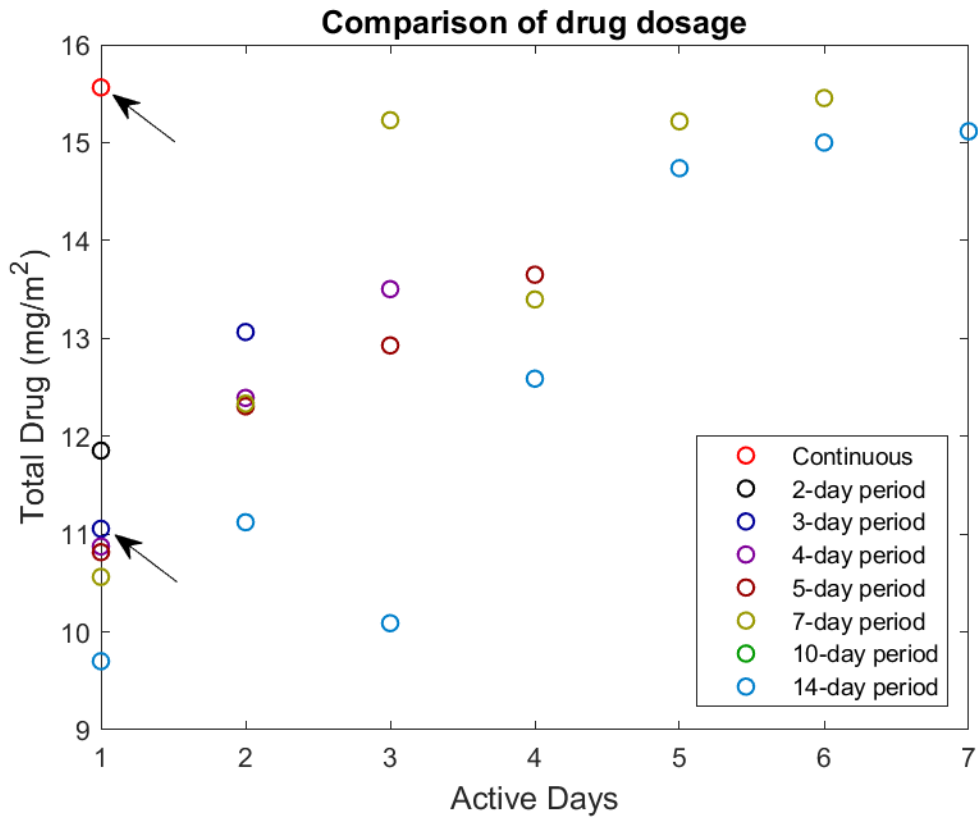


**Figure 20** – Comparison of total drug amount administered when applying a variety of periodic treatments (case 5).

The indicated case of  $[t_p/t_{on}] = [3/1]$  requires a lower amount of drug, compared to the continuous administration treatment, making it more cost-efficient.

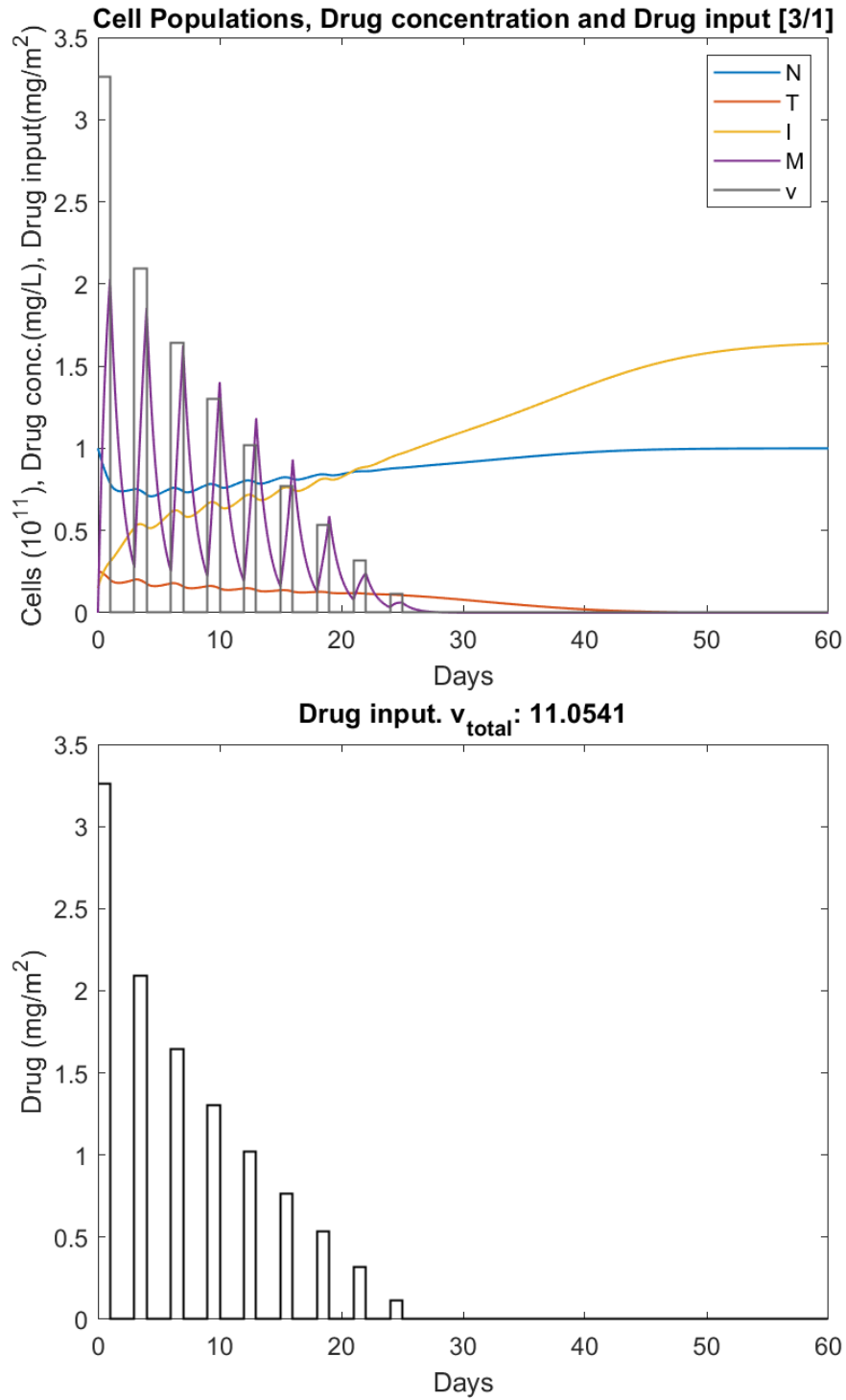


**Figure 21** – Mathematical model’s response and drug input when a periodic treatment of [3/1] days is applied, the drug input is unbounded and the input weight  $R(\underline{x}(t))$  is a decreasing function of the tumor evolution, i.e. of  $x_2(t)$ .

## Case 6 : Reevaluation of the chemotherapeutic schedule by applying a periodic bounded drug input dosage

In case 6, the periodic treatment is being applied, the control input is restricted to an upper bound  $v_{max} = 1$  and the input weight matrix remains constant  $R(\underline{x}) = r_C = 4.7$  (same as case 4). The following results compare the minimum values of normal cells  $N_{min}$  for each combination of  $[t_p/t_{on}]$  days, as well as the total amount of drug administered  $v_{total}$ .

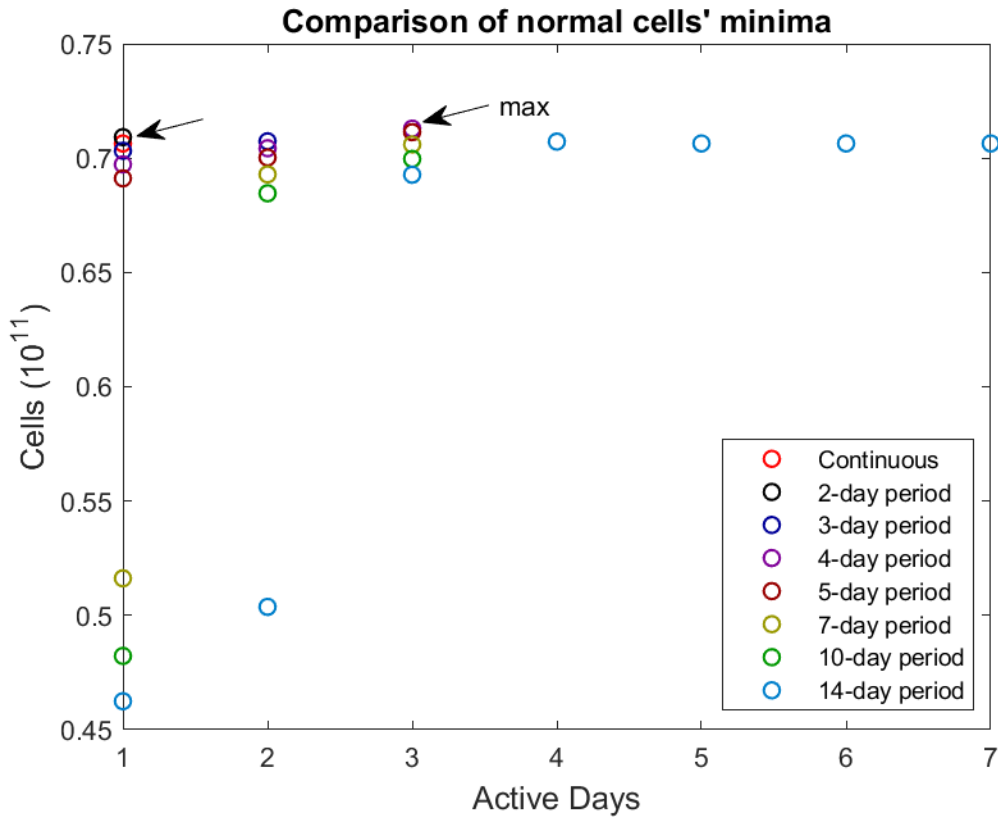


**Figure 22** – Comparison of global minima in normal cells when applying a variety of periodic treatments (case 6).

As the scatter plot shows, different combinations of active and inactive days produce different results, compared to the continuous treatment (red circle). Of particular interest is the case of  $[t_p/t_{on}] = [4/3]$ , where the drug is administered on the first three days of a four-day period, producing the maximum value of all the minima. This time, the increase is not very distinct, due to the already bounded drug input. For active days  $t_{on} \geq 3$ , the minima converge to the continuous treatment's value. Moreover, the cases of  $[7,1]$ ,  $[10,1]$ ,  $[14,1]$  and  $[14,2]$  produce very low values of minima, which translate to ineffectiveness of these combinations and uncontrollable growth of the tumor.

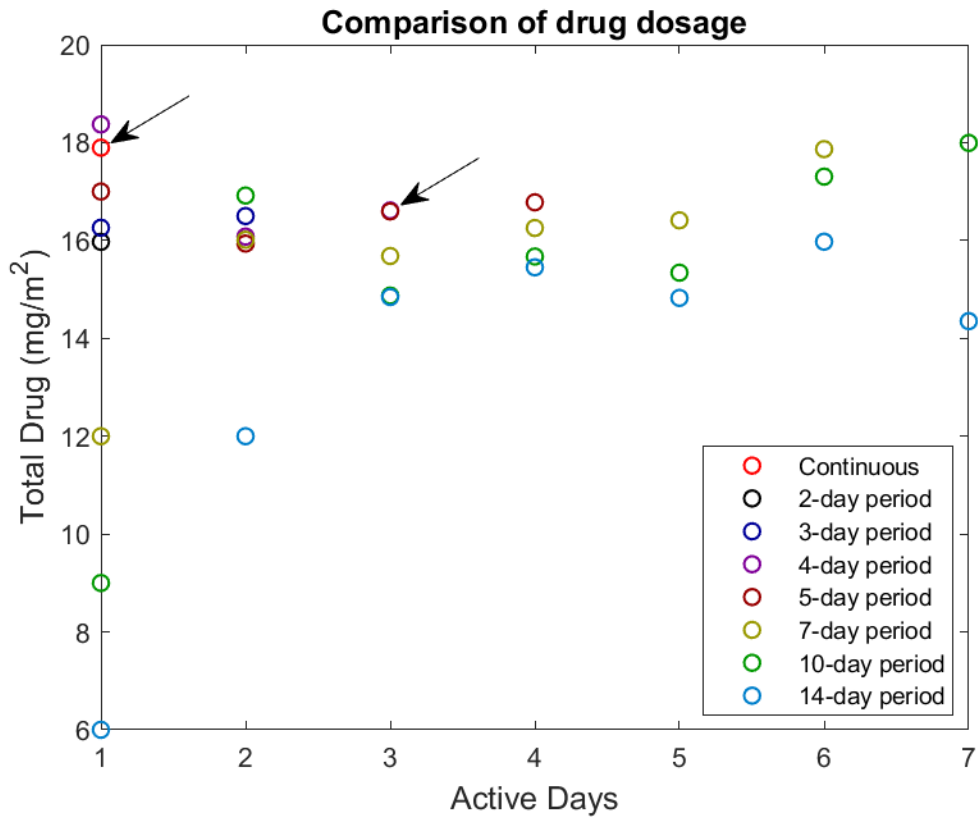


**Figure 23** – Comparison of total drug amount administered when applying a variety of periodic treatments (case 6).

The indicated case of  $[t_p/t_{on}] = [4/3]$  requires a lower amount of drug, compared to the continuous administration treatment, making it more cost-efficient.

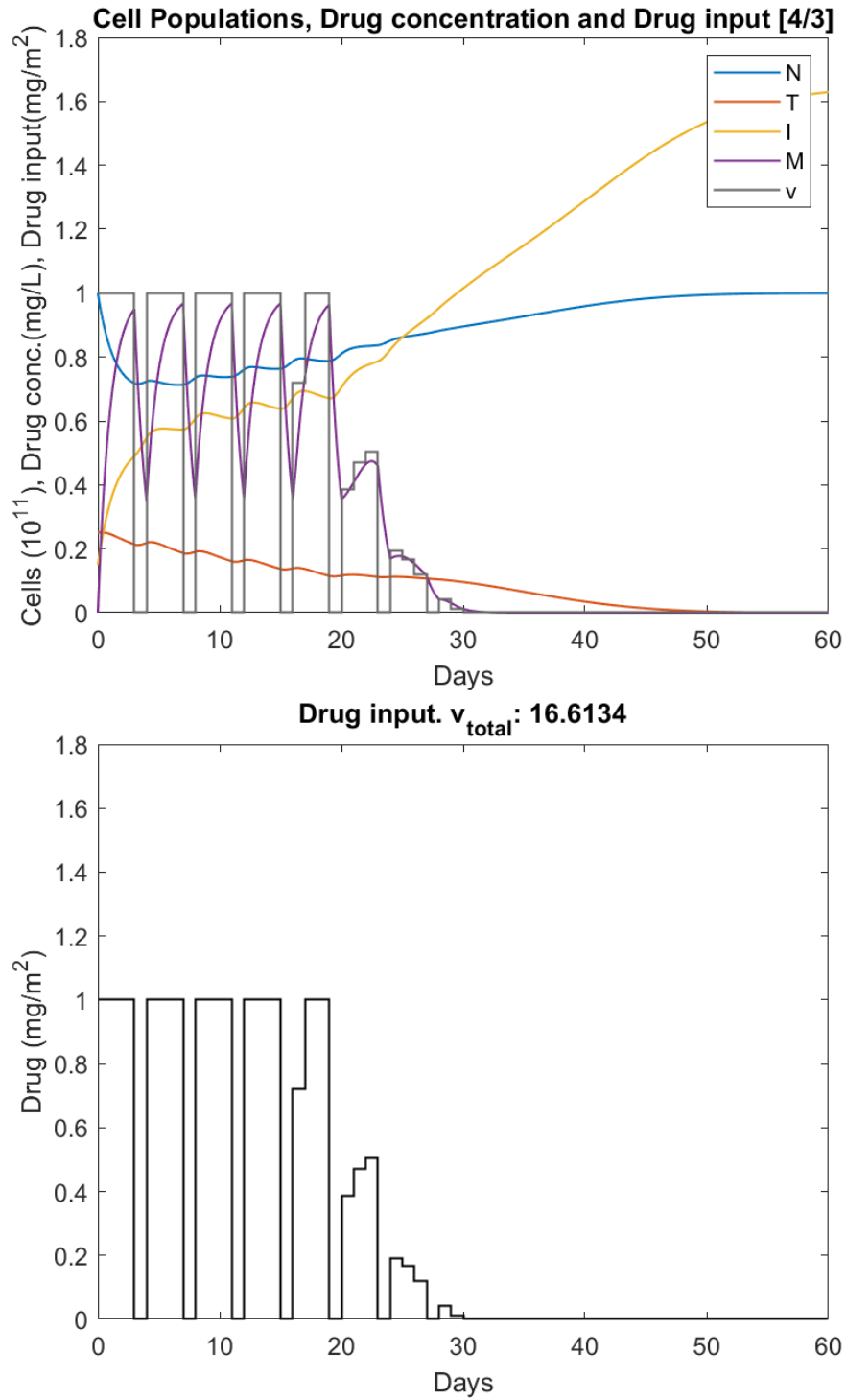


**Figure 24** – Mathematical model’s response and drug input when a periodic treatment of [4/3] days is applied, the drug input is bounded and the input weight  $R(\underline{x}(t))$  has a constant value.

A **synopsis** of the simulations' final data is presented in the tables below. The variables of particular interest are:

- $N_{min}$  (*cells*): minimum normal cells' population.
- $T_{max}$  (*cells*): maximum tumor cells' population.
- $M_{max}$  (*mg/L*): maximum drug concentration.
- $v_{total}$  (*mg/m<sup>2</sup>*): total amount of administered drug.
- $t_{zero}$  (*day*): day of tumor eradication ( $T(t_{zero}) < 0.005$ , practically 0).
- $[t_p/t_{on}]$  (*days*): total days of the period  $t_p$ , with only the first  $t_{on}$  being active, i.e., drug is administered.

**Table 2:** Continuous-SDRE treatment results

	Case 1	Case 2	Case 3	Case 4
$R(\underline{x})$	4.7	$4.7 + 2 * x_2(t)$	$4.7 - 15 * x_2(t)$	4.7
$v_{max}$	$\infty$	$\infty$	$\infty$	1
$N_{min}$	0.631064	0.630809	0.635007	0.70641
$T_{max}$	0.2511	0.2512	0.2502	0.2518
$v_{total}$	15.1177	15.071	15.564	17.8966
$t_{zero}$	32	33	31	44
$M_{max}$	2.95999	2.95907	2.98878	1

**Table 3:** Periodic-SDRE treatment results

	Case 5 – Periodic [3/1]	Case 6 – Periodic [4/3]
$R(\underline{x})$	$4.7 - 15 * x_2(t)$	4.7
$v_{max}$	$\infty$	1
$N_{min}$	0.7084	0.7129
$T_{max}$	0.2502	0.2518
$v_{total}$	11.0541	16.6134
$t_{zero}$	46	49
$M_{max}$	2.033	0.9679

The first difference which occurs is linked to the control input weight  $R(\underline{x})$  in the first three cases. When  $R(\underline{x})$  is constant (case 1), the minimum normal cells' population is relatively low ( $N_{min} = 0.631064$ ). Responsible for this issue is the high level of drug concentration in the tumor area ( $M_{max} = 2.95999$ ) which is hazardous for the healthy tissue. By relating  $R(\underline{x})$  to the tumor cells incrementally (case 2) the results become even worse. This is an expected outcome, since the existence of tumor cells is translated to a greater weight for the control input (drug), thus the controller applies a smaller amount of drug. As a result, it becomes harder to combat the tumor and at the same time the normal cells are reduced even further. On the other hand, when  $R(\underline{x})$  is related to the tumor decrementally (case 3) the treatment turns out to be more effective, allowing more drug to be administered when the population of tumor cells is large and gradually restricting it when tumor cells start to perish.

Unfortunately, in all of the above cases high toxicity levels are present. A first attempt to reduce them is by setting an upper bound  $v_{max}$  to the control input (case 4), which greatly improves the final results. The maximum drug concentration drops almost to a third of its previous value ( $M_{max} = 1$ ) and, consequently, the minimum population of normal cells reaches a higher number ( $N_{min} = 0.70641$ ). The cost for all of these advantages is an increase

to the total amount of drug given  $v_{total}$  at the order of 15% to 18% and a longer duration for the therapy (approx. 10 more days).

A second attempt to tame the drug toxicity is to apply the previously discussed periodic regimen. After selecting the two best cases from the above (case 3 & 4), a variety of simulations are conducted, under different conditions of active and inactive days. Afterwards, the least harmful treatment is selected, according to the minimum population of normal cells  $N_{min}$ . Higher values translate to a healthier organism; thus, the maximum of all minima is chosen for each case, which are  $N_{min} = 0.7084$  for case 3 and  $N_{min} = 0.7129$  for case 4. These values correspond to regimens with [total/active] days [3, 1] and [4, 3], respectively. Interestingly enough, case 3 shows a rise of 11.5%, as far as  $N_{min}$  is concerned, which is a great improvement. Additionally, maximum drug concentration is reduced ( $M_{max} = 2.033$ ), alongside with the total amount of drug required ( $v_{total} = 11.0541$ ). The results of the periodic schedule for case 4 follow the same guidelines, but at a lower scale, since the already bounded drug input had reduced the toxicity levels noticeably, leaving less room for improvement. The only drawback presented by both periodic cases is an increased treatment duration, which in either scenario does not surpass the rational period of 1.5 – 2 months.

Last but not least, the maximum tumor size  $T_{max}$  does not show any signs of noticeable oscillations in any of the examined cases. More specifically, its value is almost identical to the initial one ( $T(0) = 0.25$ ), a fact indicating that all of the approaches that have been reviewed prevent it from growing even further.

## Chapter 5 : Conclusion

---

The treatment of cancer by chemotherapy is a very complex procedure, including a plethora of interactions between the host's cells, the tumor's cells and the drug applied. In this study, a non-linear mathematical model, which is burdened by a relatively big tumor and a weakened immune response, is used to simulate a scenario of cancer. The problem of finding an optimal solution for such a case can be very challenging. For that reason, two treatment methods are implemented, tested and compared.

In the first approach, the Hermite-Simpson Direct Collocation method is used to provide an optimal regimen, yielding very effective results. However, the drawback of drug administration every day, during the whole treatment period, makes it impractical for real-world implementation. Thus, it is converted to a Bang-Bang method, maintaining the same amount of total drug, but selecting only specific days for its administration. The results obtained are equally satisfying, since the tumor is eradicated, extreme levels of toxicity are avoided and the duration of the process is reduced.

In the second approach, the State-Dependent Riccati Equation method is applied, with the crucial advantage of lower computational requirements, leading to a faster simulation time, because it does not depend on an iterative loop of optimizations, opposed to DirCol. However, the unconstrained optimal chemotherapy dosage determined using the pseudo-linear SDRE optimization introduces the issue of high toxicity, i.e. excessive drug concentration in order to eliminate the tumor. That problem is confronted successfully in the present work, either by setting an upper bound to the drug input, or by embedding a periodic application of the determined optimal chemotherapy treatment consisting of active and inactive days of the drug administration. Both scenarios offer effective regimens and, particularly, the achieved optimal periodic drug application achieves to limit even further the hazardous side-effects and to lessen the total amount of drug required.

## Interpretation of the Results

After executing the simulations of the above approaches, four scenarios are obtained, with the treatment being based on a Bang-Bang method in the first two cases (highly and less weakened immune system) and on a SDRE optimal periodic drug application method in the last two cases (unbounded and bounded input). The results of those cases, concerning the most important factors ( $N_{min}$ ,  $v_{total}$ ,  $M_{max}$ ,  $t_{zero}$ ,  $T_{max}$ ) are presented and compared below. When the color of case's bar tends to a lighter grey color, it indicates that that specific case produces a better result for the factor examined in each figure.

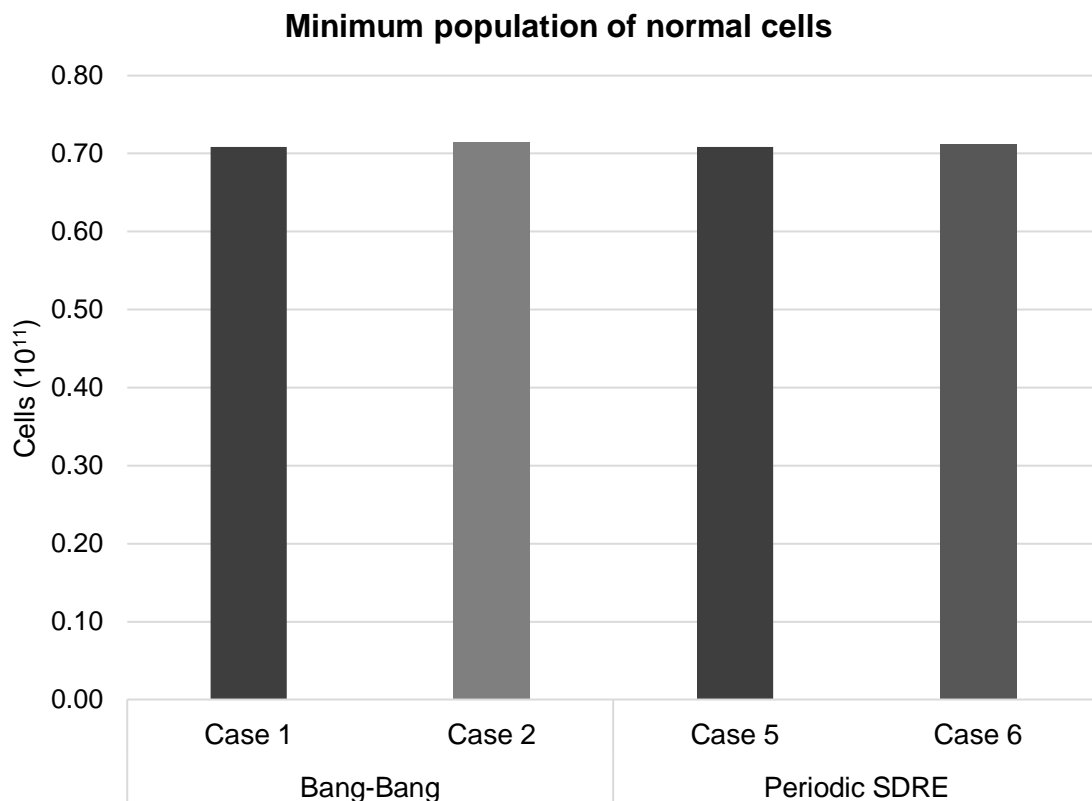


**Figure 25** – Comparison of the normal cells' minimum population (best cases).

In all four examined cases, the treatment managed to maintain the population of normal cells within a satisfying limit ( $N_{min} > 0.708$ ), showcasing their subtle impact on the healthy tissue within the tumor area.

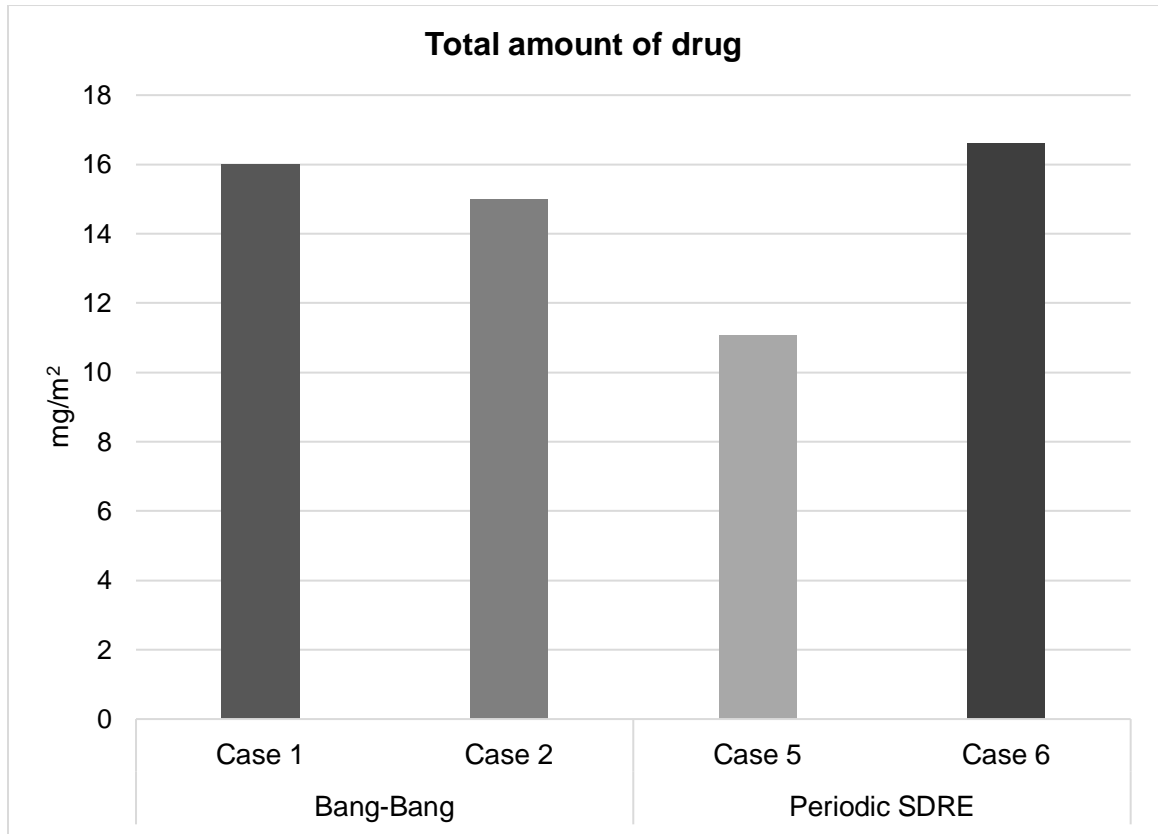


**Figure 26** – Comparison of the total amount of administered drug (best cases).

In all four examined cases, the amount of drug is kept within relatively low levels. Specifically, in case 5 a noticeable decrease is observed, which is, paradoxically, linked to an increased drug concentration (Figure 27). This phenomenon occurs (because only a small amount of drug is available and it has to be given to the patient within a short period of time) so that the treatment can be effective.

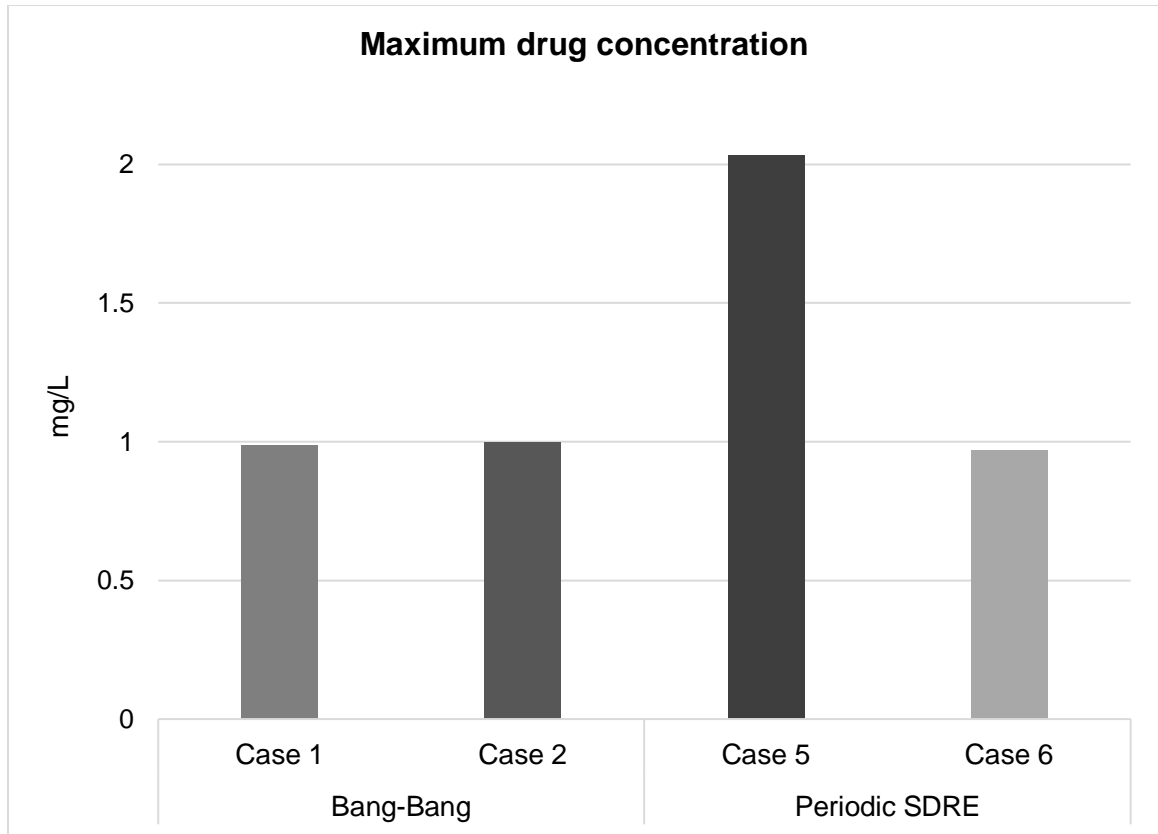


**Figure 27** – Comparison of the maximum drug concentration (best cases).

The maximum drug concentration is once again kept at low levels and is related conversely to the total amount of drug given. It is obvious that the maximum drug concentration in case 5 is double, compared to the other three cases, which occurs due to the unbounded drug input. Moreover, the controller manages these levels of drug concentration by preferring a slightly longer treatment duration to a quick one (Figure 28).

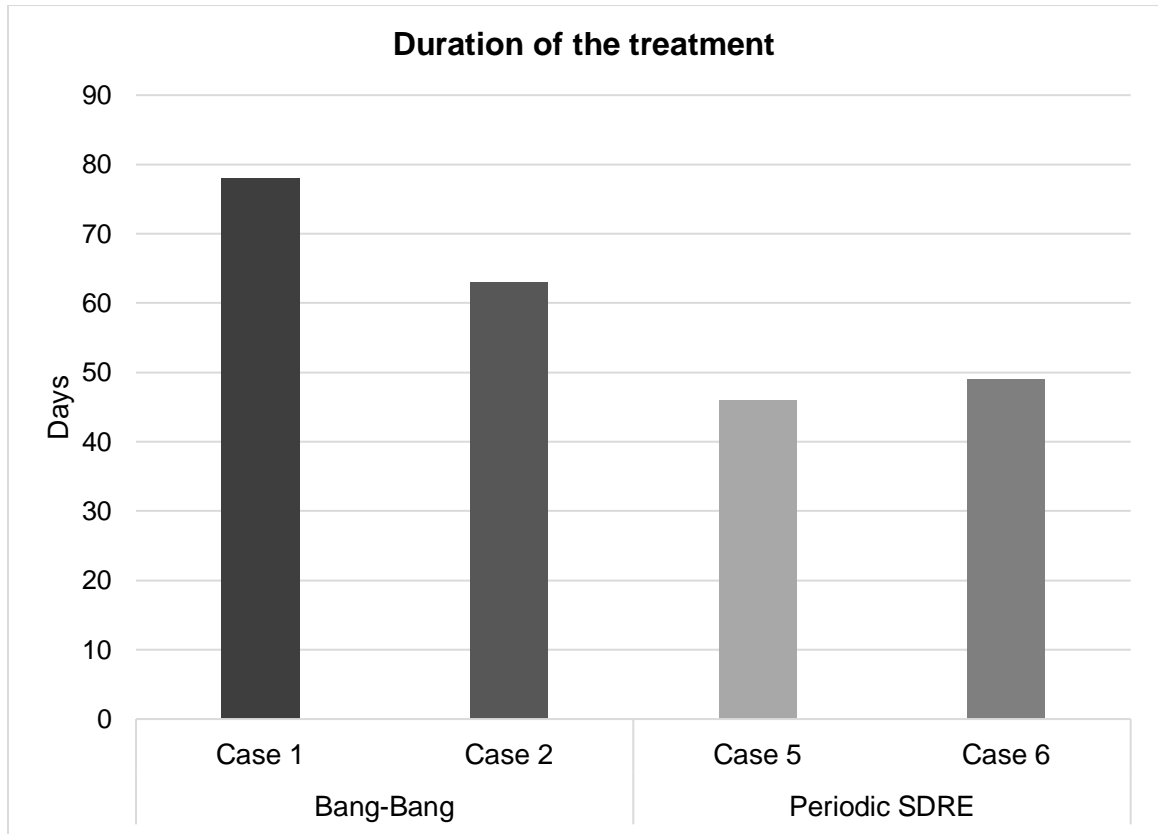


**Figure 28** – Comparison of the treatment’s duration (best cases).

When the regimens based on Bang-Bang are examined, case 1 seems to last longer, due to the highly weakened immune system ( $I_0 = 0.10$ ), compared to case 2 ( $I_0 = 0.15$ ). Moreover, the periodic-SDRE method ( $I_0 = 0.15$ ) presents a further decrease in the treatment’s duration, by taking advantage of the method’s feedback loop and a process of trial and error, through many possible variations of active and inactive days of drug administration.

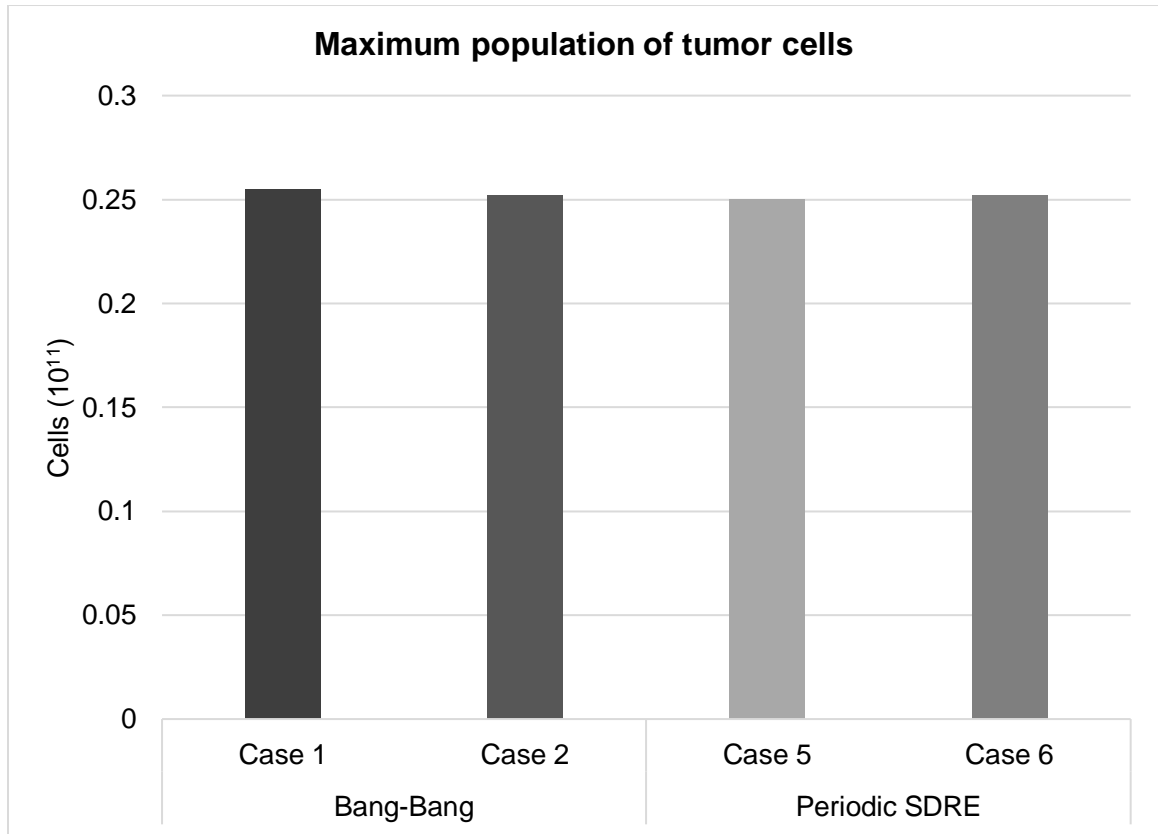


**Figure 29** – Comparison of the tumor cells’ maximum population (best cases).

In all four examined cases, the tumor size does not present any significant increase. Case 1 displays a trivial increase of 1.9%, which is the maximum among all the cases. Thus, apart from ultimately eradicating the tumor, the treatment also inhibits its further development; a very important achievement.

## Future Work

As previously mentioned, the current research depicts a simulation of a real-life scenario. Therefore, it is expected that deviations will occur when the treatment is applied to a patient, since there has always been a gap between simulated results and praxis. The scientific community is not able to counter that gap yet, and may never be, but a lot of work can be done to minimize it. As a result, an adaptive and/or predictive optimal control based chemotherapeutic treatment can be interpolated into the current analysis, so that the regimen could be reevaluated, if there are any differences between the simulation and the clinical results, e.g. the tumor's size remains the same or increases. Thus, the possibility of successfully combating cancer will undoubtedly increase.

## References

---

- [1] Adam, J. A., Panetta, J. (1995). A simple mathematical model and alternative paradigm for certain chemotherapeutic regimens. *Mathematical and Computer Modelling* 22(8), 4940.
- [2] Amerøv C., Emdin S., Lundgren B., Roos G., Söderström I., Bjersing L., Norberg C., Ångquist K. (1992). Breast carcinoma growth rate described by mammographic doubling time and S-phase fraction: Correlations to clinical and histopathologic factors in a screened population, *Cancer* 70(7), 1928-1934.
- [3] Babaei, N., Salamci, M. U., & Çimen, T. (2015). State Dependent Riccati Equation controlled drug delivery for mixed therapy of cancer treatment\*\*This work was supported by the Scientific and Technological Research Council of Turkey (TUBITAK) under the Project no. 112M209. *IFAC-PapersOnLine*, 48(25), 265–270. doi: 10.1016/j.ifacol.2015.11.098
- [4] Babaei, Naser & Salamci, Metin. (2019). Mixed Therapy in Cancer Treatment for Personalized Drug Administration using Model Reference Adaptive Control. *European Journal of Control*. 10.1016/j.ejcon.2019.03.001.
- [5] Banks, H. T., Kwon, H.-D., Toivanen, J. A., & Tran, H. T. (2006). A state-dependent Riccati equation-based estimator approach for HIV feedback control. *Optimal Control Applications and Methods*, 27(2), 93–121. doi: 10.1002/oca.773
- [6] Banks, H. T., Lewis, B. M., & Tran, H. T. (2007). Non-linear feedback controllers and compensators: a state-dependent Riccati equation approach. *Computational Optimization and Applications*, 37(2), 177–218. doi: 10.1007/s10589-007-9015-2
- [7] Borrelli R., Coleman C. (1998). *Differential equations: A modeling perspective*, John Wiley and Sons
- [8] Burden T., Ernstberger J., Fister K.R. (2004). Optimal control applied to immunotherapy, *Discrete and Continuous Dynamical Systems-Series B*, 4(1) 135-146.
- [9] Castiglione F., Piccoli B. (2007). Cancer immunotherapy, mathematical modeling and optimal control, *Journal of Theoretical Biology*, 247, 723–732.
- [10] Çimen T (2008). State Dependent Riccati Equation (SDRE) control: A survey. Plenary Session of 17th IFAC World Congress. 17. 10.3182/20080706-5-KR-1001.00635.
- [11] Cloutier, J., & Cockburn, J. (2001). The state-dependent non-linear regulator with state constraints. *Proceedings of the 2001 American Control Conference. (Cat. No.01CH37148)*. doi: 10.1109/acc.2001.945577
- [12] d’Onofrio, A., & Gandolfi, A. (2013). Modeling Immune-Mediated Tumor Growth and Treatment. In *Mathematical Oncology* (pp. 203–214). New York: Springer. doi: 10.1007/978-1-4939-0458-7\_7

- [13] De Pillis L.G., Fister K.R., Gu W., Collins C., Daub M., Gross D., Moore J., Preskill B. (2009). Mathematical model creation for cancer chemo-immunotherapy. *Computational and Mathematical Methods in Medicine* 10 (3), 165–184.
- [14] De Pillis L.G., Gu W., Fister K.R., Head T., Maples K., Murugan A., Neal T., Yoshida K. (2007). Chemotherapy for tumors: an analysis of the dynamics and a study of quadratic and linear optimal controls. *Mathematical Biosciences* 209, 292–315.
- [15] De Pillis L.G., Gu W., Radunskaya A.E. (2006). Mixed immunotherapy and chemotherapy of tumors: modeling, applications and biological interpretations. *Journal of Theoretical Biology* 238, 841–862.
- [16] De Pillis L.G., Mallet D.G., Radunskaya A.E. (2006). Spatial tumor-immune modeling. *Computational and Mathematical Methods in Medicine* 7 (2-3), 159–176.
- [17] De Pillis L.G., Radunskaya A.E. (2001). A mathematical tumor model with immune resistance and drug therapy: An optimal control approach. *Journal of Theoretical Medicine* 3, 79-100.
- [18] De Pillis L.G., Radunskaya A.E. (2003). The Dynamics of an optimally controlled tumor model: a case study. *Mathematical and Computer Modelling* 37, 1221–1244.
- [19] De Pillis L.G., Radunskaya A.E., Wiseman C.L. (2005). A validated mathematical model of cell-mediated immune response to tumor growth. *Cancer Research* 65, 7950–7958.
- [20] Dibrov, B., Zhabotinsky, A., Neyfakh, Y., Orlova, M., & Churikova, L. (1985). Mathematical model of cancer chemotherapy. periodic schedules of phase-specific cytotoxic-agent administration increasing the selectivity of therapy. *Mathematical Biosciences*, 73(1), 1–31. doi: 10.1016/0025-5564(85)90073-2
- [21] Eisen, M. (1981). *Mathematical Models in Cell Biology and Cancer Chemotherapy*. Biometrics. 37. 10.2307/2530548.
- [22] Emmett (2020). Algebraic Riccati Equation Solver [\[source\]](#), MATLAB Central File Exchange. Retrieved January 22, 2020.
- [23] Hargraves, C., & Paris, S. (1986). Direct trajectory optimization using non-linear programming and collocation. *Astrodynamics Conference*. doi:10.2514/6.1986-2000
- [24] Hedley B.D., Chambers A.F (2009). Tumor dormancy and metastasis. *Adv. Cancer Res.*102:67–101.
- [25] Holford, N. H., & Sheiner, L. B. (1981). Understanding the Dose-Effect Relationship. *Clinical Pharmacokinetics*, 6(6), 429–453. doi: 10.2165/00003088-198106060-00002
- [26] Itik, M., Salamci, M. U., & Banks, S. P. (2009). Optimal control of drug therapy in cancer treatment. *Non-linear Analysis: Theory, Methods & Applications*, 71(12). doi: 10.1016/j.na.2009.01.214

- [27] Jahanban-Esfahlan, R., de la Guardia, M., Ahmadi, D., Yousefi, B. (2017). Modulating tumor hypoxia by nanomedicine for effective cancer therapy. *J. Cell. Physiol.* 233:2019–2031. doi: 10.1002/jcp.25859.
- [28] Kelly, M. (2017). An Introduction to Trajectory Optimization: How to Do Your Own Direct Collocation. *SIAM Review*, 59(4), 849–904. doi: 10.1137/16m1062569
- [29] Kelly, M. P. (2017). Transcription Methods for Trajectory Optimization: A beginners tutorial. arXiv:1707.00284v1
- [30] Kelly, M. P. (2019). **OptimTraj**. Latest commit September 7, 2019. Retrieved from [\[source\]](#)
- [31] Kirschner D., Panetta J. C. (1998). Modeling immunotherapy of the tumor-immune interaction. *Journal of Mathematical Biology* 37, 235–252.
- [32] Knolle, H. (1988). Cell kinetic modelling and the chemotherapy of cancer. Berlin u.a.: Springer.
- [33] Kovács, L., & Eigner, G. (2018). A TP-LPV-LMI based control for Tumor Growth Inhibition. *IFAC-PapersOnLine*, 51(26), 155–160. doi: 10.1016/j.ifacol.2018.11.146
- [34] Kusama S., Spratt J., Donegan W., Watson F., Cunningham C. (1972). The gross rates of growth of human mammary carcinoma, *Cancer* 30(2), 59&599.
- [35] Kuznetsov, V., & Knott, G. (2001). Modeling tumor regrowth and immunotherapy. *Mathematical and Computer Modelling*, 33(12-13), 1275–1287. doi: 10.1016/s0895-7177(00)00314-9
- [36] Kuznetsov, V., Makalkin, I., Taylor, M., Perelson, A. (1994). Non-linear dynamics of immunogenic tumors: Parameter estimation and global bifurcation analysis, *Bull. of Math. Bio.* 56(2), 295-321.
- [37] Ledzewicz U., Schättler H. (2014). Optimal Control for Mathematical Models of Cancer Therapies, *Interdisciplinary Applied Mathematics*, 42.
- [38] Manjili M.H (2017). Tumor dormancy and relapse: From a natural byproduct of evolution to a disease state. *Cancer Res.* 77:2564–2569. doi: 10.1158/0008-5472.CAN-17-0068.
- [39] Martin R.B. (1992). Optimal Control Drug Scheduling of Cancer chemotherapy, *Automatica*, 28(6), 1113-1123, 1992.
- [40] Martin, R.B. & Fisher, M.E. & Minchin, Rod & Teo, Kok. (1990). A mathematical model of cancer chemotherapy with an optimal selection of parameters. *Mathematical biosciences.* 99. 205-30. 10.1016/0025-5564(90)90005-J.
- [41] Mehmet, I., Salamci, M. U. & Banks, S. (2010). SDRE optimal control of drug administration in cancer treatment. *Turkish Journal of Electrical Engineering and Computer Sciences.* 18. 10.3906/elk-1001-411.
- [42] Mracek, C. P., & Cloutier, J. R. (1998). Control designs for the non-linear benchmark problem via the state-dependent Riccati equation method. *International Journal of*

- Robust and Non-linear Control*, 8(4-5), 401–433. doi: 10.1002/(sici)1099-1239(19980415/30)8:4/5<401::aid-rnc361>3.0.co;2-u
- [43] Niemann, D., Li, J., Wang, H. O., & Tanaka, K. (1999). Parallel distributed compensation for Takagi-Sugeno fuzzy models: New stability conditions and dynamic feedback designs. *IFAC Proceedings Volumes*, 32(2), 5374–5379. doi: 10.1016/s1474-6670(17)56915-3
- [44] Owen, A. B. (2013). *Monte Carlo theory, methods and examples*. Monte Carlo Theory, Methods and Examples.
- [45] Paez D., Labonte M.J., Bohanes P., Zhang W., Benhanim L., Ning Y., Wakatsuki T., Loupakis F., Lenz H.J (2012). Cancer dormancy: A model of early dissemination and late cancer recurrence. *Clin. Cancer Res. Off. J. Am. Assoc. Cancer Res.*18:645–653. doi: 10.1158/1078-0432.CCR-11-2186.
- [46] Panetta J. (1996). A mathematical model of periodically pulsed chemotherapy Tumor recurrence and metastasis in a competitive environment, *Bulletin of Mathematical Biology* 58(3), 425-447.
- [47] Paris, S., Riehl, J., & Sjaww, W. (2006). Enhanced Procedures for Direct Trajectory Optimization Using Non-linear Programming and Implicit Integration. *AIAA/AAS Astrodynamic Specialist Conference and Exhibit*. doi: 10.2514/6.2006-6309
- [48] Pouliezios, A. (2015). *Modern Control Theory*. Athens: Hellenic Academic Libraries Link. <http://hdl.handle.net/11419/105>
- [49] Rao, A. (2010). *A Survey of Numerical Methods for Optimal Control*. *Advances in the Astronautical Sciences*. 135.
- [50] Shochat, E., Hart, D., Agur, Z. (1999). Using Computer Simulations for Evaluating The Efficacy Of Breast Cancer Chemotherapy Protocols. *Mathematical Models and Methods in Applied Sciences*, 09(04), 599–615. doi: 10.1142/s0218202599000312
- [51] Slotine J.J.E., Li, W. (1991). *Applied non-linear control*, Prentice Hall, London.
- [52] Souzaki, R., Kawakubo, N., Matsuura, T. et al (2019). Navigation surgery using indocyanine green fluorescent imaging for hepatoblastoma patients. *Pediatr Surg Int* 35, 551–557 doi:10.1007/s00383-019-04458-5
- [53] Steel G. (1977). *Growth kinetics of tumors*, Oxford University Press, Oxford.
- [54] Swan, G. W. (1985). Optimal control applications in the chemotherapy of multiple myeloma, *ZMA Journal of Mathematics Applied in Medicine and Biology* 4(2), 171-184.
- [55] Swan, G. W. (1987). Optimal control analysis of a cancer chemotherapy problem. IMA (Institute of Mathematics and its Applications). *Journal of Mathematics Applied in Medicine and Biology* 4(2), 171-184.
- [56] Swan, G. W. (1990). Role of optimal control theory in cancer chemotherapy. *Mathematical Biosciences*, 101(2), 237–284. doi: 10.1016/0025-5564(90)90021-p

- [57] Topputo, F., & Zhang, C. (2014). Survey of Direct Transcription for Low-Thrust Space Trajectory Optimization with Applications. *Abstract and Applied Analysis*, 2014, 1–15. doi: 10.1155/2014/851720
- [58] Unni, P., & Seshaiyer, P. (2019). Mathematical Modeling, Analysis, and Simulation of Tumor Dynamics with Drug Interventions. *Computational and Mathematical Methods in Medicine*, 2019, 1–13. doi: 10.1155/2019/4079298
- [59] Yadav, V. (2016). Direct collocation for optimal control. Retrieved from [\[source\]](#)

## Bibliography

---

- [60] Adam, J. A. (1993). The dynamics of growth-factor-modified immune response to cancer growth, One-dimensional models, *Mathematical and Computer Modelling* 17(3), 83-106.
- [61] Alamir, M., & Chareyron, S. (2006). State-Constrained Optimal Control Applied to Cell-Cycle-Specific Cancer Chemotherapy. *Positive Systems Lecture Notes in Control and Information Sciences*, 271–278. doi: 10.1007/3-540-34774-7\_35
- [62] Banks, S.P. & Dinesh, K.. (2000). Approximate Optimal Control and Stability of Non-linear Finite and Infinite-Dimensional Systems. *Annals of Operations Research*. 98. 19-44. 10.1023/A:1019279617898.
- [63] Baranyi, P., Yam, Y., & Várlaki, P. (2018). Tensor Product Model Transformation in Polytopic Model-Based Control. doi: 10.1201/9781315218045
- [64] Bartonszynski, R., Jones, B. F., & Klein, J. P. (1985). Some stochastic models of cancer metastases, *Communications in Statistics. Stochastic Models* 1(3), 317-339.
- [65] Beeler, S. & Cox, D. (2004). State-Dependent Riccati Equation Regulation of Systems with State and Control Non-linearities.
- [66] Chareyron, S., & Alamir, M. (2009). Mixed immunotherapy and chemotherapy of tumors: Feedback design and model updating schemes. *Journal of Theoretical Biology*, 258(3), 444–454. doi: 10.1016/j.jtbi.2008.07.002
- [67] Çimen, T., & Banks, S. P. (2004). Global optimal feedback control for general non-linear systems with nonquadratic performance criteria. *Systems & Control Letters*, 53(5), 327–346. doi: 10.1016/j.sysconle.2004.05.008
- [68] Coldman, A. J., Goldie, J. H. (1986). A stochastic model for the origin and treatment of tumors containing drug-resistant cells. *Bulletin of Mathematical Biology* 48(34), 279-292. *Simulation in cancer research* (Durham, N.C., 1986).
- [69] Drexler, D. A., Sápi, J., & Kovács, L. (2017). Modeling of Tumor Growth Incorporating the Effects of Necrosis and the Effect of Bevacizumab. *Complexity*, 2017, 1–10. doi: 10.1155/2017/5985031
- [70] Drexler, D. A., Sápi, J., & Kovács, L. (2017). Positive non-linear control of tumor growth using angiogenic inhibition. *IFAC-PapersOnLine*, 50(1), 15068–15073. doi: 10.1016/j.ifacol.2017.08.2522
- [71] Erdem, E., & Alleyne, A. (n.d.). Estimation of stability regions of SDRE controlled systems using vector norms. *Proceedings of the 2002 American Control Conference (IEEE Cat. No.CH37301)*. doi: 10.1109/acc.2002.1024784
- [72] Erdem, B., E. (2001). Analysis and real-time implementation of state-dependent Riccati equation controlled systems. Retrieved from [\[source\]](#).

- [73] Galambos, P., & Baranyi, P. (2015). TP $\tau$  Model Transformation: A Systematic Modelling Framework to Handle Internal Time Delays in Control Systems. *Asian Journal of Control*, 17(2), 486–496. doi: 10.1002/asjc.1077
- [74] Lamé, G. et. al. (2016). Outpatient Chemotherapy Planning: A Literature Review with Insights from a Case Study. *IIE Transactions on Healthcare Systems Engineering*. 6. 00-00. 10.1080/19488300.2016.1189469.
- [75] Martín-Castellanos, C., & Moreno, S. (1996). Regulation of G1 progression in fission yeast by the rum1 gene product. *Progress in Cell Cycle Research*, 29–35. doi: 10.1007/978-1-4615-5873-6\_3
- [76] Menon, P., Lam, T., Crawford, L., & Cheng, V. (n.d.). Real-time computational methods for SDRE non-linear control of missiles. *Proceedings of the 2002 American Control Conference (IEEE Cat. No.CH37301)*. doi: 10.1109/acc.2002.1024809
- [77] Murray J.M. (1990). Optimal control for a cancer chemotherapy problem with general growth and loss function, *Mathematical Biosciences*, 98, 273-287.
- [78] Owen M., Sherratt, J. (1998). Modelling the macrophage invasion of tumours: Effects on growth and composition. *IMA Journal of Mathematics Applied in Medicine and Biology* 15, 165-185.
- [79] Pontryagin L.S., Boltyanskii V.G., Gamkrelidze R.V., Mishchenko E.F. (1962). *The Mathematical Theory of Optimal Processes*, Gordon and Breach.
- [80] Sutton, R., Mcallester, D., Singh, S. & Mansour, Y. (2000). Policy Gradient Methods for Reinforcement Learning with Function Approximation. *Adv. Neural Inf. Process. Syst.* 12.
- [81] Swan, George & Vincent, Thomas. (1977). Optimal control analysis in the chemotherapy of IgG Multiple Myeloma. *Bulletin of Mathematical Biology*. 39. 317-337. 10.1007/BF02462912.
- [82] Swierniak, A., Polanski, A. Kimmel, M. (1996). Optimal control problems arising in cell-cycle-specific cancer chemotherapy, *Journal of Cell Proliferation* 29, 117-139.
- [83] Syed, K. (2020). Programmable Pulse Generator using Simulink's basic blocks (<https://www.mathworks.com/matlabcentral/fileexchange/35922-programmable-pulse-generator-using-simulink-s-basic-blocks>), MATLAB Central File Exchange. Retrieved January 22, 2020.
- [84] Tanaka, K., & Wang, H. O. (2001). *Fuzzy control systems design and analysis: a linear matrix inequality approach*. New York: Wiley.
- [85] Thomlinson R. (1982). Measurement and management of carcinoma of the breast, *Clinical Radiology* 33(5), 481-493.
- [86] Tomás-Rodríguez, M., & Banks, S. P. (2010). Linear Approximations to Non-linear Dynamical Systems. *Linear, Time-Varying Approximations to Non-linear Dynamical Systems Lecture Notes in Control and Information Sciences*. doi: 10.1007/978-1-84996-101-1\_2

- [87] Udagawa T (2018). Tumor dormancy of primary and secondary cancers. *Apmis: Acta Pathol. Microbiol. Immunol. Scand.* 116:615–628. doi: 10.1111/j.1600-0463.2008.01077.x.
- [88] Vaidya V., Alexandro Jr. F. (1982). Evaluation of some mathematical models for tumor growth, *International Journal of Bio-Medical Computing* 13, 19-35.
- [89] Ya-Fei D., Juan-Juan X (2018). Tumor Cell Dormancy: How It Performs in Drug Resistance and Relapse. *Prog. Biochem. Biophys.* 45:460–470.

## Appendix 1 :

# Hermite-Simpson Direct Collocation method

---

In Hermite-Simpson collocation method, the state trajectories are expressed as cubic polynomials, and the control is expressed as a piecewise linear function. The dynamic equations are imposed as constraints at collocation points that are midpoints of the discretization segments of the time domain [59]. The implementation of the method is analyzed in the following sections.

### Discretize the time domain

Suppose we discretize time  $t_f$  into  $N$  segments as,

$$t_0 = 0 \leq t_1 \leq t_2 \leq \dots \leq t_k \leq t_{k+1} \dots \leq t_N = t_f,$$

then the states between  $t_k$  and  $t_{k+1}$  can be represented as

$$x(t) = a_{k,0} + a_{k,1}t + a_{k,2}t^2 + a_{k,3}t^3,$$

which yields

$$\dot{x}(t) = a_{k,1} + 2a_{k,2}t + 3a_{k,3}t^2,$$

where  $a_{k,0}$ ,  $a_{k,1}$ ,  $a_{k,2}$  and  $a_{k,3}$  are coefficients of the polynomial approximation in  $k^{th}$  interval.

### Compute state derivatives at the collocation point

A collocation point is the midpoint of the time interval

$$t_{k,c} = \frac{t_k + t_{k+1}}{2}.$$

As the value of the state or its derivatives will not change by shifting the interval from  $[t_k, t_{k+1}]$  to  $[0, h]$ , where  $h = t_{k+1} - t_k$ , we shift the time interval. We now have

$$\begin{aligned}x(0) &= x_k, \\x(h) &= x_{k+1}, \\ \dot{x}(0) &= x_k = f(x_k, u_k), \\ \dot{x}(h) &= x_{k+1} = f(x_{k+1}, u_{k+1}).\end{aligned}$$

The same can be computed from the polynomial representations too. This gives us

$$\begin{bmatrix} x(0) \\ \dot{x}(0) \\ x(h) \\ \dot{x}(h) \end{bmatrix} = \begin{bmatrix} 1 & 0 & 0 & 0 \\ 0 & 1 & 0 & 0 \\ 1 & h & h^2 & h^3 \\ 0 & 1 & 2h & 3h^2 \end{bmatrix} \begin{bmatrix} a_{k,0} \\ a_{k,1} \\ a_{k,2} \\ a_{k,3} \end{bmatrix}.$$

Taking the inverse gives

$$\begin{bmatrix} a_{k,0} \\ a_{k,1} \\ a_{k,2} \\ a_{k,3} \end{bmatrix} = \begin{bmatrix} 1 & 0 & 0 & 0 \\ 0 & 1 & 0 & 0 \\ -\frac{3}{h^2} & -\frac{2}{h} & \frac{3}{h^2} & -\frac{1}{h} \\ \frac{2}{h^3} & \frac{1}{h^2} & -\frac{2}{h^3} & \frac{1}{h^2} \end{bmatrix} \begin{bmatrix} x(0) \\ \dot{x}(0) \\ x(h) \\ \dot{x}(h) \end{bmatrix}.$$

With these coefficients, we can compute the value of states and their derivatives at collocation points as

$$x_c = x\left(\frac{h}{2}\right) = \frac{1}{2}(x_k + x_{k+1}) + \frac{h}{8}[f(x_k, u_k) - f(x_{k+1}, u_{k+1})].$$

The time-derivative at midpoint is given by,

$$\dot{x}_c = \dot{x}\left(\frac{h}{2}\right) = -\frac{3}{2h}(x_k - x_{k+1}) - \frac{1}{4}[f(x_k, u_k) + f(x_{k+1}, u_{k+1})].$$

This derivative depends on the states and control at the interval or knot points. By choosing the states and controls appropriately, we can make sure that the derivative at the collocation point matches the dynamics. The control at the collocation point is given by

$$u_c = \frac{u_k + u_{k+1}}{2}.$$

We construct a defect  $\Delta_k$  for each interval such that,

$$\begin{aligned}\Delta_k &= \dot{x}_c - f(x_c, u_c), \\ \Delta_k &= -\frac{3}{2h}(x_k - x_{k+1}) - \frac{1}{4}[f(x_k, u_k) + f(x_{k+1}, u_{k+1})] - f(x_c, u_c), \\ \Delta_k &= -\frac{3}{2h} \left[ (x_k - x_{k+1}) + \frac{h}{6} [f(x_k, u_k) + 4f(x_c, u_c) + f(x_{k+1}, u_{k+1})] \right],\end{aligned}$$

We redefine the state constraint as

$$\Delta_k = \left[ (x_k - x_{k+1}) + \frac{h}{6} [f(x_k, u_k) + 4f(x_c, u_c) + f(x_{k+1}, u_{k+1})] \right].$$

The last term in the expression above is implicit Hermite integration of system dynamics. We call this integration implicit because the last term in the bracket is equal to the Hermite integration only when the collocation point satisfies the system dynamics.

## Express the cost function in terms of optimization parameters

The next step is to approximate the cost function. The cost function can be computed by using various numerical integration (or quadrature) schemes. Say we choose to use trapezoid method, the cost function expressed as,

$$J(u) = \Phi(x_f) + \int_{t=0}^{t_f} \mathcal{L}(t, x, u) dt.$$

We can use trapezoid integration and integrate the above in an interval as

$$J_{nlp} = \Phi(x_N) + \frac{1}{2} \sum_{k=1}^{N-1} (\mathcal{L}(t_{k+1}, x_{k+1}, u_{k+1}) + \mathcal{L}(t_k, x_k, u_k)) (t_{k+1} - t_k).$$

For the special case where we have linear quadratic regulator, with time points discretized evenly at segments of  $h$ , we have

$$J_{ntp} = \Phi(x_N) + \frac{1}{2} \sum_{k=1}^{N-1} (x_{k+1}^T Q x_{k+1} + u_{k+1}^T R u_{k+1} + x_k^T Q x_k + u_k^T R u_k) h.$$

## Define Additional Constraints

The constraints on states and controls can be expressed as

$$u_{min} \leq u_k \leq u_{max},$$

$$x_{min} \leq x_k \leq x_{max},$$

$$C_{eq}(x_k, u_k) = 0,$$

$$C(x_k, u_k) \leq 0,$$

where  $C_{eq}(x, u)$  and  $C(x, u)$  correspond to constraint equality and inequality matrices, respectively, should there be any additional restrictions for the system.

## Appendix 2 :

### State-Dependent Riccati Equation (SDRE) method

---

This appendix presents a section of [10], in order to further understand the nature of the SDRE technique.

#### Problem formulation

Consider the deterministic, infinite-horizon non-linear optimal regulation (stabilization) problem, where the system is full-state observable, autonomous, non-linear in the state, and affine in the input, represented in the form

$$\dot{x}(t) = f(x) + B(x)u(t), \quad x(0) = x_0 \quad (2.1)$$

Where  $x \in \mathbb{R}^n$  is the state vector,  $u \in \mathbb{R}^m$  is the input vector, and  $t \in [0, \infty)$ , with  $C^1(\mathbb{R}^n)$  functions  $f: \mathbb{R}^n \rightarrow \mathbb{R}^n$  and  $B: \mathbb{R}^n \rightarrow \mathbb{R}^{n \times m}$ ,  $B(x) \neq 0 \forall x$ . Without any loss of generality, the origin  $x = 0$  is assumed to be an equilibrium point, such that  $f(0) = 0$ . In this context, the minimization of the infinite-time performance criterion

$$J(x_0, u(\cdot)) = \frac{1}{2} \int_0^{\infty} \{x^T(t)Q(x)x(t) + u^T(t)R(x)u(t)\}dt \quad (2.2)$$

is considered, which is non-quadratic in  $x$  but quadratic in  $u$ . The state and input weighting matrices are assumed state-dependent such that:  $Q: \mathbb{R}^n \rightarrow \mathbb{R}^{n \times n}$  and  $R: \mathbb{R}^n \rightarrow \mathbb{R}^{m \times m}$ . These design parameters satisfy  $Q(x) \geq 0$  and  $R(x) \geq 0$  for all  $x$ . Under the specified conditions, a control law

$$u(x) = k(x) = -K(x)x, \quad k(0) = 0, \quad (2.3)$$

where  $k(\cdot) \in C^1(\mathbb{R}^n)$ , is then sought that will (approximately) minimize the cost  $J$  subject to the input-affine non-linear differential constraint  $\dot{x}(t)$ , while regulating the system to the origin  $\forall x$ , such that  $\lim_{t \rightarrow \infty} x(t) = 0$ . This problem forms the basis of the SDRE method for non-linear regulation.

## Extended linearization

Extended linearization, also known as apparent linearization or SDC parameterization, is the process of factorizing a non-linear system into a linear-like structure which contains SDC matrices. Under the assumptions  $f(0) = 0$  and  $f(\cdot) \in C^1(\mathbb{R}^n)$ , a continuous non-linear matrix-valued function  $A(x)$  always exists such that

$$f(x) = A(x), \quad (2.4)$$

where  $A: \mathbb{R}^n \rightarrow \mathbb{R}^{n \times n}$  is found by mathematical factorization and is, clearly, nonunique when  $n > 1$ . Hence, extended linearization of the input-affine non-linear system becomes

$$\dot{x}(t) = A(x)x(t) + B(x)u(t), \quad x(0) = x_0, \quad (2.5)$$

which has a linear structure with SDC matrices  $A(x), B(x)$ . The application of any linear control synthesis method to the above linear-like SDC structure, where  $A(x)$  and  $B(x)$  are treated as constant matrices, forms an extended linearization control method. These represent a rather broad class of control design methods, leading to non-linear control laws of the form of  $u(x)$  that render the closed-loop dynamics (SDC) matrix

$$A_{CL}(x) = A(x) - B(x)K(x) \quad (2.6)$$

pointwise Hurwitz.

The recoverability of non-linear state feedback laws using extended linearization control techniques has been investigated by Cloutier, Stansbery & Sznaier (1999). By recoverable it is meant that a given non-linear state feedback law of form  $u(x)$  can be obtained (or recovered) from a given control design method. Necessary and sufficient conditions for the recoverability of a given non-linear state feedback control law by some extended linearization control technique, and in particular, by the SDRE method, have been provided by Cloutier, Stansbery & Sznaier (1999).

## Controller structure

The SDRE methodology uses extended linearization as the key design concept in formulating the non-linear optimal control problem. The underlying linear control synthesis method in this case is the LQR synthesis method. Motivated by the LQR problem, which is characterized by an ARE, SDRE feedback control is an “extended linearization control method” that provides a similar approach to the non-linear regulation problem for the input-affine system  $\dot{x}(t) = f(x) + B(x)u(t)$  with cost functional  $J(x_0, u(\cdot))$ . By mimicking the LQR formulation, the state feedback controller is obtained in the form

$$u(x) = -R^{-1}(x)B^T(x)P(x)x \quad (2.7)$$

where  $P(x)$  is the unique, symmetric, positive-definite solution of the algebraic State-Dependent Riccati Equation

$$P(x)A(x) + A^T(x)P(x) - P(x)B(x)R^{-1}(x)B^T(x)P(x) + Q(x) = 0, \quad (2.8)$$

hence the name SDRE control. The resulting SDRE-controlled trajectory becomes the solution of the quasilinear closed-loop dynamics

$$\dot{x}(t) = [A(x) - B(x)R^{-1}(x)B^T(x)P(x)]x(t), \quad (2.9)$$

such that the state-feedback gain in  $A_{CL}$  for minimizing  $J(x_0, u(\cdot))$  is

$$K(x) = R^{-1}(x)B^T(x)P(x).$$

Therefore, the SDRE solution to the originally presented infinite-horizon autonomous non-linear regulator problem is a true generalization of the infinite-horizon time-invariant LQR problem, where all of the coefficient matrices are state-dependent. At each instant, the method treats the state-dependent coefficients matrices as being constant, and computes a control action by solving an LQ optimal control problem. As is evident from the algebraic State-Dependent Riccati Equation, the resulting controller relies on a solution, pointwise in  $\mathbb{R}^n$ , of an ARE thereby leading to the SDRE terminology. There is no attempt to solve the HJB equation. The clearest benefit of the SDRE algorithm is its simplicity and its apparent

effectiveness. When the coefficient and weighting matrices are constant, the non-linear regulator problem collapses to the LQR problem and the SDRE control method collapses to the steady-state linear regulator.

## Existence of stabilizing feedback controls

Cloutier, Stansbery & Sznaier (1999) derived the necessary condition on  $f(x)$  and  $B(x)$  for the existence of any feedback gain matrix,  $K(x)$ , that results in eq. (2.6) being pointwise Hurwitz. First, let us state the following system-theoretic concept definitions, pointwise in  $x$ , associated with the existence of SDRE stabilizing feedback controls.

**Definition 1.** The SDC representation (2.5) is a stabilizable (controllable) parameterization of the non-linear system (2.1) in a region  $\Omega \in \mathbb{R}^n$  if the pair  $\{A(x), B(x)\}$  is pointwise stabilizable (controllable) in the linear sense for all  $x \in \Omega$ .

**Definition 2.** The SDC representation (2.5) is a detectable (observable) parameterization of the non-linear system (2.1) in a region  $\Omega \in \mathbb{R}^n$  if the pair  $\{A(x), Q^{1/2}(x)\}$  is pointwise detectable (observable) in the linear sense for all  $x \in \Omega$ .

**Definition 3.** The SDC representation (2.5) is pointwise Hurwitz in a region  $\Omega$  if the eigenvalues of  $A(x)$  are in the open left half plane  $Re(s) < 0$  (that is, have negative real parts) for all  $x \in \Omega$ .

**Definition 4.** A  $C^1(\mathbb{R}^n)$  control law (2.3) is said to be recoverable by SDRE control in a region  $\Omega$  if there exists a pointwise stabilizable SDC parameterization  $\{A(x), B(x)\}$ , a pointwise positive-semidefinite state weighting matrix  $Q(x)$  and a pointwise positive-definite control weighting matrix  $R(x)$  such that the resulting state-dependent controller (2.7) satisfies (2.3) for all  $x$ .

**Theorem 1** (Cloutier, Stansbery & Sznaier, 1999).

A  $C^1(\mathbb{R}^n)$  control law (2.3) is recoverable by SDRE control in a region  $\Omega$  if there exists a pointwise stabilizable SDC parameterization  $\{A(x), B(x)\}$  such that the closed-loop dynamics matrix (2.6) is pointwise Hurwitz in  $\Omega$ , and the gain  $K(x)$  satisfies the pointwise minimum-

phase property in  $\Omega$ , that is, the zeros of the loop gain  $K(x)[sI - A(x)]^{-1}B(x)$  lie in the closed left half plane  $Re(s) \leq 0$ , pointwise.

Although Theorem 1 provides the necessary and sufficient conditions for recoverability of SDRE controls, it is difficult to apply this theorem due to the fact that there are an infinite number of SDC parameterizations.

## Local asymptotic stability

The following conditions are required for guaranteeing local asymptotic stability:

**Hypothesis 3.**  $A(\cdot), B(\cdot), Q(\cdot)$  and  $R(\cdot)$  are  $C^1(\mathbb{R}^n)$  matrix-valued functions.

**Hypothesis 4.** The respective pairs  $\{A(x), B(x)\}$  and  $\{A(x), Q^{1/2}(x)\}$  are pointwise stabilizable and detectable SDC parameterizations of the non-linear system (2.1) for all  $x$ . A sufficient test for the second stability condition is to check that the controllability matrix

$$M_c = [B(x) \quad A(x)B(x) \quad \cdots \quad A^{n-1}(x)B(x)]$$

has rank  $(M_c) = n, \forall x \in \mathbb{R}^n$ .

Similarly, a sufficient test for detectability is that the observability matrix

$$M_o = [Q^{1/2}(x) \quad Q^{1/2}(x)A(x) \quad \cdots \quad Q^{1/2}(x)A^{n-1}(x)]$$

has rank  $(M_o) = n, \forall x \in \mathbb{R}^n$ , which can be guaranteed by ensuring that  $Q(x)$  is positive definite  $\forall x \in \mathbb{R}^n$ .

**Theorem 2** (Mracek & Cloutier, 1998).

Consider the non-linear multivariable system (2.1) with feedback control (2.7) applied, where  $x \in \mathbb{R}^n$  ( $n > 1$ ) and  $P(x)$  is the unique, symmetric, positive-definite, pointwise-stabilizing solution of the SDRE (2.8). Then, under Hypotheses 3 and 4, the SDRE method produces a closed-loop solution which is locally asymptotically stable.

**Proof.** Using SDRE control, the closed-loop solution becomes  $\dot{x} = A_{CL}(x)x$ , where  $A(x)_{CL}$  is the closed-loop SDC matrix given by (2.6). From Riccati equation theory,  $A(x)_{CL}$

is guaranteed to be stable at every point  $x$ . Under the smoothness assumptions of Hypotheses 3,  $P(x)$  is  $C^1(\mathbb{R}^n)$  and hence so is  $A_{CL}(x)$ . Applying the Mean Value Theorem to  $A_{CL}(x)$  gives

$$A_{CL}(x) = A_{CL}(0) + \frac{\partial A_{CL}(z)}{\partial x} x,$$

where  $\partial A_{CL}(z)/\partial x$  generates a tensor, and the vector  $z$  is that point on the line segment joining the origin 0 and  $x$ . By substitution,

$$\dot{x} = A_{CL}(0)x + x^T \frac{\partial A_{CL}(z)}{\partial x} x,$$

which gives

$$\dot{x} = A_{CL}(0)x + \psi(x, z) \|x\|,$$

where  $\psi(x, z) \triangleq \frac{1}{\|x\|} x^T \frac{\partial A_{CL}(z)}{\partial x} x$ , such that  $\lim_{\|x\| \rightarrow 0} \psi(x, z) = 0$ . Hence, in a neighborhood about the origin, the linear term which has a constant stable coefficient matrix  $A_{CL}(0)$  dominates the higher-order term, yielding local asymptotic stability.

Theorem 2 presents the rather mild conditions that guarantee local asymptotic stability of the SDRE closed-loop solution. Since the characterization of the resulting SDRE controller has a similar structure to the LQR problem, in order that the SDRE (2.8) have a positive-semidefinite solution for all  $x$ , it is sufficient that  $\{A(x), B(x), Q^{1/2}(x)\}$  be pointwise stabilizable and detectable for all  $x$ . The SDRE algorithm then gives a smooth feedback.